

A Novel Anxiety Process Biomarker via Electrovestibulography

by

Cory Bosecke

A thesis submitted to the Faculty of Graduate Studies of
the University of Manitoba
in partial fulfilment of the requirements of the degree of

MASTER OF SCIENCE

Biomedical Engineering

University of Manitoba

Winnipeg

© 2022 by Cory Bosecke

Abstract

Anxiety disorders have no known biomarkers, and are thus diagnosed based on symptoms. Identifying biomarkers for these disorders could help improve the accuracy of anxiety disorder diagnoses, but may be difficult because some of the deepest brain regions are implicated in anxiety. Directly measuring activity from these regions non-invasively is highly complex; however, it may be possible to indirectly measure activity in these regions with the electrophysiological technique ‘Electrovestibulography’ (EVestG). This technique records electrical activity from the ear canals with cotton tipped wire electrodes, and detects field potentials (FPs) caused by vestibular neurons. These FPs may reveal an anxiety biomarker because they are mediated by the brainstem vestibular nucleus (VN), which receives dense projections from three anxiety-implicated brainstem regions, that in turn receive projections from anxiety-implicated regions whose homologues in rodents are known to exhibit the rhythmicity of the anxiety-implicated ‘hippocampal theta rhythm’ (hTheta). Vivally, depth recording has revealed a human analogue of hTheta in the hippocampus (HPC); and Shadli et al. [1] found an anxiety process biomarker ‘goal conflict specific rhythmicity’ (GCSR) that seems to be driven by a human analogue of hTheta, in frontal electroencephalography (EEG) data, via an anxiety-related ‘Stop Signal Task’ (SST). It may therefore be possible to test whether a human analogue of hTheta entrains vestibular FPs by eliciting this analogue with the SST while recording FPs with EVestG, where altered FP firing patterns would indicate a GCSR ‘analogue.’

The current study was comprised of two experiments: an ‘EEG Experiment’ and ‘EVestG Experiment,’ where healthy volunteers (five and four, respectively) performed the SST by pressing keyboard keys in response to images on a screen while frontal EEG or EVestG data were recorded. The ‘EEG Experiment’ was aimed at partially replicating an experiment in Shadli et al. [1] by reproducing GCSR in frontal EEG power spectra; while the ‘EVestG Experiment’ — a novel experiment — was aimed at eliciting an analogue of GCSR in vestibular FP firing patterns. The EEG Experiment showed no GCSR, indicating that frontal EEG power was not significantly altered during the anxiogenic conditions of the SST. The EVestG Experiment, however, revealed a GCSR ‘analogue’ in the right ear EVestG data of volunteers and indicated that vestibular FPs occurred at a higher than average (9 Hz) firing rate during the anxiogenic conditions of the SST. The theory behind GCSR implies that a human analogue of hTheta may have entrained these FPs. This could have caused vestibular neurons to burst fire, grouping FPs and making them easier to

detect with EVestG (which there was evidence of, in the results). Critically, the GCSR ‘analogue’ validates a novel anxiety biomarker (caused by a human analogue of hTheta) that could possibly provide objective data to clinicians that could inform anxiety disorder diagnoses, in the future. However, due to the low recruitment (related to COVID-19 lockdowns) in the current study, results should be interpreted with caution; and both experiments should be repeated with more volunteers.

Keywords: EVestG, anxiety, hippocampal theta

Acknowledgements

First, I would like to thank my advisor, Professor Brian Lithgow, for guiding me through to the end of this project. Thank you, Prof Lithgow. Your door was always open.

I would also like to thank my co-advisor, Doctor Marcus Ng, for all of his knowledge about electroencephalography that he was willing to share and for the support he provided.

I am grateful to Doctor Dana Turcotte for her dedication to the project and assistance with all of the pharmacological aspects of the study. Thank you, Doctor Turcotte.

I must thank Doctor Moussavi for first introducing me to the research and to my advisor, and for helping me navigate my graduate studies.

Thank you to a true friend, Tom Kaminski, who coded the entire SST program for me, and who has remained a dear friend through the toughest of times.

Dr. Neil McNaughton, thank you for teaching me more than I thought I would ever learn about *any* subject through emails (or perhaps any medium).

Thanks to all of you.

Table of Contents

Abstract.....	i
Acknowledgements.....	iii
List of Tables	vi
List of Figures.....	viii
List of Abbreviations	xi
Chapter 1 : Introduction	1
1.1 Motivation.....	1
1.2 Objectives.....	4
1.3 Results.....	4
1.4 Outline.....	5
Chapter 2 : Background	6
2.1 Overview	6
2.2 What is Anxiety?	6
2.3 Anxiety-Like Behaviour is Linked to hTheta.....	8
2.4 Type I & II hTheta are Independent.	11
2.5 Anxiety-Like Behaviour is Caused by hTheta.	13
2.6 Anxiety is Linked to hTheta-Like Rhythmicity.	14
2.7 hTheta Modulates Auditory Signals.	20
2.8 hTheta may Modulate Vestibular Signals.	22
2.9 Reciprocal Information Transfer: A Novel Anxiety Process Biomarker	25
2.10 A Novel Anxiety Process Biomarker via Electrovestibulography	28
2.11 Summary	30
Chapter 3 : Methods	33
3.1 Overview	33
3.2 Participants	33
3.3 Description of the Stop Signal Task (SST).....	34
3.4 EEG Experiment.....	37
3.5 EVestG Experiment	44
3.6 Summary	52

Chapter 4 : Results	54
4.1 Overview	54
4.2 EEG Experiment.....	54
4.3 EVestG Experiment	64
4.4 Summary	72
Chapter 5 : Discussion.....	75
5.1 Overview	75
5.2 EEG Experiment Discussion.....	75
5.3 EVestG Experiment Discussion.....	77
Chapter 6 : Conclusion	82
6.1 Future Work	83
References.....	85

List of Tables

Table 3-1. Demographics of participants in the EEG and EVestG Experiments. Note that three volunteers were recruited for both experiments, but one of these three (P-3) was later excluded from the EVestG Experiment due to excessive artefacts in recorded signals (* data excluded)..	34
Table 4-1. The demographic data of the participants in “Experiment 2” of Shadli et al. [1].	55
Table 4-2. SST statistics of the EEG group participants. ‘GO_RT’ is the average reaction time in ‘go’ trials; ‘Go pass’ is the success rate in ‘go’ trials; ‘Int SSD Avg’ is the average intermediate SSD value; ‘SSRT’ is ‘GO_RT’ minus ‘Int SSD Avg;’ and ‘Short,’ ‘Intermed.’ and ‘Long SSD’ are short, intermediate and long ‘stop’ trial success rates.	56
Table 4-3. Mean SST values of the EEG group for comparison with those of Shadli et al. (2016). ‘GO_RT’ is the average reaction time in ‘go’ trials; ‘Go pass’ is the success rate in ‘go’ trials; ‘Int SSD Avg’ is the average intermediate SSD value; ‘SSRT’ is ‘GO_RT’ minus ‘Int SSD Avg;’ ‘Short,’ ‘Intermed.’ and ‘Long SSD’ are short, intermediate and long ‘stop’ trial success rates.	56
Table 4-4. Numbers of included power spectra by trial condition and EEG group participant. Participants had at least 7 included spectra for each condition and therefore 6 average spectra (short stop, short go, intermediate stop, intermediate go, long stop and long go average spectra).	58
Table 4-5. Main GCSR contrast results from SPSS, showing that the quartic term for the ‘frequency’ polynomial had a p-value below 0.05. After Bonferroni correction (for the five orders that were tested), however, the result did not reach significance.	60
Table 4-6. Results of GCSR contrast for each 4-12 Hz level of ‘frequency,’ tested separately...	61
Table 4-7. Results of GCSR contrast for 5-11, 6-10 and 7-9 Hz ranges of ‘frequency.’	62
Table 4-8. Results for test of variation between effects of short and long SSDs on F8 power independent of the intermediate SSD. BIS theory predicts no variation between effects of short and long SSDs. As results were insignificant, no significant variation was detected.	63

Table 4-9. Results for test of variation between ‘stop’ and ‘go’ effects on F8 power. BIS theory predicts variation between ‘stop’ and ‘go’ effects. A ‘stopping’ effect was detected because the linear ‘frequency’ term was significant after Bonferroni correction.	64
Table 4-10. SST statistics of the EVestG group participants. ‘GO_RT’ is the mean reaction time in ‘go’ trials; ‘Go pass’ is the success rate in ‘go’ trials; ‘Int SSD Avg’ is the average intermediate SSD value; ‘SSRT’ is ‘GO_RT’ minus ‘Int SSD Avg;’ and ‘Short,’ ‘Intermed.’ and ‘Long SSD’ are short, intermediate and long ‘stop’ trial success rates.	66
Table 4-11. SST mean values of the EVestG group to compare with those of Shadli et al. (2016). ‘GO_RT’ is the average reaction time in ‘go’ trials; ‘Go pass’ is the success rate in ‘go’ trials; ‘Int SSD Avg’ is the average intermediate SSD value; ‘SSRT’ is ‘GO_RT’ minus ‘Int SSD Avg;’ ‘Short,’ ‘Intermed.’ and ‘Long SSD’ are short, intermediate and long ‘stop’ trial success rates.	66
Table 4-12. IHs included in analyses for each EVestG group participant by trial type and SSD. Each participant had at least 7 included IHs for each condition and therefore 6 average IHs (short stop, short go, intermediate stop, intermediate go, long stop and long go average IHs).	67
Table 4-13. GCSR ‘analogue’ results. The fourth and sixth order polynomials for ‘time’ were significant after Bonferroni correction.	70
Table 4-14. Results for test of variation between effects of short and long SSDs on IH values independent of the intermediate SSD. BIS theory predicts no variation between effects of short and long SSDs. As results were insignificant, no variation was detected.	71
Table 4-15. Results for test of variation between ‘stop’ and ‘go’ effects on IH values. BIS theory predicts variation between ‘stop’ and ‘go’ effects. A ‘stopping’ effect was not detected because none of the results were significant after Bonferroni correction.	71

List of Figures

- Figure 2-1. mPFC and vHPC hTheta power increased in the EPM and open field anxiety assays. (Top) Local field potential traces for the mPFC (hTheta is visible for the EPM and open field). (Bottom) Power spectra for the mPFC and vHPC had 7 Hz peaks in the EPM and open field. Source: Adapted from [21]. 9
- Figure 2-2. mPFC hTheta power inhibits exploratory behaviour. Averaged spectrograms of mPFC power (a, b) and vHPC-mPFC coherence (c, d), centered at times when mice transitioned to (b, d) and from (a, c) safe (i.e., closed) arms of the EPM. Source: Adapted from [21]. 10
- Figure 2-3. hTheta power increases with movement speed. The dotted, dashed, and solid lines represent slow, moderate, and fast movement, respectively. Source: Adapted from [21]. 11
- Figure 2-4. 4-12 Hz EEG activity via depth recording in the human HPC amid virtual movement. (a) Raw trace while subject was still, S, then moving, M; (b) raw trace during virtual movement; (c, d) power spectra during virtual movement tasks; (e, f) “percentage of time in oscillatory episode [during virtual movement tasks],” determined by “time filled with detected oscillatory episodes divided by the total time in the segment of interest” [10]. Source: Adapted from [10]. 15
- Figure 2-5. Anatomical connections between the VN and regions implicated in anxiety disorders. Various studies [12, 13, 39-46] together establish that these neural connections exist in rodents. The blue lines are bidirectional projections, and the red arrows are unidirectional projections. . 23
- Figure 2-6. Most rat DR neurons fired in synchrony with hTheta amid REM sleep and movement. (Top) Local field potentials from depth recording in the HPC. (Bottom) Single-unit activity from depth recording within a sample DR neuron. (Left) Recordings during large irregular activity. (Right) Recordings during hTheta activity. Source: Adapted from [47]. 24
- Figure 3-1. Flowchart of the possible images shown in SST trials. Source: Adapted from [31]. 35
- Figure 3-2. EOG correction of EEG data recorded during the SST. (Top to bottom) F8 before correction; F8 after vEOG correction; F8 after vEOG and hEOG correction; vEOG; hEOG. 40
- Figure 3-3. EEG recording after EOG correction and manual artefact removal (missing segments are where artefacts occurred). The vertical axis is frontal EEG activity at the F8 recording site (in millivolts); and the horizontal axis is time (in milliseconds)..... 42

Figure 3-4. Ear canal electrode placement. Note the proximity of the vestibular organs (right). Adapted from [13].....	45
Figure 3-5. Raw trace from a typical (~ 6-minute) in-ear recording.	46
Figure 3-6 1-second in-ear EEG data segment and field potentials identified by NEER within it. (Top) 1-second segment of in-ear EEG data, recorded from a participant during the SST. (Bottom) Field potentials NEER found buried in noise, in the 1-second in-ear EEG data segment. The vertical axis is voltage (volts/10,000); the horizontal axis is time (the window is 1 second).	47
Figure 3-7. An average FP shape. A data segment was excluded from analyses if the average FP shape for the segment exhibited any of the following criteria: 1) the width of the large trough in the center was narrower than the gap between the vertical black dashed lines (at the $y = 0$ line), 2) any peaks between the red dashed lines exceeded $2/3$ of the magnitude of the central trough, or 3) any trough between the red dashed lines exceeded $2/3$ of the magnitude of the central one. The vertical axis is amplitude (in μV) and the horizontal axis is time index (in sample numbers).	48
Figure 3-8. Interval histogram of FPs separated by 33 inter-FP gaps in a 1-second segment.....	49
Figure 3-9. A participant's 6 average IHs, with IHs for 'stop' and 'go' trials of the same SSD overlapped to highlight effects of 'stopping.' Top to bottom: short, intermediate and long SSDs. Here, the greatest shift between 'stop' and 'go' levels is seen to occur for the intermediate SSD.	50
Figure 4-1. SST data used to track a participant's performance of the SST. Plots that did not track a horizontal line may have indicated 'slowing' (though this was not disqualifying).	57
Figure 4-2. GCSR plot for the EEG Experiment. (GCSR did not reach statistical significance). 59	
Figure 4-3. A GCSR plot in Shadli et al. [1] that appears similar to the one in the current study (in terms of frequency distribution and peak frequency). Source: Adapted from [1].....	61
Figure 4-4. Three-point-smoothed GCSR plot from the EEG Experiment in the current study. (Note: GCSR did not reach significance).	63

Figure 4-5. The right-ear data of the EVestG group yielded a GCSR ‘analogue’ with a tall peak at 110 ms (9 Hz). Vertical axes are the GCSR ‘analogue’ residual values (in $\log \mu V^2$ units) and the horizontal axes are ‘time’ bins (in milliseconds), centered at 125 ms (8Hz)..... 68

List of Abbreviations

5-HT	5-hydroxytryptamine (serotonin)
5-HT_{1A}R	5-hydroxytryptamine (serotonin) 1A receptor
BIS	Behavioural inhibition system
DR	Dorsal raphe
EEG	Electroencephalogram
EOG	Electrooculogram
EPM	Elevated plus maze
EVestG	Electrovestibulography
FP	Field potential
GABA	Gamma-Amino Butyric Acid
GAD	Generalized anxiety disorder
GCSR	Goal conflict specific rhythmicity
GO_RT	Median 'go' trial reaction time
hEOG	Horizontal electrooculogram
hTheta	The hippocampal theta rhythm
HPC	Hippocampus
iEEG	Intracranial electroencephalography
IH	Interval histogram
mPFC	Medial prefrontal cortex
NEER	Neural Event Extraction Routine
PFC	Prefrontal cortex
REM	Rapid eye movement

SPSS	Statistical Package for the Social Sciences
SSD	Stop signal delay
SSRT	Stop signal reaction time
SST	Stop signal task
vEOG	Vertical electrooculogram
VIP	Vasoactive intestinal peptide-expressing
VN	Vestibular nucleus

Chapter 1: Introduction

1.1 Motivation

In 2019, anxiety disorders were the second “most disabling mental disorders” and one of “the top 25 leading causes of burden” worldwide [2]. One of the difficulties with these disorders is that their diagnoses “[are] still based on clinical symptom checklists, not biological causes” and, as a result, “seldom [link] to specific effective treatments” [3]. Recently, it has been suggested that “biological markers could predict treatment efficacy better than current symptom-based diagnoses, greatly improving treatment outcomes and cost-effectiveness” [3]. However, existing technologies have yet to produce biomarkers that are sufficiently robust to be used in clinical settings [3]; therefore, new technologies should be developed.

One of the difficulties in identifying biological markers for anxiety disorders with currently available non-invasive technology is that some of the smallest, deepest regions of the brain are implicated in anxiety [4]. Functional magnetic resonance imaging can provide superior spatial resolution of neural activity among the anxiety-implicated subregions of the HPC, amygdala and prefrontal cortex (PFC). However, as this activity is measured indirectly (via changes in blood flow), the temporal resolution of functional magnetic resonance imaging is inadequate for monitoring the phasic interactions among these subregions that putatively underlie anxiety [4]. Conversely, EEG and magnetoencephalography *directly* record attenuated signals from these subregions at the scalp’s surface. However, isolating these signals from the greater activity that is picked up requires source localization which for small, deep brain regions is a complex process that is seldom attempted [4].

Typically, the goal when probing deep brain regions for anxiety research is to measure the activity of a putative human analogue of a brain rhythm that has been studied extensively in rodents and linked to behaviour that is suggestive of anxiety [4] (“anxiety-like behaviour” [5]). In rodents and other mammals, the ‘hippocampal theta rhythm’ originates in the HPC, as the name suggests; but despite the nomenclature, hTheta frequencies spans the cortical alpha and theta bands [6]. Driven by brainstem nuclei [6], this 4-12 Hz [3], 1-2 mV, behaviourally-modulated, nearly-sinusoidal rhythm is the largest normal extracellular synchronous signal in the brains of mammals [6]. Although its function is unclear (for a review, see [7]), results from rodent studies suggest that hTheta may synchronize local field potentials between regions and thereby time activity within

them so that “well-defined behavioural responses” can occur [5]. However, regardless of its function, hTheta seems to elicit anxiety-like behaviour in rodents under various experimental conditions [7-9]. Thus, recording its putative human analogue (‘hTheta-like rhythmicity’) could be useful for anxiety research.

Throughout the rodent midbrain, hTheta features prominently in extracellular EEG recordings [6]. However, intracranial electrodes are required to probe these areas [6]; thus, hTheta has been recorded and studied extensively in animals, but its putative human analogue has been seldom probed — and only in studies of individuals with epilepsy who were undergoing seizure monitoring [6]. These individuals have electrodes permanently implanted through their skulls (positioned according to their individual pathologies) that are typically used to record EEGs for diagnostic purposes, but that can also be used to deliver therapeutic electrical stimulation for treating seizures [4]. Despite many limitations that are inherent to hTheta-like rhythmicity research involving such individuals, much has been discovered from the few intracranial EEG (iEEG) studies that have been performed [4]. Critically, iEEG studies confirmed rhythmicity in the human HPC spanning the same hTheta frequency range (4-12 Hz) observed in rodent studies and further showed that these oscillations are similarly modulated by behaviour [10].

Although iEEG was critical for early hTheta-like rhythmicity research [10], it is evidently not suitable as a diagnostic tool for anxiety because permanently implanted transcranial electrodes are required; thus, a non-invasive means of performing recordings is clearly needed. Furthermore, despite the scientific gains that were made from studies of individuals with epilepsy, the use of iEEG as a research tool has several limitations: 1) enrollment can take a long time because only individuals with epilepsy are eligible [4]; 2) iEEGs are recorded from existing implant locations — which are heterogeneous within groups *and* may not be optimally situated for measuring hTheta-like rhythmicity — complicating analysis [4]; and 3) results may not be generalizable, since individuals with epilepsy have abnormal physiology and consequently produce data which can appear very different from that seen in healthy individuals [4]. Clearly, non-invasive technologies are needed to record hTheta-like rhythmicity, both in lab and clinical settings.

Evidence from previous studies suggests that EVestG has facilitated the identification of numerous possible biomarkers for several neurological disorders and diseases [11]. In some studies, EVestG has shown greater than 85% accuracy in discriminating patients from healthy

controls [11]. The EVestG technique involves recording signals from electrodes placed in the outer ear canals of participants who are seated in a hydraulic chair, which can be tilted to elicit a dynamic response from the vestibular system — the brain’s primary balance mechanism [11]. The ear drums are situated close enough to the vestibular peripheries to allow measurement of peripheral afferent signals, which are shaped in part by the spontaneously active efferent vestibular system, that is in turn modulated by the brainstem VN [11].

The brainstem VN is connected to three anxiety-implicated brainstem regions, namely the dorsal raphe (DR), locus coeruleus and parabrachial nucleus; which are in turn connected to the abovementioned HPC, amygdala and PFC that are implicated in anxiety *and* exhibit hTheta [12]. It is therefore possible that direct inputs to the VN from the brainstem regions or indirect signals from the HPC, amygdala and PFC may alter VN efferent activity, thereby causing perturbations in peripheral afferent activity which EVestG could detect. Importantly, anxiety and balance disorders can be comorbid; and some of the drugs used in anxiety management may also be effective in treating some balance disorders [12], suggesting that anxiety and balance share pathways, and that anxiety signals might therefore perturb activity in the VN.

There is, in fact, already evidence that hTheta-like rhythmicity modulates EVestG signals. Lithgow et al. [13] found that EVestG features can separate participants into major depressive disorder, bipolar disorder and control groups, suggesting that EVestG features may have been impacted by emotions — which may have included anxiety, as anxiety disorders are often observed comorbidly in individuals with major depressive disorder and bipolar disorder [14, 15]. Critically, some of these features were derived from the timing of FPs that EVestG detected, and seemed to have been caused by (~ 10 Hz) low-frequency modulation of FPs [13]. Therefore, this modulation seems consistent — in etiology and frequency — with hTheta-like rhythmicity. However, an experiment designed specifically to elicit this rhythmicity would be better suited to test whether it indeed modulates the FPs that EVestG detects. This thesis will investigate: whether ‘GCSR,’ the anxiety-process biomarker that is theorized to rely on hTheta-like rhythmicity and was previously discovered in the frontal EEGs of healthy volunteers during the anxiety-related SST (task) [16], can be replicated; and whether the same SST can produce an *analogue* of GCSR in EVestG data.

1.2 Objectives

The current study had two experiments: an ‘EEG Experiment’ and ‘EVestG Experiment,’ for which healthy participants (five and four, respectively) were recruited to carry out the SST. The ‘EEG Experiment’ was aimed at partially replicating “Experiment 2” of Shadli et al. [1] by reproducing GCSR (in frontal EEG power spectra); while the ‘EVestG Experiment’ — that was a novel experiment — was aimed at eliciting an analogue of GCSR (in vestibular FP firing patterns).

The specific goals were:

1) in the EEG Experiment, to replicate GCSR via the same methods that were employed in “Experiment 2” of Shadli et al. [1];

2) in the EVestG Experiment, to detect a GCSR ‘analogue’ in vestibular FP firing patterns, using a) the SST of Shadli et al. [1] to elicit this analogue, b) data recording and pre-processing techniques from previous EVestG studies [11, 13, 17] to obtain vestibular FP firing pattern data, and c) a novel data analysis technique to detect a GCSR ‘analogue’ in vestibular FP firing patterns;

3) in *both* experiments, to verify that the program that delivered the SST worked properly, by comparing statistics generated by the program (related to how participants performed the SST) to analogous statistics in Shadli et al. [1].

1.3 Results

1) The EEG Experiment did not yield GCSR. What this entails is that frontal EEG power was not increased for certain SST conditions which were designed to activate an anxiety process that is theorized to increase frontal EEG power by increasing hTheta-like rhythmicity.

2) The EVestG Experiment revealed a GCSR ‘analogue’ in vestibular FP firing patterns that was detected in the right ear EVestG data of participants. What this ‘analogue’ entails is that vestibular FPs occurred at a certain higher than average firing rate for certain conditions of the SST that were designed to activate an anxiety process mediated by hTheta-like rhythmicity.

3) Statistics of how participants performed the SST that were reported by the SST program, in both experiments, were found to be similar to analogous statistics reported in Shadli et al. [1], suggesting that the program functioned properly and created the conditions for GCSR in the EEG Experiment and a GCSR ‘analogue’ in the EVestG Experiment.

While the EEG Experiment did not yield GCSR, and therefore failed to replicate the results in Shadli et al. [1], it was determined that the experiment should (in the future) be repeated with a larger study population (more than the five who were included) of volunteers whose demographics should be more similar to those of volunteers in Shadli et al. [1]. Meanwhile, the GCSR ‘analogue’ that was identified in the EVestG Experiment may represent a novel anxiety process biomarker. As will be discussed, this analogue may entrain vestibular neurons more generally than in the SST — whenever humans are anxious — and might therefore represent a (general) anxiety biomarker. This biomarker may provide an objective measure of anxiety that could help clinicians diagnose anxiety disorders, as patients could be fitted with in-ear EVestG recording devices to measure their hTheta-like rhythmicity throughout their day, which could reveal the triggers of a patient’s anxiety or indicate the severity of their anxiety. However, the EVestG Experiment should be repeated with a larger number of participants (more than the four who participated) to further validate the results.

1.4 Outline

This chapter (Chapter 1) provides an introduction to the motivations, objectives and results of the study that is the focus of this thesis (“the current study”). Chapter 2 will review the literature on hTheta, sensory signals and anxiety, and posit that a human analogue of hTheta may modulate vestibular signals during periods of high anxiety and be non-invasively measurable with EVestG. Chapter 3 will outline the methods that were employed in the two experiments of the current study, including the SST (anxiety-related task) that was used in both experiments, the recording protocols for the experiments (frontal EEGs in the EEG Experiment and EVestG in the EVestG Experiment), the pre-processing and data analysis techniques that differed between experiments, and finally the statistical analyses (mostly repeated measures ANOVA polynomial contrasts) in both experiments. Chapter 4 will present the results that were obtained in the two experiments of the current study, that did not reveal GCSR in the EEG Experiment that aimed to partially replicate Shadli et al. [1], but did reveal an analogue of GCSR in the EVestG Experiment that was a novel experiment. Chapter 5 will provide a discussion of the results in both experiments, and offer explanations for why GCSR was not found in the EEG Experiment, before explaining that the GCSR ‘analogue’ that was identified may represent a novel anxiety process biomarker or general anxiety biomarker. Chapter 6 will present conclusions and limitations of the current study, then suggest future work.

Chapter 2: Background

2.1 Overview

This chapter will 1) review the hTheta literature as it relates to sensory signals and anxiety, 2) show that hTheta may modulate sensory signals amid anxiety; and 3) posit that such modulation of *vestibular* signals may be an anxiety biomarker that could be detected non-invasively in humans. To develop these ideas, a neural model for anxiety from rodent studies will first be summarized. It will then be shown that hTheta increases during anxiety-like behaviour, in mouse anxiety assays. Next, hTheta will be shown to be affected by *both* type I (movement) and type II (anxiety) effects; after which it will be revealed that hTheta transmitted to the PFC *causes* anxiety-like behaviour.

Results from human studies will then be reviewed, beginning with the first study to report rhythmicity analogous to rodent *type I* hTheta in humans. Then, the study that first evidenced a human analogue of rodent *type II* hTheta via double blind placebo controlled drug test will be summarized in more detail than the other studies in this chapter because 1) it essentially represents a culmination of the hTheta literature as it relates to anxiety, 2) it is a basis to look for other sites from which hTheta rhythmicity can be detected in humans, and 3) the task it employed was adapted for the current study. Next, research involving newer versions of the above task will be reviewed.

Turning again to rodent studies, it will be revealed that hTheta occurs during high arousal (and likely anxiety) and in so doing seems to alter sensory signals. Several lines of evidence will then be presented which together suggest that *vestibular* signals likely receive hTheta modulation, and that analogous modulation in humans would represent a novel anxiety process biomarker that could be measured non-invasively.

2.2 What is Anxiety?

Calhoun and Tye [5] suggest that “anxiety represents a state of high arousal and negative valence and results in enhanced vigilance in the absence of an immediate threat.” Importantly, the term “anxiety” (when it is unmodified, as in the above definition) refers to an emotional or behavioural *state* and is synonymous with “state anxiety” [5]. State anxiety level can vary from one moment to the next; however, “trait anxiety,” which refers to an individual’s *propensity* to experience anxiety [18] or “sensitivity to threat” [18, 19], is stable over time. Individuals with sufficiently high trait anxiety are often diagnosed with an anxiety disorder such as generalized

anxiety disorder (GAD) [19]. According to “The Diagnostic and Statistical Manual of Mental Disorders” 5th edition, the diagnostic criteria for GAD include: “the presence of excessive anxiety and worry about a variety of topics, events, or activities” [20]. Therefore, anxiety is an emotional or behavioural *state*; while ‘trait anxiety’ relates to how often or how easily this state occurs; and if it occurs too often or too easily, then this may indicate GAD. Finally, it is important to highlight that anxiety is normally a healthy function that is essential for survival [5] — it is only pathological if it is persistent and there is significant difficulty controlling it [20].

To understand how anxiety disorders might occur, it may be useful to have a concept of how anxiety could operate at the neural level. From insights gained through optogenetics research on mice, researchers at the Massachusetts Institute of Technology developed a model for anxiety in which circuits that arise from networks of neurons, distributed among several specific brain regions, process stimuli to determine response [5]. The model describes four stages, namely ‘detection,’ ‘interpretation,’ ‘evaluation,’ and ‘response’ circuits, which process stimuli and, if the environment is deemed sufficiently risky, drive an anxiety-like response [5]. The *detection* stage implicates the sensory systems and thalamus that first process stimuli before sending information forward to the amygdala, bed nucleus of the stria terminalis, ventral HPC (vHPC) and medial PFC (mPFC) to be *interpreted* [5]. These “interpretation” regions then cause their downstream effector *response* circuits, namely the hypothalamus, brainstem nuclei and motor cortex, to trigger the observable effects of anxiety (e.g., increases in glucocorticoid circulation, heart rate and risk avoidance, respectively) [5]. Finally, information travels backward from the mPFC and vHPC to the bed nucleus of the stria terminalis and amygdala which *evaluate* interpretation and “prevent unchecked activation of pro-anxiety circuits” [5]. Critically, *threat* is interpreted if more basolateral amygdala neuronal populations are recruited by projections of circuits pushing for defensive behaviour than by projections of circuits pushing for exploration [5].

Calhoun and Tye [5] suggest that anxiety disorders could arise from disturbances occurring *anywhere* within the circuits of their model (that was described, above), because any of these disturbances may upset the equilibrium of the whole network and thereby cause neutral stimuli to be habitually misinterpreted as threatening. Interestingly, serotonin (5-HT) 1A receptor knockout mice — a mouse model of high trait anxiety — lack the 5-HT 1A receptor (5-HT_{1AR}) that is normally expressed in large concentrations among the brain regions that were described above [5,

21], demonstrating that a single perturbation within these regions indeed seems capable of producing a feature that resembles pathological anxiety. As discussed in the following section, anxiety-like behaviour and hTheta are both hyperactive in 5-HT_{1AR} knockout mice [21].

2.3 Anxiety-Like Behaviour is Linked to hTheta.

Lesion and inactivation studies have shown that the vHPC is necessary for mice to exhibit anxiety-like behaviour in free-roaming assays that model anxiety [21-23]. Based on this knowledge, Adhikari et al. [21] attempted to identify a mechanism involving the vHPC that could play a role in causing anxiety-inducing ('anxiogenic') effects in rodents. The authors placed mice in an elevated plus maze (EPM) and an open field (which are anxiogenic arenas) as well as an anxiety-reducing ('anxiolytic') familiar arena and recorded EEG signals intracranially from the vHPC and mPFC [21].

The authors found that mPFC and vHPC hTheta were increased in the anxiogenic arenas compared to the familiar one [21]. Local field potential traces showed prominent hTheta for mice in the EPM and open field, but not for mice in the familiar arena (Figure 2-1, top) — where the other mode of the HPC, large irregular activity [6], occurred; and power spectra revealed large peaks at 8 Hz in the anxiogenic arenas, but no 4-12 Hz peaks in the familiar one (Figure 2-1, bottom) [21]. These results were found to be robust from the first day of exposure to the familiar arena; thus, novelty could not explain them [21]. While vHPC hTheta power was increased *throughout* the EPM and open field, mPFC hTheta power was high only in the anxiogenic zones of these arenas [21]. Therefore, vHPC hTheta predicted when mice were in an anxiogenic arena; while mPFC hTheta predicted when mice were in an anxiogenic *zone*, within a given arena.

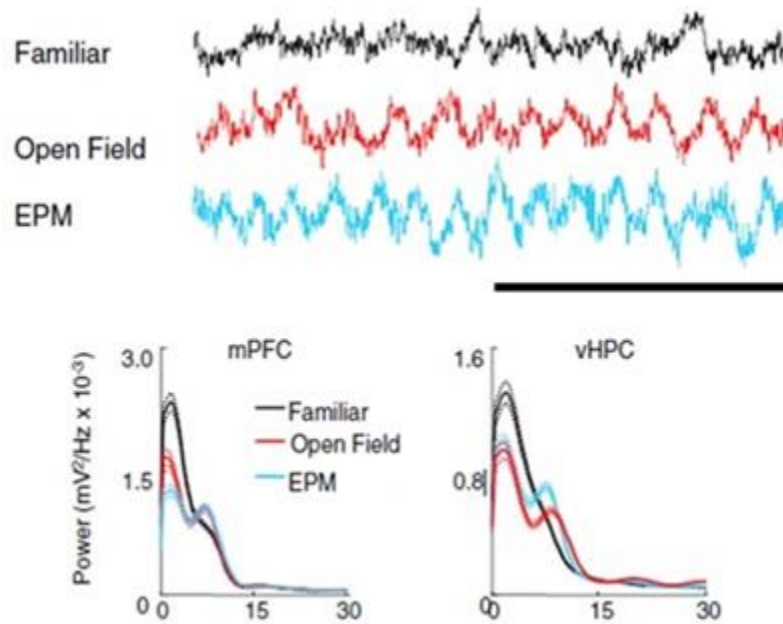


Figure 2-1. mPFC and vHPC hTheta power increased in the EPM and open field anxiety assays. (Top) Local field potential traces for the mPFC (hTheta is visible for the EPM and open field). (Bottom) Power spectra for the mPFC and vHPC had 7 Hz peaks in the EPM and open field.

Source: Adapted from [21].

vHPC-mPFC hTheta power coherence was also increased specifically in the safe zones of the EPM and open field, and it was found that mice tended to exit the safe zones of the EPM and open field 2-3 seconds after coherence decreased (Figure 2-2a) and re-entered 2-3 seconds after it increased again (Figure 2-2b) [21]. As neither locomotion nor position changed with coherence, Adhikari et al. [21] suggested that coherence does not relate to movement — but instead inhibits exploratory behaviour. Additionally, the authors discovered that both anxiety-like behaviour and coherence were highest in 5-HT_{1A}R knockout mice [21]. Together, the above results suggest that anxiety-like behaviour is linked to vHPC-mPFC hTheta power coherence.

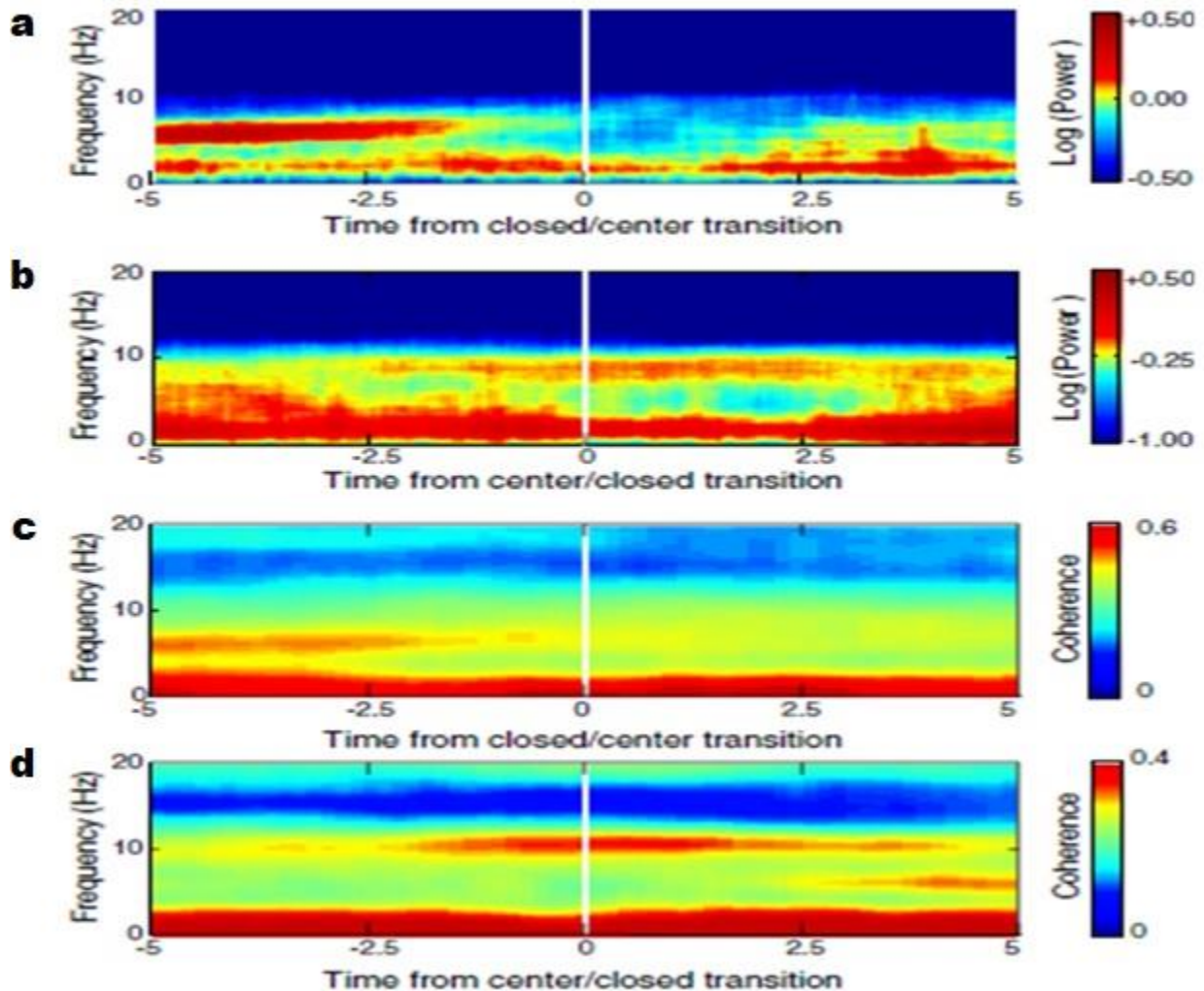


Figure 2-2. *mPFC hTheta power inhibits exploratory behaviour. Averaged spectrograms of mPFC power (a, b) and vHPC-mPFC coherence (c, d), centered at times when mice transitioned to (b, d) and from (a, c) safe (i.e., closed) arms of the EPM. Source: Adapted from [21].*

Based on the above findings — which showed that hTheta power coherence between the vHPC and mPFC was associated with anxiety-like behaviour, and that vHPC hTheta power predicted when mice were in an anxiogenic arena [21] — analogous activity in brain regions homologous to these could predict anxiety, if a human analogue of rodent hTheta exists. As will be reviewed in section 2.6, Ekstrom et al. [10] found behaviourally-modulated 4-12 Hz oscillations in the human HPC; and McNaughton et al. [16] developed an anxiety process biomarker that seems to be caused by a human analogue of (4-12 Hz) vHPC-mPFC hTheta power coherence.

2.4 Type I & II hTheta are Independent.

It is important to note that movement modulates hTheta and can therefore confound results (Figure 2-3) [10, 21]. Critically, there are putatively two types of hTheta [24, 25]: type I is *atropine-resistant* and occurs during movement, perceived movement and rapid eye movement (REM) sleep [7, 24]; while type II is *eliminated by atropine* and can occur without movement [7, 25]. Type II occurs when animals freeze in the presence of a predator [7]; therefore, type II is the type of interest to anxiety research. Importantly, it has been shown that mechanisms for type I and type II can be active at the same time, in which case they produce an “overall hTheta frequency” [7]. In the study that was reviewed in the previous section, Adhikari et al. [21] controlled for the effects of movement (on hTheta) by comparing data that were recorded at similar running speeds.

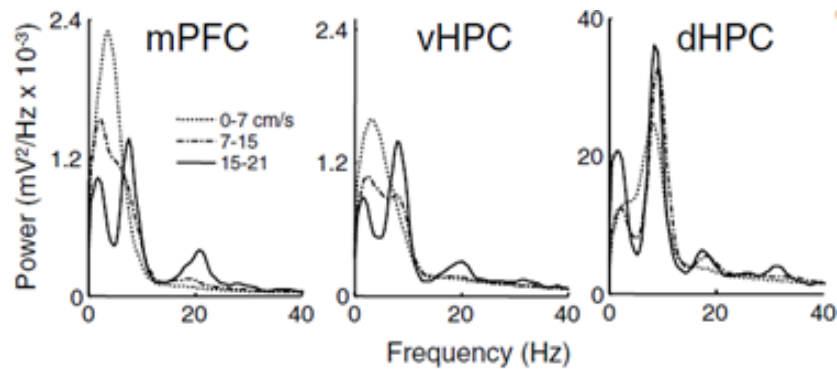


Figure 2-3. hTheta power increases with movement speed. The dotted, dashed, and solid lines represent slow, moderate, and fast movement, respectively. Source: Adapted from [21].

While it is known that type I and type II mechanisms *both* impact overall hTheta frequency, whether these mechanisms are independent has been a matter of debate [7]. In their review of studies that collectively illustrate the “dual functionality” of hTheta, Korotkova et al. [7] describe a model for the relationship of overall hTheta frequency to type I and II in rodent anxiety assays, such as the EPM and open field. The model describes a linear relationship between the overall hTheta frequency (the outcome variable) and the running speed of an animal (the independent variable), where novelty of the environment modulates the slope of the function, and type II hTheta mechanisms determine the intercept [7]. To test this model, Wells et al. [26] predicted that giving mice an anxiolytic drug would lower the intercept without affecting the slope. This prediction was based on the idea that type II hTheta relates to anxiety (which was discussed) and the findings of McNaughton et al. [27], who had studied the results of “the anxiolytic drug test” (for a review, see

[27])¹ for every drug that had been tested and reported that 1) those drugs which were clinically effective at treating GAD *also* lowered the frequency of hTheta elicited by electrical stimulation of the brainstem reticular formation, and 2) those that were not clinically effective at treating GAD (including *those* antipsychotics and sedatives which are not anxiolytic) lacked this effect — with no false positives or false negatives having been found [7, 27].^{2,3} The prediction by Wells et al. [26] has since been validated, as all four anxiolytic drugs with diverse primary targets they tested reduced the type II effects (i.e., intercept) on overall hTheta frequency *without* affecting the rate at which overall hTheta frequency changes with running speed (i.e., slope) [7]. Furthermore, Wells et al. [26] also demonstrated the converse, namely that novelty lowers the rate of change (i.e., slope) without impacting type II effects (i.e., intercept) on overall hTheta frequency [7]. Together, the above results suggest that type I and type II hTheta mechanisms do not interfere with each other and therefore independently modulate the single overall frequency⁴ that hTheta exhibits [7].

¹ In the anxiolytic drug test, a rodent is kept immobile (either by anaesthetising or manually handling the animal) and the reticular formation of the rodent is electrically stimulated via intracranial electrodes, which artificially generates hTheta in the rodent HPC [27]. Increasing the amount of stimulation has been shown to increase the frequency of reticular formation-elicited hTheta [27]. However, anxiolytic drugs have been shown to lower this increase in hTheta frequency [27]. This method of testing a drug's ability to lower the frequency of hTheta generated by reticular formation stimulation is called "the anxiolytic drug test" [27].

² This process of artificially generating hTheta by electrically stimulating the reticular formation and testing a drug's ability to lower the frequency of this hTheta presents a challenge because animals must remain motionless, otherwise movement (that elicits type I hTheta, as was discussed) will confound results. To prevent subjects from moving, they can be anaesthetised; however, caution must be used as anaesthetics alter hTheta production (albeit in a predictable way that can be corrected for, during analysis [27]). Alternatively, animals can be awake; however, in this case it is necessary to manually handle them to keep them from moving — and even the slightest movement causes type I hTheta, confounding results [27].

³ While anxiolytics lower hTheta (when it is elicited by the anxiolytic drug test), and hTheta is linked to anxiety-like behaviour, single-dose administrations of novel anxiolytics seem to reduce anxiety-like behaviour only in certain anxiety assays such as the Morris Water Maze, where it is believed that corticosterone — which has anxiogenic effects and is released by these drugs but is blocked by classical anxiolytics — does not interfere in these tests [27].

⁴ Korotkova et al. [7] highlight that this single overall frequency for hTheta is at odds with a strict interpretation of the most popular dual functionality theory — that the dorsolateral HPC and vHPC separately control cognition and emotion, respectively [7]. However, they confirm that in terms of frequency the HPC does exhibit "a single travelling [hTheta] wave," but add that amplitude varies, and phase systematically changes, from dorsal to ventral aspects of the HPC [27]. Regardless of how type I and type II effects separately impact the single travelling hTheta wave, Korotkova et al. [27] indicate that the above results could one day lead to quantitative measures of cognition and emotion. Interestingly, quantitative measures would make it possible to subtract the effects of movement from overall hTheta frequency, leaving only the desired type II effects, which would improve upon current methods of controlling for movement, such as: 1) either skillfully keeping animals still but awake or fully anaesthetizing them, when testing a drug's ability to lower the frequency of reticular formation-elicited hTheta in the anxiolytic drug test [27]; or 2) specifying a range of speeds over which the variable effects of movement will be ignored, as in the Adhikari et al. [21] EPM and open field experiments (reviewed in the previous section).

2.5 Anxiety-Like Behaviour is Caused by hTheta.

As was reviewed in section 2.3, Adhikari et al. [21] *linked* anxiety-like behaviour and hTheta, though the direction of causality between the two remained unclear. Recently, however, two optogenetics studies that examined mice in the EPM and applied phasic light stimulation (albeit on different neuronal populations) revealed that technicians could strongly influence rodent behaviour in an anxiogenic or anxiolytic way, either by 1) *activating* vHPC terminals in the mPFC via 8-Hz light input [9] or 2) *inhibiting* vasoactive intestinal peptide-expressing (VIP) interneurons that gate mPFC hTheta input from the vHPC [8], respectively.

Padilla-Coreano et al. [9] showed that stimulating vHPC neuron terminals in the mPFC using light that oscillated sinusoidally in intensity at 8 Hz *increased* anxiety-like behaviour, while stimulation delivered outside the hTheta frequency range (at 2 or 20 Hz) lacked this effect. Critically, this stimulation also increased vHPC-mPFC neural transmission as well as entrained vHPC hTheta and spiking of mPFC neurons to the 8 Hz optical stimulation, thereby synchronizing vHPC hTheta and mPFC spiking. Interestingly, the degree of synchrony between stimulation and mPFC spiking was higher in the EPM (relative to a familiar arena) and highest in its (anxiogenic) open arms; while synchrony between mPFC spiking and vHPC hTheta was primarily increased in the open arms [9]. This led Padilla-Coreano et al. [9] to hypothesize that this dependency of synchrony on location related to the behaviour of VIP interneurons that Lee et al. [8] had previously shown were responsible for gating mPFC hTheta from the vHPC.

Lee et al. [8] reported that *activating* the abovementioned interneurons when mice were in the centre of the EPM (where mice had equal opportunity to enter either the open or closed arms) caused the cells to *disinhibit* vHPC-mPFC hTheta transmission and *increased* open arm avoidance; while *inhibiting* the cells *blocked* this transmission and *decreased* avoidance of the open arms, showing that the interneurons gate vHPC-mPFC hTheta transmission and thereby sway behaviour in an anxiogenic or anxiolytic way. The authors also found that when not applying stimulation, VIP interneuron activity predicted avoidance of the open arms *and* was increased within them [8]. This led Lee et al. [8] to conclude that these VIP interneurons gate mPFC hTheta transmission from the vHPC, which the mPFC uses to form “representations” of information relevant to anxiety. Together, the results that were reviewed in this section reveal a *causal* role for vHPC-mPFC hTheta transmission on anxiety-like behaviour and therefore extend the findings of Adhikari et al. [21],

who had established that anxiety-like behaviour and vHPC-mPFC hTheta transmission are linked (as was reviewed in section 2.3).

2.6 Anxiety is Linked to hTheta-Like Rhythmicity.

An important question for anxiety research is whether a human analogue of rodent hTheta (hTheta-like rhythmicity) exists. As was mentioned in Chapter 1, EEG recordings of HPC activity in individuals with epilepsy who were undergoing seizure monitoring have been performed via intracranial electrodes with the goal of measuring hTheta-like rhythmicity in humans on a few occasions. In one such study of particular importance, Ekstrom et al. [10] recorded signals from the HPC proper while patients navigated a virtual environment on a computer screen. Intriguingly, EEG data revealed prominent activity within the hTheta range that is seen in rodents (Figure 2-4) [10]. As was observed in the rodent studies discussed in previous sections, signals increased in power and frequency with movement speed [10]. Ekstrom et al. [10] declared that this was the first demonstration of behaviourally-modulated 4-7 Hz oscillations in the human HPC, and noted that while the study had focused on identifying rhythmicity within the traditional theta range, “broadening the theta band to include frequencies classically analyzed in the rat [did] not affect [their] overall findings” (where 8-9 Hz power was most robust in some tasks; Figure 2-4f). These results thus seem to reveal a human analogue of rodent hTheta (‘hTheta-like rhythmicity’); however, since the task involved movement, type I mechanisms are implicated;⁵ suggesting that it should be determined whether this rhythmicity is also caused by type II mechanisms because it would be this ‘type II hTheta-like rhythmicity’ that could represent an anxiety process biomarker.⁶ (Notably, patients in the above study may have experienced anxiety that could have contributed to 4-12 Hz rhythmicity; however, results from rodent studies in prior sections suggest that movement would have confounded results, making it difficult to assess anxiety based on 4-12 Hz activity).

⁵ Both real and virtual movement have been shown to elicit type I hTheta in rodents as well as the human analogue of this hTheta (“type I hTheta-like rhythmicity”) in humans [10].

⁶ Section 2.3 showed that vHPC hTheta power predicted when mice were in an anxiogenic arena; and section 2.5 revealed a causal role for vHPC-mPFC hTheta transmission on anxiety-like behaviour.

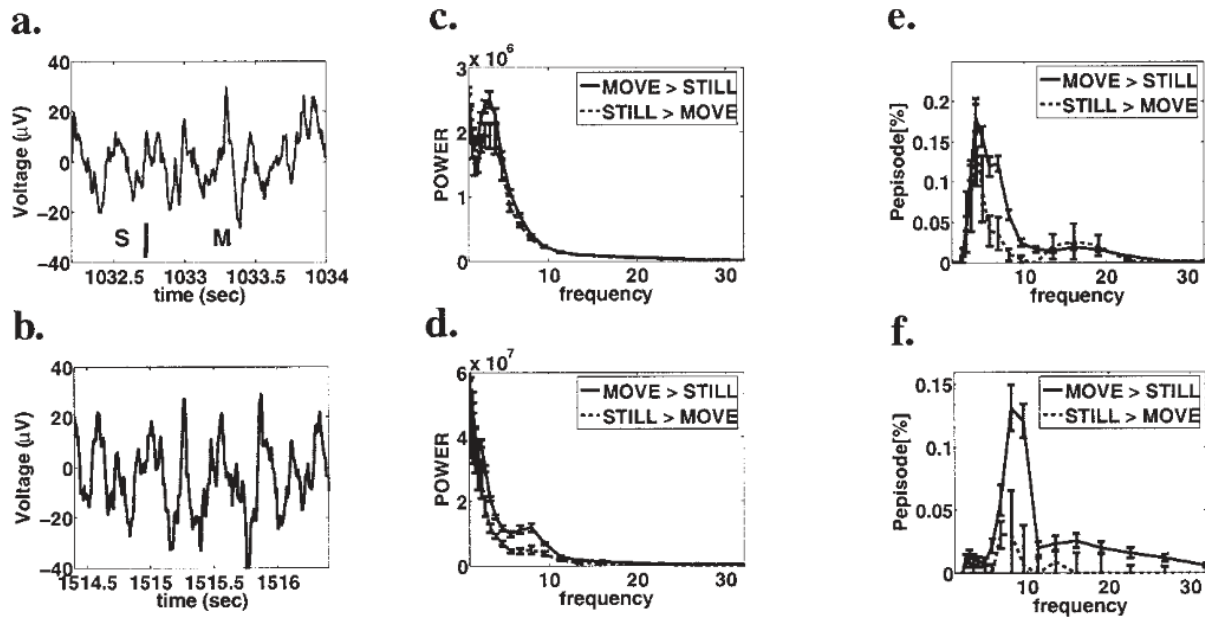


Figure 2-4. 4-12 Hz EEG activity via depth recording in the human HPC amid virtual movement. (a) Raw trace while subject was still, S, then moving, M; (b) raw trace during virtual movement; (c, d) power spectra during virtual movement tasks; (e, f) “percentage of time in oscillatory episode [during virtual movement tasks],” determined by “time filled with detected oscillatory episodes divided by the total time in the segment of interest” [10]. Source: Adapted from [10].

As reviewed in the previous three sections, Adhikari et al. [21] found that vHPC-mPFC hTheta transmission and anxiety-like behaviour were linked; after which Padilla-Coreano et al. [9] and Lee et al. [8] showed that this transmission of hTheta to the mPFC in fact *causes* anxiety-like behaviour. If this causal relationship that Padilla-Coreano et al. [9] and Lee et al. [8] demonstrated in rodents has a human analogue, then transmission between homologous regions may predict anxiety in humans. Furthermore, it might be possible to detect these transmissions in healthy participants because EEGs from the PFC (recipient of the transmissions) can be measured with surface electrodes [28], eliminating the need to recruit individuals with epilepsy who are undergoing seizure monitoring. Therefore, it might be possible to detect transmissions analogous to those which cause anxiety-like behaviour in rodents [8, 9] in EEG data recorded from humans via surface electrodes.

Based on results similar to those that were reviewed in previous sections, albeit that linked mPFC hTheta transmission from the *dorsal* rather than the ventral HPC⁷ to anxiety-like behaviour [29], McNaughton et al. [16] realized that a human analogue of this transmission (from the HPC to the PFC, more generally; “HPC-PFC hTheta-like transmission”) would entrain hTheta-like rhythmicity in the PFC that could be measured with surface electrodes and therefore designed an experiment to elicit this rhythmicity in healthy participants whose frontal EEGs they planned to record non-invasively. Furthermore, the authors developed the experiment into a double-blind, placebo-controlled drug study, in which thirty-four (34) participants would be randomly assigned to one of three groups that would each receive one of the following three treatments prior to testing: 0.25 mg of triazolam, 10 mg of buspirone, or a placebo [16]. Based on a ‘behavioural inhibition system’ (BIS) theory that they developed in rodents, McNaughton et al. [16] predicted that the drug groups would exhibit reduced hTheta-like rhythmicity during the experiment.⁸

McNaughton et al. [16] describe the BIS in rodents as necessary for anxiety (defined as defensive approach) and unrelated to fear (defined as simple defensive avoidance) which depends instead on the fight, flight, freeze system. ‘Goal conflict’ is said to activate the BIS when simultaneous goals that are incongruent vie for control of behaviour, to which the system responds by initiating ‘goal-conflict resolution’ that is mediated by repeated HPC-PFC hTheta waves [28]. “The BIS is defined originally by the effects of anxiolytic drugs” on the structures that support it (Neil McNaughton, personal communication, 8 July 2021), namely the amygdala, medial septum, HPC, medial hypothalamus, periaqueductal gray, posterior cingulate, and prefrontal dorsal stream [16]. Vitaly, hTheta has been found in each of these structures [16]; and McNaughton et al. [16] hypothesize that anxiolytics decrease BIS function and goal conflict resolution by reducing hTheta.

At the centre of the experiment that McNaughton et al. [16] conducted was their Stop Signal Task (SST). The SST is delivered by a computer program, and is designed to elicit varying degrees of goal conflict (at various stages of the task) by assigning to participants simultaneous,

⁷ As discussed, Korotkova et al. [7] suggested that the HPC exhibits a single hTheta frequency, and that the dorsal HPC and vHPC only differ in phase (systematically) and amplitude; thus, it is unsurprising that Adhikari et al. [21] and Young & McNaughton [29] were able to link anxiety-like behaviour and hTheta transmission to the mPFC from different HPC subregions.

⁸ McNaughton et al. [27] had reviewed all drugs that were subjected to the “anxiolytic drug test” and found that those which are used to treat GAD reduced the frequency of reticular formation-elicited hTheta, while those which are not lacked this effect — with no false positives or false negatives having been found (for a review, see [27]).

incompatible goals, which are meant to create maximal goal conflict when brought into maximal temporal alignment [16]. The goals involved are called ‘going’ and ‘stopping,’ and the SST informs participants which goal to pursue by respectively displaying an arrow (a ‘go signal’) on a computer monitor or playing an audible tone (the ‘stop signal’) via headphones [16]. During ‘go trials’, the SST merely issues a ‘go’ signal (a left or right arrow displayed on the monitor, the direction indicating the mouse button to click); while ‘stop trials’ at first issue a ‘go’ signal, before next — after a variable ‘stop signal delay’ (SSD) — issuing the ‘stop’ signal (informing participants not to click) and, in theory, producing goal conflict [16].

The SST consists of 128 consecutive (~3-second) trials: 32 ‘stop’ and 96 ‘go’ trials that are randomly ordered, where each ‘stop’ trial and its ‘paired go trial’ (the ‘go’ trial that immediately precedes the ‘stop’ trial) are analyzed in ‘trial pairs’ [16]. During ‘stop’ trials, a ‘go’ signal (arrow) is first issued to activate circuits in the brain that promote ‘going’ (clicking), before the ‘stop’ signal (tone) is then issued to activate circuits which promote ‘stopping’ (not clicking), thus forcing these circuits to compete to determine whether clicking occurs. McNaughton et al. [16] state that the amount of delay determines the temporal alignment of the two goals (‘stopping’ and ‘going’) and therefore the amount of resulting goal conflict (which is high when alignment is high). Variability in this alignment is introduced by random assignment of either a short, intermediate, or long delay to ‘stop’ trials [16]. To maintain correct alignment, the values for these SSDs are adjusted throughout the task to ensure success rates of ~ 20, 50, and 80% in ‘stop’ trials for ‘short,’ ‘intermediate,’ and ‘long’ SSDs, respectively — where a successful ‘stop’ trial is defined as one in which a participant withholds clicking [16]. The variable values of the ‘short,’ ‘intermediate’ and ‘long’ SSDs are also called ‘short,’ ‘intermediate’ and ‘long’ “staircases,” respectively [16].

The intermediate SSD is believed to *maximally align* the opposite ‘going’ and ‘stopping’ goals temporally because it causes participants to click in about half of all ‘stop’ trials to which it is assigned and to *not* click in the other half [16]. Assuming ‘going’ and ‘stopping’ function independently, as in the ‘horse race model’ [28, 30], such maximal temporal alignment of opposite goals is predicted by BIS theory to elicit maximal goal conflict in the ‘stop’ trials with intermediate SSDs (‘intermediate stop trials’); while less goal conflict is predicted in ‘stop’ trials with short (‘short stop trials’) or long SSDs (‘long stop trials’) since temporal alignment of opposite goals is decreased in them; and no goal conflict is predicted in each of their ‘paired go trials’ (with which

they respectively form ‘intermediate,’ ‘short,’ and ‘long SSD trial pairs’) because goal conflict requires more than one goal [16].

Since the BIS is theorized to be activated in proportion to level of goal conflict, and BIS activation entails goal conflict resolution that is mediated by HPC-PFC hTheta-like transmission, McNaughton et al. [16] believed that maximal HPC-PFC hTheta-like transmission would occur during ‘intermediate’ as opposed to ‘short’ or ‘long’ stop trials. Specifically, the authors hypothesized that (stop – go) differences in 4-12 Hz frontal EEG power between ‘trial pairs’ would be significantly larger for ‘intermediate’ SSD trial pairs than for the average of ‘short’ and ‘long’ SSD trial pairs — the contrast that is referred to as ‘GCSR’ [16]. McNaughton et al. [16] therefore predicted that GCSR would be identified in the placebo group, however not in the drug groups (where it was expected that the anxiolytics would sufficiently reduce BIS activity, and therefore goal conflict resolution via HPC-PFC hTheta-like rhythmicity, to prevent increased 4-12 Hz frontal EEG power from the intermediate ‘stop’ trials).

To determine whether their prediction was correct, McNaughton et al. [16] used repeated measures ANOVA to look for differences in 4-12 Hz frontal EEG power between trial conditions that would indicate the presence of GCSR and included ‘type’ and ‘SSD’ as repeated measures factors, where ‘type’ could either be ‘stop’ or ‘go,’ and the levels for ‘SSD’ (from lowest to highest) were ‘short,’ ‘intermediate,’ and ‘long.’ The authors predicted that 4-12 Hz EEG power would go from low, to high, to low, as SSD went from short, to intermediate, to long, and therefore used a within-subjects *quadratic* contrast to look for this pattern [16]. Additionally, McNaughton et al. [16] included a *linear* contrast for ‘type’ (‘stop’ or ‘go’) to isolate the effect of the ‘stop signal’ (Neil McNaughton, personal communication, 12 July 2021) because ‘stop’ trials contain the ‘stop’ signal but are otherwise identical to ‘go’ trials; and the difference in EEG power between a ‘stop’ and its ‘paired go trial’ should only include the effect of the stop signal. Therefore, the authors examined the overall within-subjects ‘type’ x ‘SSD’ interaction (linear x quadratic) — which if statistically significant ($p < 0.05$) would confirm GCSR [16].⁹

⁹ Mathematically, the contrast can be performed via the following steps: 1) EEG power spectra for ‘paired go’ trials are subtracted from their associated ‘stop’ trials, 2) the resulting differences are averaged for each SSD (short, intermediate, and long), and 3) the contrast is then the intermediate average minus the average of the short and long averages [31].

As they had predicted, McNaughton et al. [16] found GCSR only in the placebo group, which showed significantly higher EEG power at the frontal F4, Fz and F8 sites in the intermediate (compared to the short and long) SSD trials, specifically within the frequency range of 9-10 Hz. This effect was reduced at F8 “(Stop–Go x SSD x frequency x channel x group, dev x quadratic x cubic x quartic, $F(2,30) = 9.75$, $P < 0.001$);” and similar reductions occurred at the Fz and F4 sites, in the drug groups — one of which received buspirone, with activity at 5-HT_{1a} receptors, and the other was given triazolam, which interacts with gamma-aminobutyric acid (GABA)_a receptors — suggesting that these drugs, despite their diverse primary targets and side effects, blocked GCSR as had been predicted [16].

The above results therefore suggest that GCSR is a biomarker [16]; while the (BIS) theory that accurately predicted GCSR implies that this possible biomarker should be caused by a human analogue of rodent hTheta transmission from the HPC to the PFC [16], which furthermore seems to be caused by type II hTheta mechanisms, because: 1) the SST was designed to engage the anxiety-mediating circuits of the BIS [16]; 2) movement, which is linked to type I effects [7], was not involved [16]; and 3) Wells et al. [26] have shown that anxiolytic drugs specifically reduce type II effects on overall hTheta (as was reviewed in section 2.4). The results of McNaughton et al. [16] therefore suggest that GCSR is an anxiety process biomarker that is caused by a human analogue of rodent HPC-PFC type II hTheta transmission; and, as McNaughton et al. [16] declare, their results reveal “a distinct rhythmic system in humans that is sensitive to both classical/GABAergic and novel/serotonergic anxiolytics.”

In a later study that aimed to expand on the above results of McNaughton et al. [16], Shadli et al. [31] further developed GCSR as a potential novel biomarker in two ways: 1) by showing that it was lowered by pregabalin — an anxiolytic drug that, unlike buspirone and triazolam, acts on calcium channels — further linking it to rodent hTheta (which is known to be lowered by all three drugs), and 2) by achieving greater GCSR over a wider range of hTheta frequencies in their own experiment (which Shadli et al. [31] attributed to improvements they had made to the SST). Additionally, a more recent Shadli et al. [1] study tested a modified version of the SST that used a visual cue (an exclamation mark) as the ‘stop signal’ instead of the auditory stimulus (an audible tone); and, as with previous studies [16, 31], GCSR was identified in the control group, but not in

the (triazolam and buspirone) drug groups (which was hypothesized), further validating GCSR as an anxiety process biomarker and illustrating the translatability of the ‘stop signal’ [1].

The above studies [1, 16, 31] provide strong evidence for a human analogue of rodent type II hTheta because they all accurately predicted (based on a theory developed from rodent studies; for a review, see [3]) that: 1) 4-12 Hz behaviourally modulated rhythmicity would be elicited in a specific brain region *only* if a stimulus was presented at a very precise time, and 2) this rhythmicity would be lowered by multiple chemically distinct anxiolytic drugs with diverse primary targets and side effects. This 4-12 Hz rhythmicity was therefore consistent both in etiology and frequency with rodent type II hTheta *and* was reduced by all three anxiolytic drugs that were selected for the above experiments because of their previously demonstrated ability to lower hTheta in rodents [3].

Together, the results that were reviewed in this section — from the first three studies that aimed to produce GCSR and lower it with anxiolytic drugs — suggest that GCSR is an anxiety process biomarker, caused by a human analogue of rodent HPC-PFC hTheta transmission [3]; and the findings from Wells et al. [26] indicate that this hTheta is caused by type II effects because it was reduced by anxiolytic drugs [26]. In summary, humans appear to exhibit behaviourally-modulated, anxiolytic-sensitive, 4-12 Hz EEG rhythmicity that is elicited by anxiety-related tasks [3] — and therefore analogous to the hTheta that has been reported in rodent anxiety assays [7].

2.7 hTheta Modulates Auditory Signals.

The anxiety process biomarker ‘GCSR’ that McNaughton et al. [16], Shadli et al. [31] and Shadli et al. [1] developed (as reviewed in the above section) might soon provide clinicians with objective data that could assist them in diagnosing some anxiety-related issues, as researchers in New Zealand have been testing whether GCSR can predict treatment response “better than current symptom-based diagnoses [because if it can], this would validate the first human biological marker for a theoretically-defined ‘anxiety’ *syndrome*” [3]. Critically, GCSR would not classify *all* illnesses related to anxiety, as it seems to be a biomarker of “one specific anxiety process” (i.e., goal-conflict resolution) [31] that causes emotional or behavioural traits which *today* end up “diagnosed as some type of anxiety disorder” when there is “hyperreactivity (hypersensitivity to input)” in this process [3]. Nevertheless, GCSR appears to be caused by a human analogue of rodent hTheta (as discussed in the above section); and since rodent hTheta occurs in multiple brain regions where it is linked to anxiety-like behaviour (as was reviewed in this chapter), this apparent

human analogue could provide additional anxiety process biomarkers in brain regions other than the PFC (where GCSR was found). As will be discussed, hTheta seems to modulate the spiking activity of auditory neurons in rodents *when they are aroused* [32], suggesting that analogous modulation in humans should be a biomarker of arousal — as well as anxiety, because anxiety is “arousal with negative valence” (as was reviewed in section 2.2) [5].

Studies have shown that when a stationary animal is presented with a stimulus, it will often exhibit hTheta in the HPC that is sensitive to atropine [33], leading some to suspect that type II hTheta is a sign of HPC involvement in sensory processing [7, 25, 32, 34, 35]. Critically, some stimuli (e.g., an audible tone) only elicit hTheta if another stimulus that on its own produces hTheta (e.g., an owl sound) or one that does not itself cause hTheta but seems to “prime” the animal for it (e.g., a cat odour) is presented first [25], suggesting that whether hTheta occurs depends on the animal’s “internal state” [34] — specifically its level of arousal (which if sufficiently high leads to type II hTheta being elicited by stimuli [25]). Furthermore, Liberman et al. [32] showed that hTheta seems to *time* activity outside the HPC because auditory neurons in the inferior colliculus central nucleus phase locked to the rhythm, which arose for several seconds when guinea pigs were exposed to changes in auditory stimulation. This suggests that hTheta modulates auditory signals, which is plausible because they are known to be shaped not only by sound, but also by the central nervous system — which maintains constant control of auditory processing, including within the inferior colliculus central nucleus where it modifies the frequency and pattern of neuronal spiking between behavioural states [32, 36].

While its function when it arises in the HPC during periods of increased arousal is unclear, Liberman et al. [32] state that hTheta “may affect the excitability of distant neurons by inducing membrane potential oscillations” and thereby provide “temporal coding” for auditory information. However, regardless of the function that hTheta may serve if it indeed affects auditory processing, the above results suggest that a human analogue of this modulation could be a biomarker of arousal — and anxiety (since this is “arousal with negative valence” [5]). As discussed in the next section, hTheta might similarly modulate vestibular signals; and if peripheral neurons are affected, then this modulation should be measurable with non-invasive technology.

2.8 hTheta may Modulate Vestibular Signals.

The apparent discovery of hTheta modulation in auditory signals during increased arousal (as discussed in the above section) suggests that hTheta might similarly modulate vestibular signals because peripheral auditory and vestibular neurons (which are responsible for sensing sound and balance, respectively) occupy the same structure (“the bony labyrinth”) within the inner ear and communicate with the central nervous system via the same (eighth) cranial nerve [13]. Importantly, hTheta impacts the signals of other sensory systems (touch, smell, vision and pain) [32], suggesting that vestibular signals are probably affected by it as well. While the literature seems to contain no mention of vestibular signals being modulated by hTheta, several lines of evidence indicate that such modulation likely occurs during anxiety (as will be discussed).

A key question for research aimed at detecting modulatory effects of anxiety on vestibular signals is whether hTheta perturbs activity in the VN, because 1) hTheta is linked to anxiety (as was discussed in this chapter), and 2) the VN is a major hub for afferent and efferent vestibular signals [13]. Critically, the VN modulates the efferent vestibular system, which influences peripheral afferent signals that can be recorded from the ear canal [13] (which will be discussed in the next section). Meanwhile, the VN receives direct projections from multiple brainstem nuclei that are implicated in anxiety [12] and are highly interconnected, namely the locus coeruleus, DR and parabrachial nucleus (Figure 2-5). Furthermore, these nuclei are directly connected to several anxiety-implicated regions that exhibit hTheta [5] and are themselves highly interconnected, namely the HPC, bed nucleus of the stria terminalis, amygdala, PFC and hypothalamus (Figure 2-5). Therefore, hTheta could reach the VN *directly* from the above brainstem nuclei, or *indirectly* from the other abovementioned regions, since hTheta is known to entrain regions with which it has only multisynaptic connections [35]. Critically, as Poppi et al. [37] have pointed out: “the vestibular periphery is not the only site along the vestibular pathway where modulation of sensory signals can occur” (for a review, see [38]); and the efferent vestibular system has polysynaptic inputs from the hypothalamus, reticular formation and DR [37] (that are implicated in anxiety or exhibit hTheta, as discussed).

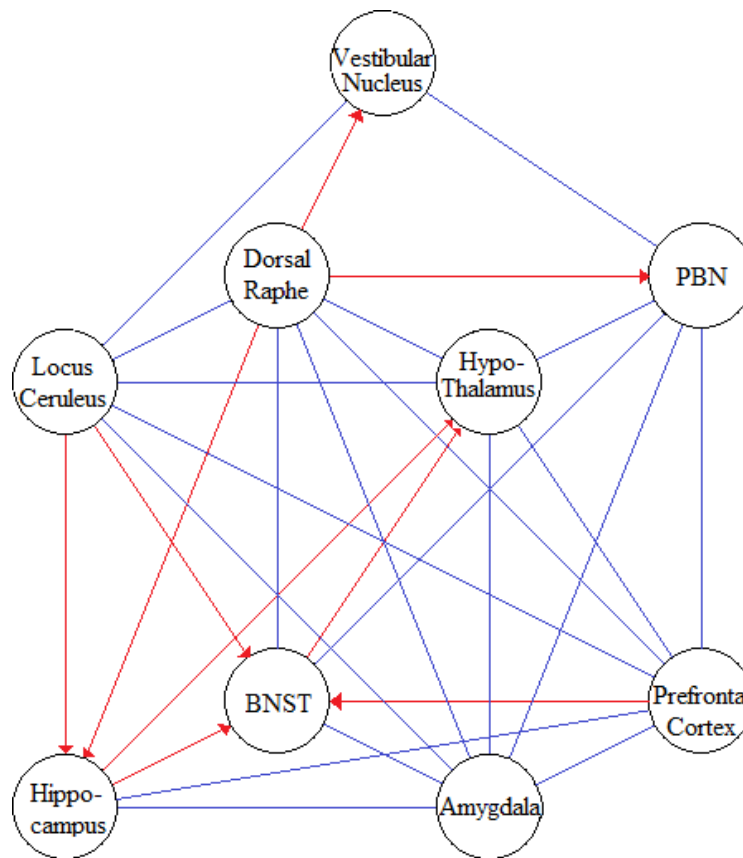


Figure 2-5. Anatomical connections between the VN and regions implicated in anxiety disorders. Various studies [12, 13, 39-46] together establish that these neural connections exist in rodents. The blue lines are bidirectional projections, and the red arrows are unidirectional projections.

The high degree of interconnectivity that was described (above) between the VN and eight anxiety-implicated regions — of which five are known to exhibit hTheta — suggests that hTheta may have several pathways to the VN. While the literature seems to contain no mention of hTheta in local field potentials from the DR, locus coeruleus and parabrachial nucleus (that all send dense *direct* projections to the VN [12]), these nuclei (which are largely serotonergic, noradrenergic, and cholinergic, respectively [12]) have been implicated in anxiety (as was discussed in this section) which itself has been linked to hTheta (as was discussed in this chapter), together suggesting that hTheta may in fact occur in these regions. Critically, it has been shown that a majority of neurons in at least one of them, namely the serotonergic DR, appear to be modulated by hTheta during REM sleep and movement in rats [47].

In a sample of 30 DR neurons, Kocsis and Vertes [47] found that 20-25% of these cells “discharged rhythmically” with hTheta in the HPC; and that firing in “approximately another 30%” correlated with hTheta (albeit to a lesser degree) in REM sleep and while rats walked (Figure 2-6). The authors hypothesized that the firing of these DR neurons might be linked to activity in the medial septum because the region is known to drive hTheta in the HPC [6]. These authors therefore proposed three scenarios for when hTheta arises: 1) the medial septum drives DR neurons in the same manner that it drives HPC neurons, 2) the DR modulates medial septum neurons when they drive neurons in the HPC, or 3) reciprocal signals are sent back and forth between the DR and medial septum [47].¹⁰

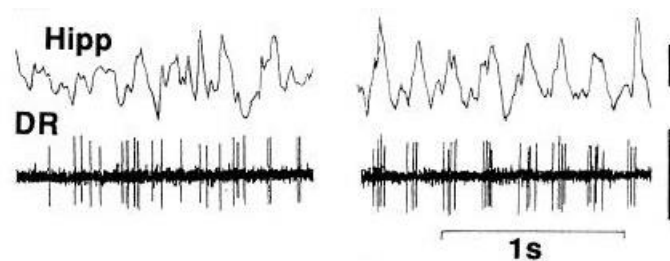


Figure 2-6. Most rat DR neurons fired in synchrony with hTheta amid REM sleep and movement. (Top) Local field potentials from depth recording in the HPC. (Bottom) Single-unit activity from depth recording within a sample DR neuron. (Left) Recordings during large irregular activity. (Right) Recordings during hTheta activity. Source: Adapted from [47].

Irrespective of any hypothetical link between the DR and medial septum, however, the above results (suggesting most DR neurons fire in synchrony with hTheta) seem to establish hTheta’s signature in the brainstem (where the critical VN lies). Interestingly, these findings, together with previous results showing that the DR projects throughout the cortex [48, 49], led Kocsis and Vertes [47] to hypothesize that the DR coordinates widespread cortical activity by relaying hTheta throughout the cortex. Critically, if the DR relays hTheta to brainstem regions, then the VN is a plausible target because it receives dense descending DR projections (as was discussed). Importantly, although REM sleep and movement (as opposed to anxiety assays) were used by Kocsis and Vertes [47] to elicit hTheta, type I (movement) and type II (anxiety) effects

¹⁰ Kocsis and Vertes [47] pointed out that the first scenario is plausible because it is known that the medial septum sends dense descending projections to the DR [34]; while the second is conceivable because the DR primarily uses 5-HT (as was mentioned), which has been linked both to hTheta generation and inhibition. Importantly, the authors noted that those cells whose activity correlated most with hTheta appeared to be non-serotonergic [47].

together create “a single travelling [hTheta] wave” in the HPC [7]; therefore, type I and type II effects should together modulate any neurons that become entrained by hTheta — suggesting that anxiety assays should elicit similar synchrony of DR neurons with hTheta (though, it is unclear whether hTheta indeed entrained the DR cells that Kocsis and Vertes [47] reported).

In a similar study, Sirota et al. [35] conducted experiments with the same species (rats) and tasks (REM sleep and movement); and while the DR was not probed, simultaneous recordings of local field potential and single unit activity from the HPC and several cortical areas were performed. Notably, the results confirmed that hTheta phase modulates (entrains) activity in multiple forebrain regions, and showed that this entrainment occurs both in areas with direct connections to the HPC *and* in the primary somatosensory area — that has only multisynaptic connections to the HPC [35]. Although it is unclear whether DR neurons were involved (as Kocsis and Vertes [47] predicted), these could explain the widespread entrainment because the DR sends projections throughout the cortex; and most DR neurons fire in synchrony with hTheta, as was discussed [47]. Critically, if this entrainment indeed related to the firing of DR neurons in synchrony with hTheta (as observed by Kocsis and Vertes [47]), then the VN might have also received this entrainment because, like the forebrain, it too receives extensive projections from the DR [12] (as was discussed). As reviewed in the following section, the entrainment of cortical neurons that Sirota et al. [35] identified could be a biomarker of a process that utilizes hTheta to transfer information to the HPC — and during anxiety likely entrains peripheral vestibular signals that can be recorded non-invasively.

2.9 Reciprocal Information Transfer: A Novel Anxiety Process Biomarker

As discussed in the above section, Sirota et al. [35] found that neural activity in multiple cortical regions was entrained by hTheta when rats were engaged in REM sleep or movement. To explain the nature of this entrainment, the authors theorized that it was caused by hTheta “temporally biasing activity in the [cortex], creating time windows within which the [HPC] most effectively receive[s] information,” in a process they named “reciprocal information transfer” [35]. In this process, transmission is *initiated* when hTheta biases the activity of “source structures” to

synchronize and time their outputs so they arrive at the HPC at the point in the hTheta cycle when plasticity is highest — thereby causing maximal long term potentiation [35].¹¹

Reciprocal information transfer could also explain the results of Kocsis and Vertes [47] (that were outlined in the above section), where the DR neurons that fired in synchrony with hTheta when rats were engaged in REM sleep or movement [47] would have been the source structures whose activity hTheta biased. Interestingly, as Sirota et al. [35] pointed out, “[hTheta] has been suggested to... gate sensory information” and to both time and synchronize sensory outputs, suggesting that reciprocal information transfer could also explain the results of Liberman et al. [32] (which were outlined in section 2.7), where hTheta seemed to modulate the firing of inferior colliculus central nucleus neurons when guinea pigs were exposed to changes in auditory stimuli.

Importantly, reciprocal information transfer may have played a role in a more recent study [50] that reported atropine-sensitive hTheta in the rat HPC during vestibular stimulation. In this study, Tai et al. [50] aimed to verify that the low frequency EEG rhythmicity which is blocked by atropine [51] and known to occur in the rat HPC during immobile rotation [52-55] is both 1) caused by vestibular signals, and 2) mediated by medial septum inputs to the HPC (which putatively drive hTheta, as stated in the above section [50]).

The authors found that when rats were rotated in a chamber, they exhibited 4-7 Hz EEG rhythmicity in the HPC; where fixed speed rotation elicited a stable peak frequency, and increasing the speed of rotation caused this frequency to rise (but did not alter peak power) [50]. This rhythmicity was blocked by atropine sulfate, but was unaffected by atropine methyl nitrate (which does not cross the blood brain barrier); and lesioning the cholinergic medial septum inputs to the HPC (via 192 IgG-saporin) greatly reduced the rhythm, together suggesting that this was type II hTheta, driven by the medial septum [50]. Critically, bilateral vestibular lesions via intratympanic sodium arsenilate greatly lowered the rhythmicity that was observed during passive rotation, indicating that vestibular signals are essential for rotation to elicit hTheta in the rat HPC [50].

Consistent with previous studies [25, 32, 33] in which type II hTheta was detected when stimuli were presented to animals, Tai et al. [50] attributed this rhythmicity to sensory processing;

¹¹ Notably, Kocsis and Vertes [47] indicated that “[long term potentiation] is best elicited at hTheta frequency,” and that DR neurons firing synchronously with hTheta could support long term potentiation.

however, unlike in these studies, Tai et al. [50] did not assess whether arousal played a role in the generation of type II hTheta. Vitaly, rats in the Tai et al. [50] study *must* have been aroused when hTheta occurred (unless vestibular stimulation is unlike other sensory stimuli and can elicit hTheta absent arousal) because Sainsbury et al. [25] previously showed that sensory stimulation appears to elicit hTheta only when animals are sufficiently aroused (as was reviewed in section 2.7).

Interestingly, arousal seems to have persisted throughout rotation (that lasted one minute), since “rotation was invariably accompanied by a steady and stable theta rhythm” [50]. Importantly, however, this persistent hTheta during rotation seems to contradict prior similar studies [51-55], in which hTheta only lasted for the first several seconds of rotation — until habituation occurred. To explain this discrepancy, Aitken et al. [56] noted that the studies in which hTheta lasted mere seconds had all used turntables and slow speeds (15-50 rpm) that would suggest smooth rotation; whereas a power drill spun the chamber in the Tai et al. [50] study at higher speeds (20-70 rpm), which likely caused vibrations that the rats could not habituate to (thereby causing hTheta to persist throughout rotation [56]).

The above results suggest that hTheta occurs for several seconds when rats begin rotating. This hTheta, that is caused by vestibular signals (as discussed), might in turn entrain the firing of vestibular neurons because (as was outlined in section 2.7) hTheta arose for the first several seconds when guinea pigs were exposed to auditory stimulation — and in so doing appeared to entrain the firing of auditory neurons [32]. Critically, such entrainment should be a biomarker of arousal because sensory stimulation has been shown to elicit hTheta *only* when rats are sufficiently aroused [25] (as was discussed).

Tai et al. [50] concluded that type II hTheta occurs in the rat HPC during passive rotation as a result of vestibular signals (via the hypothalamus-septohippocampal pathway) modulating cholinergic inputs to the HPC “which release ACh that modulates hippocampal apical dendritic synaptic transmission.” Importantly, the authors noted that vestibular activity may be mediated by hTheta [50], suggesting that the vestibular neurons that cause hTheta may themselves become modulated by it. Critically, if hTheta entrains the firing of any *peripheral* vestibular neurons, then it may be possible to detect this entrainment with existing non-invasive technology (as discussed in the next section). Furthermore, if these neurons are entrained by hTheta *whenever* they are active (i.e., even if they did not themselves trigger hTheta), then, because they are spontaneously active

[57] and continuously receive stimulation from gravity and inner bodily forces [56], these neurons may be entrained by hTheta even *absent* additional vestibular stimuli during arousal. Such entrainment could be a biomarker of arousal *or* anxiety because (as was discussed in this chapter) these functions have *both* been linked to type II hTheta (i.e., the type that Tai et al. [50] reported) and anxiety is simply “arousal with negative valence” (as defined by Calhoun and Tye [5]).

2.10 A Novel Anxiety Process Biomarker via Electrovestibulography

As discussed in the above section, vestibular neurons trigger type II hTheta in the rat HPC during passive rotation [56] and might (in turn) become entrained by this rhythmicity (because auditory stimuli elicit hTheta that seems to entrain auditory neurons [32]), through a theoretical process referred to as “reciprocal information transfer” [35]. However, this hTheta and its entrainment of vestibular neurons should occur only if arousal is high (because sensory stimuli appear to elicit hTheta only when rats are aroused [25]); therefore, such entrainment should be a biomarker of arousal — or anxiety (since anxiety is simply “arousal with negative valence” [5]). As will be shown, if a human analogue of this entrainment affects *peripheral* vestibular neurons, then this analogue might be an anxiety process biomarker that could be detected using EVestG — even without applied vestibular stimulation (because the vestibular system is always active [58]).

As was discussed in Chapter 1, EVestG is an electrophysiological technique that has already revealed possible biological markers (which have shown greater than 85% accuracy in separating patients from controls) for numerous neurological disorders and diseases [13]. This non-invasive technique involves recording EEGs near the ear drums from the outer ear canals with soft cotton tipped wire electrodes, and can be performed either during resting state or while participants undergo passive whole-body movements in a hydraulic chair [13]. The goal of recording in the ear is to measure electrical activity caused by vestibular neurons, as there are “substantial neurobiological links between brain processes regulating vestibular activity and brain regions implicated in the neurobiology of [multiple pathologies]” [13]. Peripheral vestibular neurons lie close enough to the ear drum that — when they fire with sufficient synchrony — the cells generate FPs that can be detected in recordings via “a wavelet-based signal processing technique called the Neural Event Extraction Routine (NEER)” [11].

If the vestibular neurons that cause these FPs become entrained by hTheta-like rhythmicity amid vestibular stimuli as auditory neurons seem to be entrained by hTheta amid auditory stimuli,

(i.e., *when arousal is high*; as was discussed in section 2.7), then these FPs should themselves become entrained; and such entrainment should indicate arousal. Furthermore, because hTheta can modulate the firing rates of individual neurons outside the HPC [32], hTheta-like rhythmicity may increase the regularity and power of FPs by synchronizing the firing of the vestibular neurons that cause them, making the FPs easier to detect. Therefore, entrainment by hTheta-like rhythmicity should be a biomarker of arousal (or anxiety; i.e., “arousal with negative valence;” Calhoun and Tye [5]) and could furthermore make FPs easier to detect, if such rhythmicity does indeed entrain peripheral vestibular neurons during periods of high arousal (which is plausible because auditory stimuli elicit hTheta that appears to entrain auditory neurons, and this seems to occur only when rats are aroused [25, 32]).

Notably, modulation of FPs within the hTheta frequency range has in fact been reported in previous EVestG studies [11, 13, 17] of individuals with mood disorders and was apparent in histograms of the time intervals between FPs (or “interval histograms;” IHs). In all of these EVestG studies, the (~10 Hz) modulation of FPs that was apparent in IH data differed in frequency between individuals with mood disorders and controls, possibly due to differences in levels of anxiety because trait anxiety is higher among individuals with mood disorders [14, 15]. Together, these results seem to reveal modulation of peripheral vestibular signals that is consistent with hTheta-like rhythmicity because the frequency of the modulation was within the hTheta range and differed between controls and individuals with mood disorders (the latter of which have more anxiety).

While type II (anxiety-implicated) hTheta-like rhythmicity could explain the modulation in the above mood disorder studies, replicating this modulation through various deliberate anxiety or arousal conditions would further show that it is in fact caused by type II hTheta-like rhythmicity. To provide a ‘pure’ anxiety condition (and avoid confounding results by including mood disorders) individuals with GAD (rather than mood disorders) could be recruited, along with healthy controls; and the experiments from the mood disorder studies could be repeated, namely various whole-body motions (supplied by a hydraulic chair) — though particularly rotation, because immobile rotation has been shown to generate type II theta in rodents (as discussed in the above section). Here, the expectation would be for type II hTheta-like rhythmicity to be more prominent in individuals with GAD (vs. controls) during chair motions because these individuals *generally* experience increased anxiety (in all manner of situations [20]).

Alternatively, the task (instead of the groups) could provide the variable anxiety conditions, where healthy volunteers would be recruited to perform a task that elicits varying levels of anxiety. For example, the SST that Shadli et al. [1] employed to elicit their anxiety process biomarker (i.e., GCSR, which was discussed in section 2.6) could be utilized, as it seems to cause varying levels of an anxiety process that anxiolytics mediate — and the theory that predicted GCSR suggests that hTheta-like rhythmicity causes this biomarker [1]. Critically, vestibular stimulation would not need to be applied *if* hTheta-like rhythmicity entrains peripheral vestibular neurons *whenever* they are active and hTheta-like rhythmicity is occurring (i.e., even if the neurons did not themselves trigger the rhythmicity) because peripheral vestibular neurons are spontaneously active and receive constant stimulation from gravity and bodily forces [58]. As these neurons exhibit some of the fastest action potential firing rates in the human body, with average intervals of about 3.3 milliseconds between action potentials [58], their signals are clearly ideal for modulation by hTheta-like rhythmicity and detection by EVestG and NEER.

In the remaining chapters of this thesis, a study (“the current study”) that employed the latter of the above two designs will be reviewed. The study had two experiments that each included 4-5 healthy volunteers who executed the SST: an ‘EEG Experiment’ and an ‘EVestG Experiment.’ The hypothesis for the EEG Experiment was that GCSR would be identified at the frontal F8 site (i.e., that ‘stop – go’ differences in 4-12 Hz frontal EEG power at the F8 recording site between ‘trial pairs’ would be significantly larger for ‘intermediate’ SSD trial pairs than for the average of ‘short’ and ‘long’ SSD trial pairs); and the hypothesis for the EVestG Experiment was that an analogue of GCSR would be identified (where this analogue of GCSR would contrast IHS of FPs analogously to how GCSR contrasts frontal power spectra, between the same SST trial conditions).

2.11 Summary

4-12 Hz hTheta activity predicts anxiety-like behaviour in rodents [7], as Adhikari et al. [21] linked vHPC-mPFC hTheta transmission to anxiety-like behaviour; and Padilla-Coreano et al. [9] and Lee et al. [8] later found that the former *causes* the latter. Crucially, all known *anxiolytic* drugs lower this hTheta; while all other drugs that have been tested do not [3].

McNaughton et al. [16], Shadli et al. [31] and Shadli et al. [1] reported rhythmicity in the human scalp that was: 4-12 Hz, over the PFC, sensitive to anxiolytics and caused by the SST (anxiety task), suggesting that the rhythmicity was analogous to rodent hTheta (and thus entrained

by the HPC). Vivally, behaviourally-modulated rhythmicity in the rodent hTheta frequency range has been established in the human HPC via depth recording, in individuals with epilepsy [10]. This rhythmicity may entrain the PFC, but could entrain other brain regions during anxiety as well, as rodent hTheta is linked to anxiety-like behaviour in multiple brain areas [5]. Interestingly, hTheta seems to entrain auditory cells in rodents that are aroused [32], suggesting that analogous entrainment in humans might be an indicator of high arousal — or perhaps (at times) anxiety — because “[a]nxiety represents a state of high arousal and negative valence” [5].

If hTheta entrains auditory cells, then it may also entrain vestibular cells because peripheral auditory and vestibular neurons occupy the same structures (for a review, see [13]). Interestingly, hTheta is known to affect other (sight, smell, touch and pain) sensory systems [32], suggesting that it may affect the vestibular system as well. Importantly, hTheta modulates the anxiety-implicated HPC, bed nucleus of the stria terminalis, amygdala, PFC and hypothalamus [5] that project to the brainstem locus coeruleus, DR and parabrachial nucleus (Figure 2-5), that are themselves implicated in anxiety [12] and project to the brainstem VN (Figure 2-5), which in turn mediates activity of the efferent vestibular system [13]. It is also worth noting that the efferent vestibular system has been shown to receive polysynaptic inputs from the hypothalamus, reticular formation and DR [37], and that hTheta is known to entrain areas with only multisynaptic connections to the HPC [35].

hTheta seems to entrain cells in at least one of the above regions that projects to the VN because Kocsis and Vertes [47] found that most *DR* neurons fire in synchrony with hTheta. This hTheta may in turn entrain the VN (that receives dense DR projections [12]) because the DR seems to transmit hTheta to many regions, to coordinate activity [47]. While the authors used REM sleep and movement (as opposed to anxiety assays) to elicit hTheta, type I (movement) and type II (anxiety) effects together create “a single travelling [hTheta] wave” in the HPC [7]; therefore, both types should together affect any cell that hTheta entrains.

Tai et al. [50] showed that vestibular stimulation, like other forms of sensory stimulation [25], elicits hTheta in the HPC that is sensitive to atropine (and is thus type II). Critically, hTheta occurs for the first several seconds when rodents are rotated [56], *and in so doing might entrain vestibular cells* because hTheta arose for the first several seconds when guinea pigs were exposed to auditory stimuli, and in so doing seemed to entrain auditory cells [32]. Importantly, Tai et al.

[50] showed that *vestibular neurons* trigger this hTheta which occurs during rotation, and indicated that vestibular neurons may in turn be mediated by hTheta, together suggesting that the vestibular neurons that trigger hTheta could themselves become entrained by it.

If vestibular neurons become entrained by hTheta *whenever* both they and hTheta are active (i.e., even if the cells did not themselves elicit hTheta), then, because they are spontaneously active [57] and continuously receive stimulation from gravity and many inner bodily forces [56], these cells might become entrained by hTheta even when animals are at rest. Furthermore, such entrainment of vestibular cells should be a biomarker of high arousal because sensory stimuli have been shown to elicit hTheta *only* when arousal is high [25].

EVestG involves recording EEG data in the ear canals and using NEER to find (in the data) the FPs that peripheral vestibular cells cause when they fire synchronously [11]. If a human analogue of rodent hTheta entrains peripheral vestibular cells (and the FPs they elicit) amid vestibular stimulation just as hTheta seems to entrain auditory cells amid auditory stimulation [32], then EVestG may reveal entrainment of FPs by this analogue amid arousal.

EVestG studies [11, 13, 58] reported modulation of FPs within the frequency range of hTheta that differed between individuals with mood disorders and controls, and was thus consistent both in frequency and etiology with a human analogue of type II rodent hTheta (given that individuals with mood disorders tend to show increased trait anxiety [14, 15]). To test the prediction that type II hTheta-like rhythmicity could explain this apparent modulation, the SST that Shadli et al. [1] employed to elicit their anxiety process biomarker (i.e., GCSR) in healthy volunteers could be tested on participants during EVestG recordings. The remainder of this thesis will review a study (“the current study”) that used the SST to cause hTheta-like rhythmicity in healthy volunteers, and that aimed to detect 1) GCSR in frontal EEG data, in a replication of a Shadli et al [1] experiment, and 2) an “analogue” of GCSR in EVestG data, in a novel experiment. The hypothesis for the first experiment was that GCSR would be identified at the frontal F8 site; and the hypothesis for the second was that an *analogue* of GCSR would be found in EVestG data.

Chapter 3: Methods

3.1 Overview

The current study had two experiments: an ‘EEG Experiment’ and ‘EVestG Experiment.’ The ‘EEG Experiment’ was aimed at partially replicating “Experiment 2” of Shadli et al. [1] by recreating GCSR at the frontal F8 site, while the ‘EVestG Experiment’ was a *novel* experiment designed to elicit an analogue of GCSR that would be detectable in EVestG data (recorded from the outer ear canal). The SST employed by Shadli et al. [1] was used for both experiments and involved pressing keys on a keyboard in response to images that were presented on a monitor.

3.2 Participants

Due to the COVID-19 pandemic, which has been ongoing since March 2020, recruitment for the current study was greatly limited. All volunteers recruited for the study were healthy adults who were either a colleague, superior or relative of the student principal investigator. None of the participants self-reported being prescribed any psychiatric drug while participating, or having received psychiatric treatment in the previous year. All experiments were approved by the University of Manitoba Biomedical Research Ethics Board, and participants signed a written consent form before the experiments and received no compensation for participating in the study.

Five volunteers (two male; two left-handed; age 28-62 years) formed an ‘EEG group’ that performed an ‘EEG Experiment’ meant to partially replicate “Experiment 2” of Shadli et al. [1] by recreating GCSR at F8 (see Table 3-1); while five volunteers (three male; one left-handed; age 31-63 years) formed an ‘EVestG group’ that performed a *novel* ‘EVestG Experiment’ designed to elicit a GCSR ‘analogue’ in EVestG data. Notably, three volunteers were in *both* groups, initially; however, one of these individuals was excluded from the EVestG group (due to excessive artefacts in their recorded electrophysiological data), which left only four participants in the EVestG group (three male; one left-handed; age 31-63 years) and two volunteers who participated in both groups. Participants in both experiments performed the SST while their electrophysiological data were recorded (namely, frontal EEG data in the EEG group, and in-ear EEG data in the EVestG group).

Table 3-1. Demographics of participants in the EEG and EVestG Experiments. Note that three volunteers were recruited for both experiments, but one of these three (P-3) was later excluded from the EVestG Experiment due to excessive artefacts in recorded signals (data excluded).*

Participant (code)	EEG Experiment			EVestG Experiment		
	Age (Years)	Sex (Male/Female)	Handedness (Left/Right)	Age (Years)	Sex (Male/Female)	Handedness (Left/Right)
P-1	33	Female	Left	-	-	-
P-2	62	Male	Left	62	Male	Left
P-3	62	Male	Right	62*	Male*	Right*
P-4	28	Female	Right	-	-	-
P-5	-	-	-	31	Male	Right
P-6	61	Female	Right	61	Female	Right
P-7	-	-	-	58	Female	Right

3.3 Description of the Stop Signal Task (SST)

The same SST and order of trials were used for both of the experiments in the current study (for a review of the many variables and functions involved in the task, as well as the theory behind the SST and GCSR, see section 2.6). For both experiments in the current study, participants were instructed on how to perform the SST via instructions (outlined below) that were 1) shown to participants on a monitor in the experiment, and 2) verbally explained to participants before the experiment. Any questions that participants had about the SST were answered verbally by the principal investigator of the study. Importantly, the instructions on the monitor were identical to those from “Experiment 2” of Shadli et al. [1]; though, there may have been differences in the way that these instructions were verbally conveyed in the current study compared to the way that they were verbally conveyed in Shadli et al. [1].

The SST described by Shadli et al. [1] was coded in html and run with Google Chrome. All images or messages that the program displayed were presented over a solid black background. The program began by displaying a message (in white, size 12, Calibri font) which was centered and said “Respond as FAST as you can with your index and middle fingers once you see an arrow.

Press the left button if you see the left arrow. Press the right button if you see the right arrow.” Participants could then press either the left or right arrow key to start a ten second countdown that appeared in the center of the screen (in white, size 12, Calibri font) and counted down from 9 to 0.

A series of 30 back-to-back “pure-go” trials then began, where each trial (Figure 3-1) showed a white “fixation” circle (centered; 5 cm in diameter) for 500 ms before the circle turned green and a left or right arrow (white; 2.5 cm tall x 2.5 cm wide) was displayed (centered, within the circle). If the correct key was then pressed within 1000 ms, the trial was recorded as successful, the circle and arrow were removed, and a gray “smiley” emoji (centered; 5 cm in diameter) was displayed; otherwise, the trial was recorded as unsuccessful, the circle and arrow were removed, and a gray “frowney” emoji (centered; 5 cm in diameter) was displayed when the incorrect key was pressed — or after 1000 ms if neither key had been pressed. Whichever emoji was displayed, it remained on the screen for 500 ms, after which the solid black background displayed for 0–3.75 seconds (where this time varied between trials) until the next trial began (if any ‘pure-go’ trials remained).

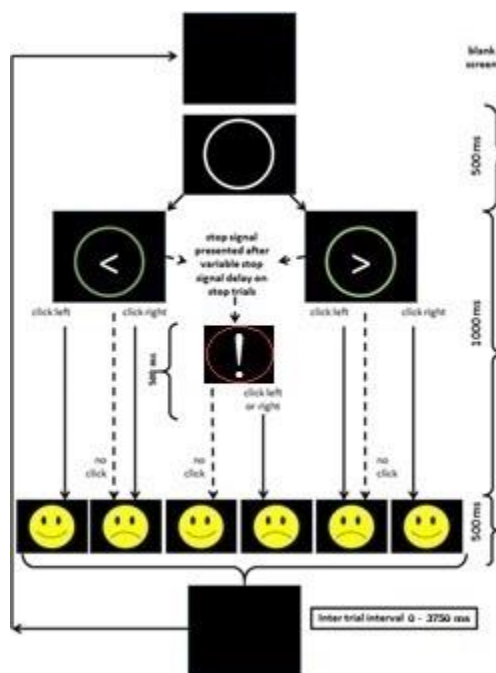


Figure 3-1. Flowchart of the possible images shown in SST trials. Source: Adapted from [31].

After the above trials, a displayed message (centered, in white, size 12, Calibri font) said: “NOW YOU WILL START HAVING STOP TRIALS. Remember, respond as fast as you can

once you see an arrow. However, if you see the exclamation mark (!), your task is to STOP yourself from pressing. Stopping and going are equally important. Press the thumb switch to proceed.” Participants then pressed a thumb switch (with their left hand) to start a ten second countdown that appeared in the center of the screen (in white, size 12, Calibri font) and counted down from 9 to 0.

A series of 132 back-to-back “stop–go” trials then began, in which each trial first displayed a white fixation circle (centered; 5 cm in diameter) for 500 ms before the circle turned green and a left or right arrow (white; 2.5 cm tall x 2.5 cm wide) was displayed (centered, within the circle). In 33 trials (randomly distributed among the 132; block size of four), after a variable (SSD) delay, the green circle became red and an exclamation mark (white; centered; 2.5 cm tall x 0.5 cm wide) replaced the arrow. If neither arrow key were then pressed while the exclamation mark was shown, the trial was recorded as successful, the circle and exclamation mark were removed after 1000 ms (minus the variable delay), and a gray “smiley” emoji (centered; 5 cm in diameter) was displayed; otherwise, once either arrow key was pressed, the trial was recorded as unsuccessful, the circle and exclamation mark were removed, and a gray “frowney” emoji (centered; 5 cm in diameter) was displayed. Whichever emoji was displayed, it remained on the screen for 500 ms, after which the solid black background displayed for 0–3.75 seconds (where this time varied between trials) until the next trial began (if any ‘stop–go’ trials remained). The other 99 ‘stop–go’ trials behaved as ‘pure–go’ (i.e., the first 30) trials, except that if *neither* arrow key was pressed within 1.5 times the average time before either key was pressed in the series of 30 ‘pure–go’ trials, then the circle and arrow were removed and a displayed message (in orange, size 30, Calibri font) said: “SLOW!”

Once the last ‘stop–go’ trial concluded, the SST program exported all of the trial variables in each trial, namely: 1) how long it took before an arrow key was pressed (or the “reaction time”), 2) whether success was achieved, 3) the arrow key that was pressed, 4) whether a key was pressed *before* the exclamation mark appeared; 5) the direction of the displayed arrow, 6) the SSD values, 7) the duration of the trial, 8) the current values for the short, intermediate and long SSD staircases, and 9) the median reaction time over the last 16 trials in which no exclamation mark was displayed. Most of the above variables were used to verify that participants had performed the SST properly, which (it was expected) would ensure that the relevant brain processes were engaged by the task. In addition to the above variables, the program exported timestamps (created throughout the SST, specifically at the beginning and end of each countdown as well as at the beginning of each trial).

For both experiments, the files with the SST variables and timestamps were converted from .json to .csv format before being analyzed in Matlab (Version: 9.8.0.1417392, R2020a, Update 4). Based on statistics of these variables, each participant's performance in the SST was evaluated; and the recorded electrophysiological data of participants who did not perform the task reasonably well (by meeting certain pre-determined standards, described below) were excluded from analyses.

The main statistics of interest were the success rates during 'stop' trials for the three SSDs. As was discussed in section 2.6, the short, intermediate and long SSDs are continually adjusted to ensure success rates of ~ 20, 50 and 80% in the short, intermediate and long 'stop' trials of the SST, respectively, to ensure (in theory) that the correct amount of goal conflict for each SSD is elicited [1]. However, inclusion criteria did not require specific ranges of values for SSD — merely that success rates decreased (at each step) as SSD went from short, to intermediate, to long.

Participant performance during 'go' trials was of secondary importance, and was primarily examined to determine whether participants were "slowing" their responses (i.e., reaction times). "Slowing" occurs when participants (in anticipating the 'stop' signal) wait longer before pressing a key after seeing the arrow ('go' signal) to avoid failure (in the event that the trial is a 'stop' trial). Three statistics were used to assess whether a participant was slowing, namely 1) their 'go reaction time' (i.e., how fast they responded), 2) the consistency of their reaction time, and 3) their 'go accuracy' (i.e., the percentage of 'go' trials that they passed). There was no standard for 'go reaction time,' because the SST adapts to different reaction times [1]; however, if reaction times doubled over the course of the task and 'go accuracy' was low (< 90%), then these factors together indicated slowing (though participants were not excluded based on whether 'slowing' occurred).

3.4 EEG Experiment

3.4.1 Procedure

Ten surface electrodes were connected to the heads of each participant prior to the SST (using the 10-20 EEG system), namely at F7, Fz and F8 (for analysis); at aFz (to act as ground); left of the left eye and above, below and right of the right eye for electrooculogram (EOG) removal; and on both mastoids (whose signals would be averaged, to serve as a reference for the other sites). All ten (Biopac EL258S) electrodes were filled with (Parker SignaGel) conductive gel before being adhered with (Biopac ADD208) adhesive collars to all recording sites that were first prepared by

rubbing skin with (Q-tip) cotton swabs coated in (Nuprep) Skin Prep Gel to remove dead cells. Impedances at each site were then verified (via Model 1089 MK III Checktrode) to be under 5 k Ω .

With their electrodes in place, volunteers were seated in a chair inside an anechoic chamber (that reduced sound from outside the chamber up to 30 dB and was electromagnetically shielded). The ten electrodes for recording frontal EEGs were then connected to a Biopac MP150 amplifier (10 k gain, 1 Hz high-pass and 35 Hz low-pass 2nd order Butterworth filters, 1 kHz sampling rate). A total of six channels were used, where: aFz served as ground for every channel (as mentioned); F7, F8, Fz and M2 were connected to the positive inputs for channels 1, 2, 3 and 4, respectively; the reference for channels 1–4 during recording was M1 [but for analysis was $(M1 + M2) / 2$]; and vertical (vEOG) and horizontal EOG (hEOG) recorded in bipolar on channels 5 and 6, respectively. Critically, the same filter settings were used for the EEG and EOG channels, which is a necessary condition for the linearity that EOG correction assumes (for a review, see [59]). Data from the above six channels were sent over ethernet cable to a computer outside the chamber and recorded with BIOPAC systems AcqKnowledge 4.1.1 data acquisition and analysis software.

During the SST, participants remained in the chair in front of a laptop that stood on a table, with their right palm on the laptop's palm rest and eyes fixated on the centre of the laptop's screen (where the centre of this 14-inch screen was at eye level and 24 inches from the participants' eyes). At one point, participants used their left thumb to press a thumb switch connected to an Arduino that initiated the final part of the SST and started the recording. When pressed, this switch caused an ASCII character to be sent from the Arduino to the laptop (via 6-foot USB cable through which the Arduino was also powered) to start the SST, and a low-high-low (0V-5V-0V) signal to be sent (via 6-foot 3.5mm audio cable) to the MP150 to start the data recording. Participants were told to breathe and blink normally but to otherwise not move *except* to press the left and right arrow keys with their index and middle fingers, respectively, whenever such actions were required by the task. Participants were then left alone in the chamber and started the SST by pressing either arrow key.

3.4.2 Pre-Processing

After the SST, the frontal EEG data files from AcqKnowledge were converted from .acq to .mat format, to prepare the data for pre-processing (and analysis, as discussed in the next section) with Matlab. In Matlab, timestamps from the SST program located the points in each frontal EEG data recording when each of the 132 'stop-go' trials (lasting a total of approximately 6 minutes)

started and ended, while the program's SSD values were used to position analysis windows relative to these points.

The F7, F8 and Fz channels were all recorded using the M1 (left mastoid) site as reference but later *re*-referenced to the average of the two mastoids (M1 and M2), which was accomplished by subtracting the M2 channel (that also had M1 as reference), after dividing its amplitude by two, from the F7, F8 and Fz channels. Below, the algebra is shown for re-referencing the F8 channel:

$$(F8 - M1) - \frac{M2 - M1}{2} = F8 - M1 - \frac{M2}{2} + \frac{M1}{2} = F8 - \frac{M1}{2} - \frac{M2}{2} = F8 - \frac{M1 + M2}{2} \quad [3-1]$$

Next, ocular artefacts were removed from the F7, F8 and Fz channels, which was especially important because the eyes 1) are close to the frontal sites, and 2) remained open during the task. Critically, the cornea and retina form an electric dipole strong enough that its movements perturb surface EEGs; and eye blinks have been shown to have similar effects, even absent eyeball motion [59]. Importantly, it has been shown that the signals generated by these sources can be recorded around the eyes and largely removed from EEG sites of interest after being scaled [59]. While it would have made sense to remove such signals with the same technique that was used by Shadli et al. [1] (as the current study aimed to replicate their results), due to software compatibility issues, it was determined that an alternative method had to be used. Vitaly, an author of Shadli et al. [1] indicated that any eye blink removal method which was generally as effective as the one that they used would be sufficient for a replication, and suggested that EOG regression may in fact be superior (Neil McNaughton, personal communication, 20 October 2019). vEOG and hEOG were thus recorded because, as Croft and Barry [59] have pointed out, “[i]t has been consistently demonstrated that it is best to correct with at least VEOG and HEOG channels;” and *simultaneous* multiple regression was used on the two EOG channels because it appears to be the most robust multiple regression for EOG correction (for a review, see [59]).

EOG correction, which “remov[es] the estimated effect of ocular activity from the EEG” [59], was performed in Matlab. First, ‘fitlm’ (fit linear regression model) was used to find the linear regression model that minimized the least squares error in estimating the F8 data via a linear combination of the vEOG and hEOG data that were recorded simultaneous to F8. The coefficients for this model that Matlab returned were used to scale the vEOG and hEOG data, and the resulting

scaled vEOG and hEOG data were subtracted from F8 to remove ocular artefacts. These two operations (scaling by coefficients, then subtracting from F8) are in Matlab code, below:

$$F8 = F8 - (b1 \times vEOG) - (b2 \times hEOG) \quad [3-2]$$

The EOG channels were then similarly scaled and subtracted from the F7 and Fz channels, after which eyeblink effects were no longer visible in any of the F7, F8 or Fz traces (Figure 3-2); and it was apparent that more of the artefacts in the traces of the F7, F8 and Fz channels were removed by subtracting the scaled vEOG data (than were removed by subtracting the scaled hEOG data). Correspondingly, subtracting the scaled vEOG data from the F7, F8 and Fz channels lowered the standard deviations of signals from these channels more than subtracting the hEOG channel did. Importantly, neither of the EOG channels were found to saturate at any point during the recordings; therefore, EOG data did not need to be replaced with missing values [59]. Also, none of the F7, F8 or Fz data needed to be replaced with missing values because of saturation.



Figure 3-2. EOG correction of EEG data recorded during the SST. (Top to bottom) F8 before correction; F8 after vEOG correction; F8 after vEOG and hEOG correction; vEOG; hEOG.

Once EOG correction was completed, it was necessary to remove other suspected artefacts from the EEG data because the corrected F7, F8 and Fz traces for all participants exhibited at least one obvious anomaly (usually lasting 1–2 seconds) that was not removed by the EOG correction. While these anomalies were typically short in duration, they were also mostly large in amplitude, suggesting they could have confounded results — despite there being very few in most recordings. As the sources of these anomalies were assumed to be muscle movement that could not be isolated,

all short sections of data containing such anomalies were replaced with missing values, as this was the protocol in Shadli et al. [1] (which the EEG Experiment was aimed at replicating).¹²

3.4.3 Data Analysis

As was discussed in section 2.6, GCSR occurs when (stop – go) differences in 4-12 Hz frontal EEG power are significantly larger, on average, for ‘intermediate’ SSD trial pairs than for ‘short’ and ‘long’ SSD trial pairs in the SST. In the current study, to test the hypothesis that GCSR would occur during the SST, it was therefore essential to analyze and compare 4-12 Hz frontal EEG power during various ‘stop’ and ‘go’ trials; and the aim was to mimic the analysis in ‘Experiment 2’ of Shadli et al. [1] as much as possible (for a review of GCSR, see section 2.6).

In total, 66 segments of data (each 1001 samples in length, sampled at 1 kHz) were analysed from each frontal EEG channel of interest (F7, F8, Fz) for each volunteer in the EEG group (N=5), where each of the 66 segments was recorded during a different trial (of the 132 trials in the SST); and the set of trials during which the 66 segments were recorded was the same for all volunteers. (Recall that each SST ‘trial’ lasts 2-5 seconds, and that each data ‘segment’ is a 1-second portion of EEG data recorded during an SST trial). Also, the starting points of segments were defined by the times of the ‘stop’ signals, that in turn depended on how each volunteer performed in the task (as reaction times during ‘go’ trials determined the values of the short and long SSDs, while performance in intermediate ‘stop’ trials set the value of the intermediate SSD throughout the task).

The 66 trials that were associated with the 66 analyzed segments included: 11 ‘short stop,’ 11 ‘short go,’ 11 ‘intermediate stop,’ 11 ‘intermediate go,’ 11 ‘long stop’ and 11 ‘long go’ trials. The order of these trials and the remaining 66 that were not analyzed (out of the total 132 trials), was pseudorandom, generated ahead of time, and (as mentioned) the same for every participant. (‘Stop’ and ‘go’ trials were in blocks of 4; short, intermediate and long SSDs were in blocks of 3).

Timestamps created when the thumb switch was pressed and when each of the trials started, along with SSD values, together pinpointed the segments in the EEG data that were to be analyzed, as the timestamps located each of the points within the EEG data recordings when each trial started;

¹² It is possible that excluding sections of data not removed by EOG correction that seemed to contain muscle artefacts may have selectively removed segments in which anxiety occurred (as anxiety might be expected to trigger muscle movements); however, investigating this possibility was beyond the scope of the current study.

and the SSD values gave the positions — relative to these points — where analysis windows began (as the SSD values determined when the exclamation mark “‘stop’ signal” occurred in ‘stop’ trials, and the ‘stop’ signals in turn determined the point in each trial when analysis was to be performed). Specifically, 1-second analysis windows began 0.25 seconds before the ‘stop’ signal in each of the 33 ‘stop’ trials *and*, however many samples into each ‘stop’ trial this was, *also* that many samples into its ‘paired go’ trial, thus creating the abovementioned 66 (1001-sample) EEG data segments.

The \log_{10} power spectrum for each of the 66 segments that were recorded for each channel (F7, F8, Fz) of each volunteer was calculated via the Matlab ‘fft’ (fast Fourier transform) function, after a (1001-sample) Hann window¹³ was applied to each segment via the Matlab ‘hann’ function. Note: for ‘stop’ trials in which a participant pressed a key *before* the exclamation mark appeared, the participant’s EEG data segment for that trial consisted entirely of missing values; and for segments that included one or more missing values, the spectra that were created from the segments were also set to missing values. Notably, all frontal EEG recordings (for all channels and participants) had somewhere between one and eight small sections (~ 500 ms) of missing values (for example, a recording is shown in Figure 3-3, after EOG correction); however, a given section of missing values only affected analysis if it coincided with one of the 66 analysis windows.

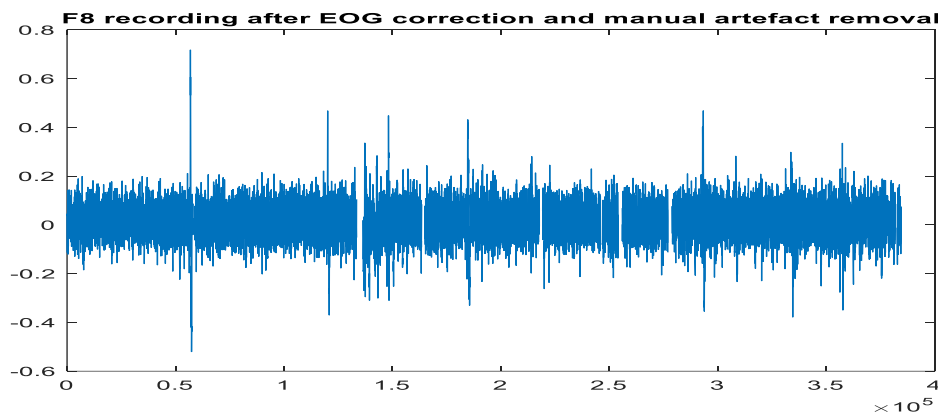


Figure 3-3. EEG recording after EOG correction and manual artefact removal (missing segments are where artefacts occurred). The vertical axis is frontal EEG activity at the F8 recording site (in millivolts); and the horizontal axis is time (in milliseconds).

¹³ A single cycle of a raised cosine function (with a value of 1, in the centre; and 0, at both ends), that Shadli et al. [1] used because it “extracts maximum power from the middle 0.5 s period... and doubles the frequency resolution of the subsequent Fourier transform [vs. a square window].”

For each volunteer (N=5) and EEG channel (F7, F8, Fz), the 66 spectra were averaged for all trials of the same type (stop, go) and SSD (short, intermediate, long), thus creating (6) “average” ‘short stop,’ ‘short go,’ ‘intermediate stop,’ ‘intermediate go,’ ‘long stop’ and ‘long go’ spectra (each of which was the average of 11 spectra) for each participant and EEG channel (F7, F8, Fz); however, spectra that contained missing values were excluded from these averages; and if five or more spectra for the same trial type and SSD contained missing values, then the entire average was excluded from analyses. F8 produced the most robust GCSR in prior studies [16, 31] and was the focus of analyses in Shadli et al. [1]; therefore, analyses herein focused on F8 as well.

To determine if the hypothesized GCSR occurred at the F8 site in the EEG group, repeated measures ANOVA (in IBM SPSS Statistics 28.0) contrasted 4-12 Hz frontal EEG power between average ‘short stop,’ ‘short go,’ ‘intermediate stop,’ ‘intermediate go,’ ‘long stop’ and ‘long go’ spectra via the repeated measures factors ‘type’ (stop, go), ‘SSD’ (short, intermediate, long) and ‘frequency’ (4-12 Hz, 1 Hz bins; for a review of statistical analyses that were replicated, see [1]).

The *quadratic* contrast for ‘SSD’ was tested because (as discussed) GCSR occurs when (stop – go) differences in 4-12 Hz frontal EEG power are larger, on average, for ‘intermediate’ SSD trial pairs than for ‘short’ and ‘long’ SSD trial pairs in the SST, suggesting EEG power should go from low, to high, to low as SSD goes from short, to intermediate, to long [1]. A *linear* contrast was also added for ‘type’ (‘stop’ or ‘go’) because this contrast was expected (in Shadli et al. [1] and the current study aimed at replicating Shadli et al. [1]) to isolate the effect of the ‘stop’ signal.¹⁴

If statistically significant ($p < 0.05$), the within-subjects ‘type’ x ‘SSD’ (linear x quadratic) interaction would validate the hypothesis that GCSR occurred during the SST [1]. Meanwhile, the within-subjects ‘type’ x ‘SSD’ (linear x linear) interaction was examined, to find “the amount of variation between the short and long conditions independently of the medium one” [1], and was expected to be *insignificant*; while the within-subjects ‘type’ (linear) that related to the effect of stopping (averaged across the levels of ‘SSD:’ short, intermediate, long) was likewise assessed but expected to be *significant* (and thus reveal an effect of the ‘stop’ signal). Vitaly, the same threshold for statistical significance ($p < 0.05$) was used for all statistical tests; and to maximize statistical

¹⁴ ‘Stop’ trials have a ‘stop’ signal but are otherwise identical to ‘go’ trials, thus the difference in EEG power between trial pairs should represent the effect of the ‘stop’ signal [1].

power, the main analysis focused on the data from the frontal F8 site because Shadli et al. [1] found that F8 showed the most robust GCSR in prior studies (as discussed).

To visualize the result of the quadratic contrast (GCSR) for the EEG group, the (6) average spectra of each participant were averaged among participants (N=5) across trials of the same ‘type’ and ‘SSD’ (‘short stop,’ ‘short go,’ ‘intermediate stop,’ ‘intermediate go,’ ‘long stop,’ ‘long go’) and entered in the formula below that performed the GCSR contrast using only the group averages:

$$\begin{aligned} & (\text{intermediate stop} - \text{intermediate go}) - [(\text{short stop} - \text{short go}) \\ & \quad + (\text{long stop} - \text{long go})] / 2 \end{aligned} \quad [3-3]$$

the result of which was plotted as a function of ‘frequency’ (4-12 Hz; 1 Hz bins) and compared to results in previous studies [1, 16, 28, 31]. In some instances, data were three-point smoothed to make finding trends across studies easier. Post hoc analyses were performed for frequencies at which large peaks were apparent in the plot, if the within-subjects ‘type’ x ‘SSD’ (linear x quadratic) contrast showed significance ($p < 0.05$).

3.5 EVestG Experiment

Whereas the ‘EEG Experiment’, previously described, was aimed at replicating “Experiment 2” of Shadli et al. [1] by causing and detecting GCSR in frontal EEG data; the ‘EVestG Experiment’ (that will be outlined in this section) was a novel experiment aimed at causing and detecting a GCSR ‘analogue’ in EVestG data, using methods *analogous* to those that were employed in “Experiment 2” of Shadli et al. [1].

3.5.1 Procedure

Participants had their ear canals inspected with an otoscope before electrodes were placed, to rule out irregularities that could have made recording in the ear canals unsafe or unproductive (such as an injury, or excess ear wax that might have caused poor electrode contact, respectively). If no irregularities were found, five electrodes were positioned to record EEGs from the ear canals: one near the ear drum in each ear canal (Figure 3-4); one just outside each ear canal; and one at Fpz. The Fpz (Biopac EL258S) electrode was filled with (Parker SignaGel) conductive gel and adhered (Biopac ADD208) to skin that was prepped with (Q-tip) cotton swabs and (Nuprep) Skin Prep Gel. First, however, the other four electrodes (each consisting of a single wire conductor

made of silver and flexible plastic insulation) had their (soft cotton) tips soaked in 50% (Baxter NaCl 0.9%) saline and 50% (Parker SignaGel) conductive gel before being fixed in their positions with medical tape. Bipolar EEGs were recorded, with each in-ear electrode and the one just outside the ipsilateral ear designated as an active lead and its reference (respectively); while Fpz was ground for both pairs.

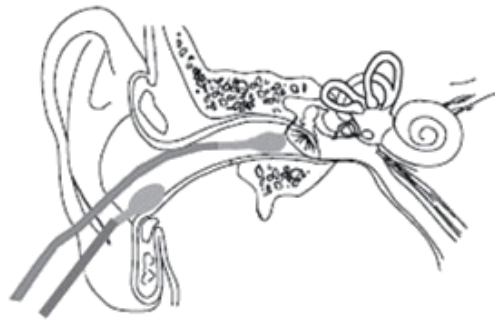


Figure 3-4. Ear canal electrode placement. Note the proximity of the vestibular organs (right).

Adapted from [13].

With their electrodes in place, volunteers were seated in a chair inside an anechoic chamber (that reduced sound from outside the chamber up to 30 dB and was electromagnetically shielded). For the in-ear data recording, a CED1902-11-2B 2 channel electrode adaptor box was used, where: the Fpz electrode was connected to the common input connector; the right and left ear canal electrodes were plugged into the channel 0 and channel 1 (positive) input connectors, respectively; and the right- and left-ear reference electrodes went into channels 0 and 1 (negative), respectively. (Note: all five electrodes had 1.5 mm connectors). Both channels were set to bipolar mode, and each of them was connected (via 6-foot, 6-pin DIN plug) to a separate CED-1902 signal amplifier (10 k gain, 60 Hz notch filter, 1 Hz high pass filter). The outputs of the two amplifiers were sent (via 6-inch coaxial cables with BNC connectors) to a CED Micro1401-3 data acquisition unit that digitized the data (at a sampling rate of 41667 Hz) and sent it (via 15-foot coaxial cables with BNC connectors) to a computer outside the chamber that recorded the data with CED Spike2 software. Before each recording, time signals and power spectra (for both channels) were observed to ensure: 1) voltage saturation did not occur, and 2) signal-to-noise ratio was above 20, respectively.

During the SST, participants remained in the chair in front of a laptop that stood on a table, with their right palm on the laptop's palm rest and eyes fixated on the centre of the laptop's screen

(where the centre of this 14-inch screen was at eye level and 24 inches from the participants' eyes). At one point, participants used their left thumb to press a thumb switch connected to an Arduino that initiated the final part of the SST and started the recordings. When pressed, this switch caused an ASCII character to be sent from the Arduino to the laptop (via 6-foot USB cable through which the Arduino was also powered) to start the SST, and a low-high-low (0V-5V-0V) signal to be sent (via 6-foot coaxial cable with BNC connectors) to the CED-1902, to start the data recordings. Participants were told to breathe and blink normally but to otherwise not move *except* to press the left and right arrow keys with their index and middle fingers, respectively, as required by the task. Participants were then left alone in the chamber and started the SST by pressing either arrow key.

3.5.2 Pre-Processing

The in-ear EEG data files recorded with Spike2 were converted from .smr to .mat format, prior to pre-processing in Matlab and Microsoft Excel (Version 2112, Build 14729.20254, 64-bit). In Matlab, timestamps from the SST program located the points in each (approximately 6-minute) in-ear EEG data recording (Figure 3-5) when each of the total 132 'stop-go' trials started and ended; and SSD values from the program were used to position analysis windows relative to these points.

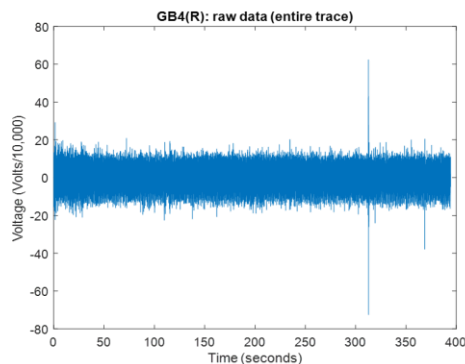


Figure 3-5. Raw trace from a typical (~ 6-minute) in-ear recording.

Analysis windows in the EVestG Experiment were akin to those in the EEG Experiment (i.e., 1-second-long, started 0.25 seconds before the 'stop' signal in each of the 33 'stop' trials *and*, however many samples into each 'stop' trial this was, that many samples into its 'paired go' trial) and thus created 66 in-ear EEG data segments (Figure 3-6). EVestG data was sampled at 41,667 Hz; thus, each segment contained 41,668 samples (while segments in the EEG Experiment

contained 1001 samples, as the frontal EEG data was sampled at 1000 Hz; as was discussed in section 3.4.3).

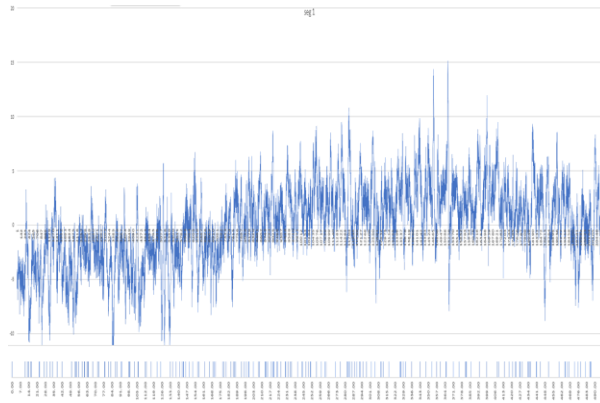


Figure 3-6 1-second in-ear EEG data segment and field potentials identified by NEER within it.

(Top) 1-second segment of in-ear EEG data, recorded from a participant during the SST.

(Bottom) Field potentials NEER found buried in noise, in the 1-second in-ear EEG data segment.

The vertical axis is voltage (volts/10,000); the horizontal axis is time (the window is 1 second).

While *frontal* EEG data segments were simply converted to power spectra before analysis, *in-ear* EEG data segments were processed by a “wavelet-based signal processing technique” [11], “NEER” (as was discussed in Chapter 2; for a review, see [11]), that located FPs (putatively caused by the simultaneous firing of vestibular cells) in each data segment and exported the segment’s “EVestG data” (average FP shape and time of each FP) to a .xlsx file. EVestG data associated with a participant’s left ear were stored in the participant’s ‘left ear’ file, and the data associated with a participant’s right ear were stored in the participant’s ‘right ear’ file. (Note: The NEER algorithm [13] used a 60-Hz notch filter to remove interference from the power grid and a high pass filter with a 300-Hz corner frequency to reduce artefacts from muscle movement).

For each segment, its average FP shape was viewed in Excel to determine if FPs (Figure 3-7) were detected or if NEER [13] had instead mistaken noise in the segment for FPs. Guidelines established prior to the current study (for a review, see [60]), that were employed in previous studies [11, 13, 17, 61], were used to determine whether NEER detected FPs in a given segment; and all EVestG data for segments in which NEER appeared to have mistaken noise for FPs were excluded from analysis and further pre-processing. For each participant, EVestG data were also

excluded from analysis and further pre-processing for segments recorded during ‘stop’ trials in which the participant responded before the ‘stop’ signal.

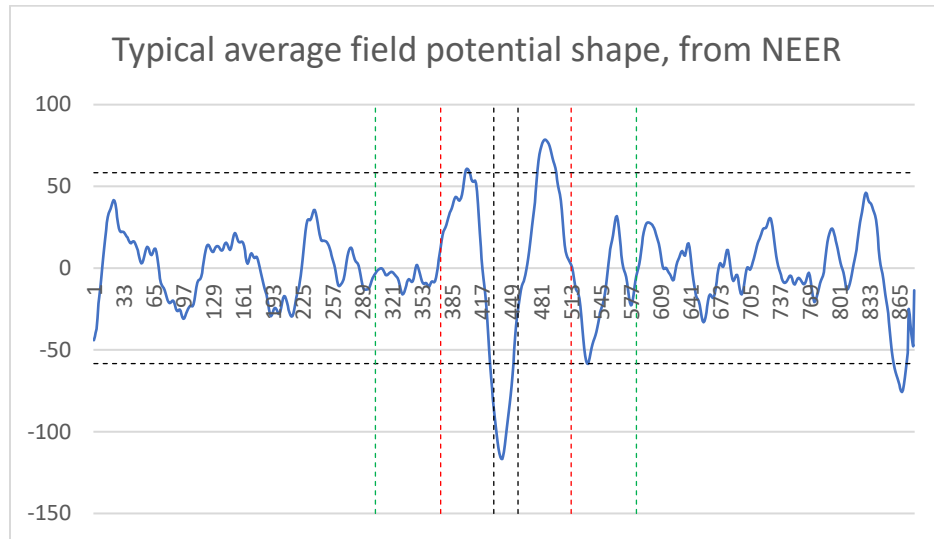


Figure 3-7. An average FP shape. A data segment was excluded from analyses if the average FP shape for the segment exhibited any of the following criteria: 1) the width of the large trough in the center was narrower than the gap between the vertical black dashed lines (at the $y = 0$ line), 2) any peaks between the red dashed lines exceeded $2/3$ of the magnitude of the central trough, or 3) any trough between the red dashed lines exceeded $2/3$ of the magnitude of the central one. The vertical axis is amplitude (in μV) and the horizontal axis is time index (in sample numbers).

3.5.3 EVestG Data Analysis

In the EVestG Experiment, the hypothesis was that the SST would produce a GCSR ‘analogue’ that, like GCSR, would be characterized by (on average) significantly larger (stop–go) differences in the outcome variable for ‘intermediate’ SSD trial pairs than for ‘short’ and ‘long’ SSD trial pairs (for a review of GCSR, see section 2.6). Because rodent hTheta has been shown to entrain the *firing patterns* of neurons outside the HPC [32], the outcome variable for the EVestG Experiment related to firing patterns of FPs (rather than the *other* form of data that is generated by NEER, namely average FP shapes).

In EVestG studies [11, 13, 17, 61], the firing patterns of FPs in a segment were analyzed by creating a histogram (IH) of each interval between pairs of FPs in the segment that were separated by 33 inter-FP gaps (creating the segment’s “IH-33” data; Figure 3-8). This value of ‘33’

for the IH was chosen because the average inter-FP gap was found to be ~ 3.3 ms; and 33 gaps of this duration would yield (on average) an overall ~ 100 -ms interval spanning one (typical 10-Hz) cycle of alpha waves — the suspected source of FP modulation in EVestG studies (for a review, see [17]). Centering these IHs at 100-ms was intended to highlight frequency shifts relative to the expected average frequency of the modulation and therefore make such shifts the primary outcome variable (Brian Lithgow, personal communication, 21 June 2021). In the current study, however, IHs were centered at 125-ms to highlight shifts in frequency relative to the centre of the expected 4-12 Hz range (i.e., 8 Hz, the reciprocal of 125 ms) because the hypothesis was that a human analogue of (4-12 Hz) rodent hTheta would entrain FPs (as was discussed in Chapter 2); and an IH was made for each of the 66 in-ear EEG data segments of a recording (participant, ear).

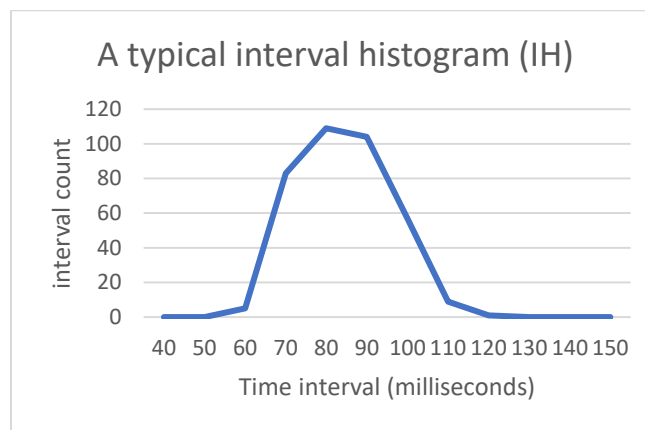


Figure 3-8. Interval histogram of FPs separated by 33 inter-FP gaps in a 1-second segment.

For each volunteer (N=4) and in-ear EEG channel (left, right), 66 IHs were averaged across all trials of the same type (stop, go) and SSD (short, intermediate, long), thus creating (6) “average” ‘short stop,’ ‘short go,’ ‘intermediate stop,’ ‘intermediate go,’ ‘long stop’ as well as ‘long go’ IHs (Figure 3-9; each was the average of 11 IHs) for each recording (participant and in-ear EEG channel). Each participant’s 6 IHs were therefore analogous to each participant’s 6 spectra in the EEG group. (IHs excluded in pre-processing were excluded from these averages, and if five or more IHs of the same trial type and SSD were excluded, then the entire average was excluded from data analyses).

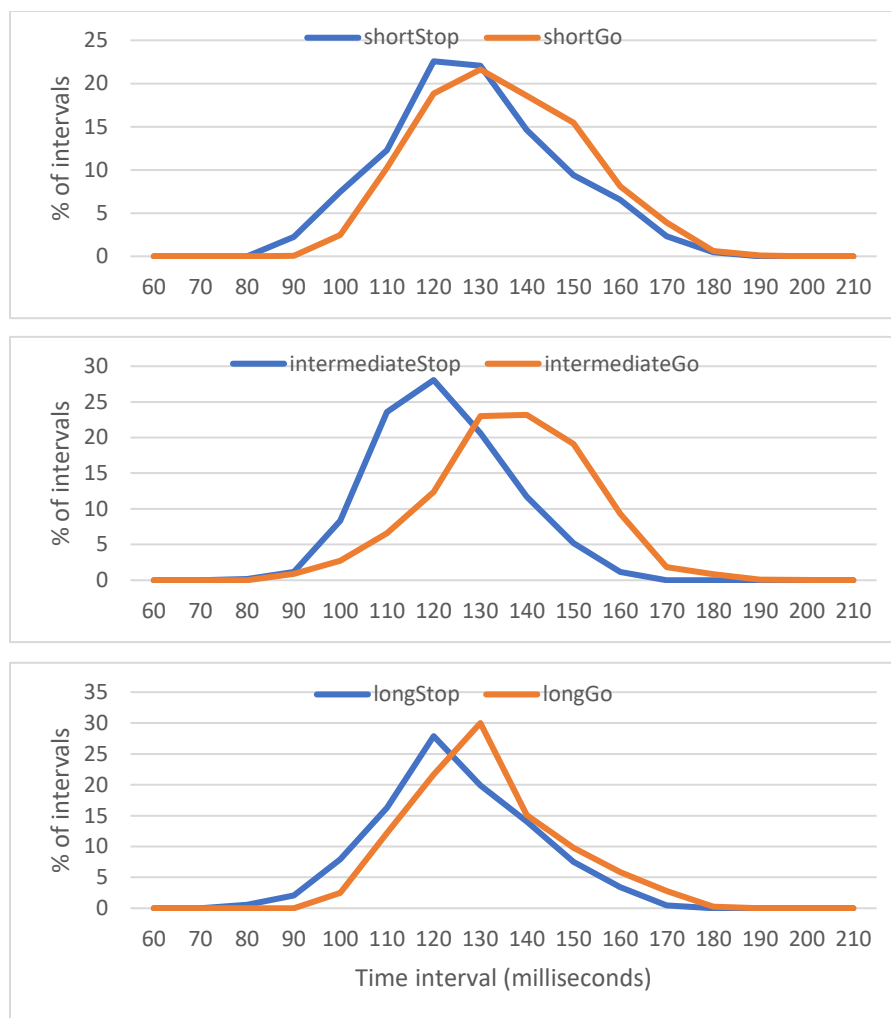


Figure 3-9. A participant's 6 average IHs, with IHs for 'stop' and 'go' trials of the same SSD overlapped to highlight effects of 'stopping.' Top to bottom: short, intermediate and long SSDs. Here, the greatest shift between 'stop' and 'go' levels is seen to occur for the intermediate SSD.

Whereas every IH in previous EVestG studies [11, 13, 17, 61] was based on the same number (33) of inter-FP gaps (as the goal was to center all IHs around the same 100 ms interval based on the same ~ 3.3 ms experimentally measured average inter-FP gap), for each recording (participant, ear) in the current study, to maintain a constant 125 ms centering, the number of inter-FP gaps used for an IH depended on the average inter-FP gap *for the recording*. (Specifically, each IH was based on a number of inter-FP gaps equal to the average number of FPs per 1-second segment of the 66 segments in a recording, multiplied by the time interval; 0.125 s). This caused all IHs for all recordings to collectively center around 125 ms while allowing IHs for the same recording to shift relative to 125 ms. This departure from the above prior studies [11, 13, 17, 61]

was intended to correct for differences in basal firing rates and noise levels *between participants* that could underly differences in average inter-FP gaps between participants (which were not under investigation, as the goal was to identify *within-subjects* differences caused by the trial conditions).

Statistical tests in the EVestG Experiment were identical to those in the EEG Experiment; however, the outcome variable related to IHs of FP intervals instead of frontal EEG power spectra — and the independent variable ‘time’ (60-210 ms) was analysed instead of ‘frequency’ (4-12 Hz). Therefore, to determine whether a GCSR ‘analogue’ occurred, repeated measures ANOVA (SPSS) contrasted average ‘short stop,’ ‘short go,’ ‘intermediate stop,’ ‘intermediate go,’ ‘long stop’ and ‘long go’ IHs using repeated measures factors ‘type’ (stop, go), ‘SSD’ (short, intermediate, long) and ‘time’ (60-210 ms, 10 ms bins; for a review of GCSR statistical analysis, see [1]). Importantly, the range of 60-210 ms for ‘time’ was used because this was the minimum range needed to contain all data that fell within all interval histograms of all participants (in the EVestG group).

As with the EEG Experiment, a *quadratic* contrast was tested for ‘SSD’ because (as discussed) like GCSR, a GCSR ‘analogue’ should be characterized by (stop–go) differences in the outcome variable significantly larger for ‘intermediate’ SSD trial pairs than for ‘short’ and ‘long’ SSD trial pairs (on average); thus, the outcome variable should go from low, to high, to low as SSD goes from short, to intermediate, to long [1]. Additionally (as was done in the EEG Experiment), a linear contrast was added for ‘type’ (‘stop’ or ‘go’) because this contrast was expected (in Shadli et al. [1] and the current study) to isolate the effect of the ‘stop’ signal.¹⁵

As with the EEG Experiment, the within-subjects ‘type’ x ‘SSD’ (linear x quadratic) interaction if statistically significant ($p < 0.05$) would validate the hypothesis for the experiment (which in the EVestG Experiment was that a GCSR ‘analogue’ would occur during the SST). Additionally (as with the EEG Experiment), the within-subjects ‘type’ x ‘SSD’ (linear x linear) interaction was predicted to be *insignificant*; while ‘type’ (linear) was expected to be *significant*. To maximize statistical power, the only order of polynomial for the independent variable ‘time’ in the ‘type’ x ‘SSD’ x ‘time’ (linear x quadratic x order) interaction that was inspected was the one that was found to be significant for the independent variable ‘frequency’ in the EEG Experiment.

¹⁵ ‘Stop’ trials have a ‘stop’ signal but are otherwise identical to ‘go’ trials; therefore, differences in IHs between trial pairs should represent the effect of the ‘stop’ signal alone [1].

However, data from both ears, with and without using data from opposite sides for individuals who were left-handed, were examined (and Bonferroni correction was used to address type I errors).

To visualize the result of the quadratic contrast for the EVestG group, the (6) average IHS of each participant were averaged among participants (N=4) and across trials of the same ‘type’ and ‘SSD’ (‘short stop,’ ‘short go,’ ‘intermediate stop,’ ‘intermediate go,’ ‘long stop,’ ‘long go’) and plugged into equation 3-3 that performed the GCSR contrast using only the group averages. The result was then plotted as a function of ‘time’ (60-210 ms; 10 ms bins) and compared to the GCSR plot from the EEG Experiment, with the two plots being expected to reveal similar maxima at corresponding ‘frequency’ and ‘time’ values (in the EEG and EVestG Experiment, respectively) for which post hoc tests would assess significance. Specifically, post hoc analyses were performed for values of ‘time’ at which large peaks were apparent in the plot of the contrast, assuming the within-subjects ‘type’ x ‘SSD’ (linear x quadratic) contrast was statistically significant ($p < 0.05$).

3.6 Summary

The current study involved two groups performing the same task but with EEGs recorded from different locations (namely three frontal sites or both ear canals, respectively) during the task. The SST involved pressing keys on a keyboard in response to images presented on a monitor, where a key had to be pressed if an arrow appeared (but not if followed by an exclamation mark). Timestamps from a program that delivered the SST located segments in the EEG data for analysis; and variables from the program were analyzed to gauge each participant’s performance of the task. Ten electrodes were used to record frontal EEGs (and remove ocular artefacts) in an “EEG” group; while five electrodes (with one near each ear drum) recorded in-ear EEGs in an “EVestG” group.

In the EEG Experiment, pre-processing removed ocular artefacts via correction by multiple regression (to scale vertical and horizontal EOG channels and subtract them from F7, F8 and Fz); and sections of data that contained residual artefacts were manually replaced with missing values. The data were then analyzed in (66) 1-second segments (for each participant and frontal EEG site); and the (66) power spectra for the segments were averaged across trials of the same type and SSD, creating (6) average spectra for each volunteer in the EEG group that were then analyzed in SPSS. A within-subjects repeated measures ANOVA contrasted 4-12 Hz power between average spectra; and if the ‘type’ x ‘SSD’ (linear x quadratic) interaction was statistically significant ($p < 0.05$), then this supported the hypothesis that GCSR would occur during the SST.

In the EVestG Experiment, pre-processing entailed 1) sending (66) 1-second data segments to a (NEER) program that found (for each segment) *when* FPs occurred and the average FP shape; and 2) excluding from analyses all segments whose average FP shapes did not meet certain criteria. The times when FPs occurred in segments were then analyzed by creating a histogram (IH) of each interval between pairs of FPs in a segment that occurred a certain number of inter-FP gaps apart, thereby highlighting frequency shifts in firing patterns relative to a (8 Hz) frequency of interest. Each participant's (66) IHs were then averaged across trials of the same type and SSD, creating (6) average IHs that were then analyzed with the (6) averages of each other EVestG group member by the same within-subjects repeated measures ANOVA that was used for the EEG group (above). Finally, if the 'type' x 'SSD' (linear x quadratic) interaction was statistically significant ($p < 0.05$), then it validated the hypothesis that a GCSR 'analogue' would occur during the SST.

Chapter 4: Results

4.1 Overview

This chapter will summarize the results of the EEG Experiment and EVestG Experiment. It will begin by presenting the demographic data and statistics from the SST for each volunteer in the EEG group before comparing these to the analogous data and statistics in Shadli et al. [1], which will reveal wide differences in demographics but similar statistics from the SST. Results from the EEG Experiment will then be reviewed, including the one for the main quadratic (GCSR) contrast which did *not* reveal significant GCSR. Next, results from several post-hoc tests that were performed to scrutinize specific frequencies and frequency ranges for the GCSR contrast in the EEG Experiment will be explained; and other results from ANOVA tests of some hypotheses from (BIS) theory will then be reviewed. Importantly, the main GCSR contrast will be plotted and its features (including its 9 Hz peak frequency) highlighted and compared to plots in prior studies.

The demographics and statistics from the SST for each volunteer in the EVestG group will then be provided and compared to their analogous data and statistics in Shadli et al. [1]; which will again reveal wide demographics differences but similar statistics from the SST. Results from the EVestG Experiment will then be covered, including the one for the main quadratic (GCSR) contrast which revealed a GCSR ‘analogue.’ Next, results from several post-hoc tests that were performed to scrutinize specific time bins and time bin ranges for the GCSR contrast in the EVestG Experiment will be explained; and other results from ANOVA that tested some hypotheses from (BIS) theory will then be reviewed. Importantly, the GCSR ‘analogue’ will be plotted and its large, singular peak that occurred at 110 ms (corresponding to 9 Hz) will be highlighted.

4.2 EEG Experiment

4.2.1 Demographics and SST Statistics

In this section, the demographic data and SST statistics for the EEG group in the current study will be presented and compared to the demographic data and SST statistics in the experiment (“Experiment 2”) of Shadli et al. [1] that the EEG Experiment was aimed at partially replicating. The purpose of comparing demographic data from the current study to those of Shadli et al. [1] was to identify any differences between study populations that could cause discrepancies between EEG data recorded during the SST in the current study and those reported by Shadli et al. [1].

Meanwhile, the goal of contrasting statistics from the SST between the studies was to determine whether the SST program in the current study elicited results similar to those in Shadli et al. [1] *despite* the SST program in the current study having been recreated based on the description of the program in the Shadli et al. [1] publication (and despite demographic differences alluded to above). Critically, as Shadli et al. [1] did not include raw data or standard deviations for demographics or SST statistics, only the means were compared across studies for most of these data and statistics. (It is also worth noting that Shadli et al. [1] assessed measures of anxiety via questionnaires that were analyzed alongside GCSR, whereas the current study merely attempted to produce GCSR).

As outlined in the previous chapter, five volunteers participated in the “EEG Experiment:” two males (1 left-handed) and three females (1 left-handed) with an average age of 49 ± 17 years (SD; see Table 3-1). These demographic data are quite unlike those in the Shadli et al. [1] study (that the EEG Experiment in the current study was aimed at partially replicating; see Table 4-1). Importantly, Shadli et al. [1] included only right-handed volunteers (whereas 40% of participants in the EEG Experiment were left-handed); and mean participant age in Shadli et al. [1] was only 20 years (or about 2.5 times lower than in the EEG Experiment). However, males and females were nearly balanced in both Shadli et al. [1] (44% males) and the EEG Experiment (40% males).

Table 4-1. The demographic data of the participants in “Experiment 2” of Shadli et al. [1].

	Average Age	Sex	Handedness
Shadli et al. (2016)	20 years	8 Males, 10 Females	All were right-handed

Meanwhile, the SST statistics of the EEG group (see Table 4-2) that determined whether a volunteer’s EEG data were included in analyses were similar to those in prior studies [16, 28, 31] (including Shadli et al. [1]). The EEG group successfully ‘stopped’ (did not press a key) after the ‘stop’ signal (exclamation mark): most often in short SSD ‘stop’ trials (M=91, SD=16%), less often in intermediate SSD ‘stop’ trials (M=58.2, SD=15.5%) and least often in long SSD ‘stop’ trials (M=22.4, SD=8.3%; see Table 4-3), indicating that the ‘alignment’ of the above three SSD ‘staircases’ was correct (for the group); however, means were slightly higher than in Shadli et al. [1] (M=83, 44 and 8% for short, intermediate and long SSDs, respectively). Crucially, the SSD staircases were properly aligned for all participants in the EEG group; therefore, none of the participants’ EEG data were excluded from analyses because of improper SSD staircase alignment.

Additionally, success rates in ‘go’ trials were above 90% for all participants in the EEG group ($M=94.4$, $SD=2.3\%$); and no participants’ reaction times in ‘go’ trials varied widely across trials (Figure 4-1), furthermore indicating that no EEG group participant exhibited significant ‘slowing.’

Table 4-2. SST statistics of the EEG group participants. ‘GO_RT’ is the average reaction time in ‘go’ trials; ‘Go pass’ is the success rate in ‘go’ trials; ‘Int SSD Avg’ is the average intermediate SSD value; ‘SSRT’ is ‘GO_RT’ minus ‘Int SSD Avg;’ and ‘Short,’ ‘Intermed.’ and ‘Long SSD’ are short, intermediate and long ‘stop’ trial success rates.

Participant (code)	GO_RT (ms)	Go pass (%)	SSRT (ms)	Int SSD Avg (ms)	Short SSD (%)	Intermed. SSD (%)	Long SSD (%)
P-1	596	95	295	301	91	64	30
P-2	453	98	189	264	100	55	20
P-3	550	94	306	244	64	45	22
P-4	471	92	289	181	100	45	30
P-5	557	93	248	309	100	82	10

Table 4-3. Mean SST values of the EEG group for comparison with those of Shadli et al. (2016). ‘GO_RT’ is the average reaction time in ‘go’ trials; ‘Go pass’ is the success rate in ‘go’ trials; ‘Int SSD Avg’ is the average intermediate SSD value; ‘SSRT’ is ‘GO_RT’ minus ‘Int SSD Avg;’ ‘Short,’ ‘Intermed.’ and ‘Long SSD’ are short, intermediate and long ‘stop’ trial success rates.

Group	GO_RT (ms)	Go pass (%)	SSRT (ms)	Int SSD Avg (ms)	Short SSD (%)	Intermed. SSD (%)	Long SSD (%)
EEG group	525	94	265	260	91	58	22
Shadli group	426	?	227	?	83	44	8

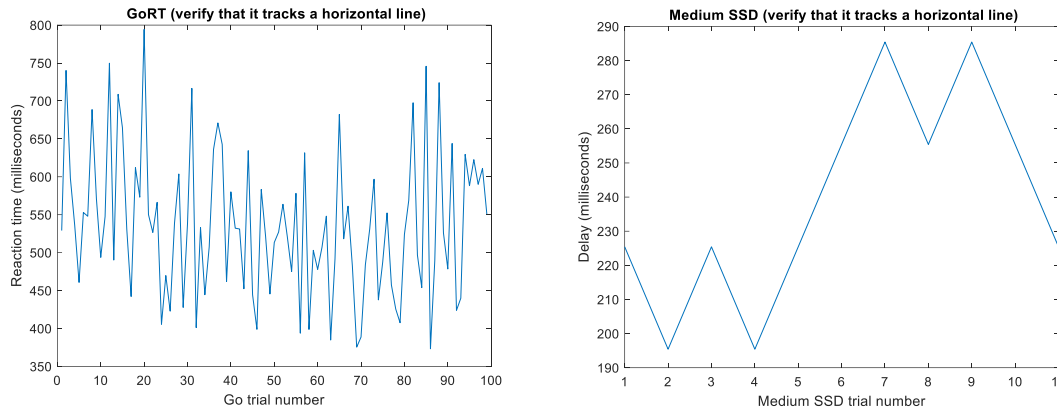


Figure 4-1. SST data used to track a participant's performance of the SST. Plots that did not track a horizontal line may have indicated 'slowing' (though this was not disqualifying).

Other SST statistics were also similar to those that were reported in Shadli et al. [1]. Most participants' intermediate SSD values ($M=260, SD=51$ ms) tracked a horizontal line (Figure 4-1), indicating consistent performance during the task; while others' rose over time (but still oscillated), suggesting improvement with time. Notably, these two types of behaviour had been observed during the SST in prior studies (Neil McNaughton, personal communication, 13 November 2019). Interestingly, 'go' reaction time (GO_RT; which is the average reaction time across all 'go' trials for a participant) when averaged across all participants in the EEG group was nearly 100 ms higher ($M=525, SD=61$ ms) than the GO_RT group average ($M=426$ ms) in Shadli et al. [1] (see Table 4-3); however, this average in Shadli et al. [1] was close to one GO_RT (453ms) in the current study (see Table 4-2). Despite this GO_RT difference, stop signal reaction time (SSRT; $M=265, SD=48$ ms), which is the average intermediate SSD subtracted from the abovementioned GO_RT, when averaged across all participants was similar to the group average ($M=227$ ms) that was reported by Shadli et al. [1] (see Table 4-3). Together, the results that were described in this section suggest that the program used in the current study to deliver the SST did not deviate widely from the one that delivered the SST in Shadli et al. [1].

4.2.2 EEG Experiment Results did not Reveal GCSR

As was discussed in section 3.4.3, (6) 'average' power spectra ('short stop,' 'short go,' 'intermediate stop,' 'intermediate go,' 'long stop' and 'long go' averages) were calculated for every EEG channel (F7, F8, Fz) of every participant ($N=5$) in the EEG group, where each of the 6 'average' power spectra averaged 11 power spectra (for 11 EEG data segments recorded during

SST trials of the same ‘type’ and ‘SSD’); however, any of these 11 power spectra that contained missing values were not included in an ‘average’ power spectrum; and an ‘average’ power spectrum was excluded if fewer than 7 of the spectra that it averaged had no missing values. Note: this section only presents results for analyses performed on ‘F8’ because this site was the focus of “Experiment 2” in Shadli et al. [1] (which the current study was aimed at replicating) that found F8 elicited the most robust GCSR (F7 and Fz results will be available after publication).

For the F8 site, each participant in the EEG group ended up with 6 ‘average’ power spectra, since each participant had at least 7 power spectra to average (that did not contain missing values) for each ‘type’ and ‘SSD’ of ‘average’ power spectrum (included spectra are listed in Table 4-4). For each volunteer, the quadratic (GCSR) contrast of their 6 ‘average’ power spectra was found using equation 3-3 (these results will be plotted separately and made available after publication); and the resulting 5 contrasts (1 per volunteer) were averaged to form the ‘group quadratic contrast’ that is visualized in Figure 4-2 (where this ‘group quadratic contrast’ is plotted against ‘frequency’). Note: data from the F7 sites of left-handed participants were used for the ‘group quadratic contrast’ while F8 data were used for right-handed individuals because (as discussed in the prior section), Shadli et al. [62] previously showed that F7 in left-handed volunteers responds similarly to F8 in right-handed volunteers (during the SST); and EEG data from left- and right-handed volunteers can thus be combined, using F7 for left-handed individuals and F8 for right-handed individuals.

Table 4-4. Numbers of included power spectra by trial condition and EEG group participant. Participants had at least 7 included spectra for each condition and therefore 6 average spectra (short stop, short go, intermediate stop, intermediate go, long stop and long go average spectra).

Participant (code)	Short Stop spectra (#)	Short Go spectra (#)	Inter Stop spectra (#)	Inter Go spectra (#)	Long Stop spectra (#)	Long Go spectra (#)
P-1	10	9	10	11	8	10
P-2	11	11	11	10	9	10
P-3	11	11	11	11	9	11
P-4	11	11	11	11	10	11
P-5	11	11	9	11	10	11

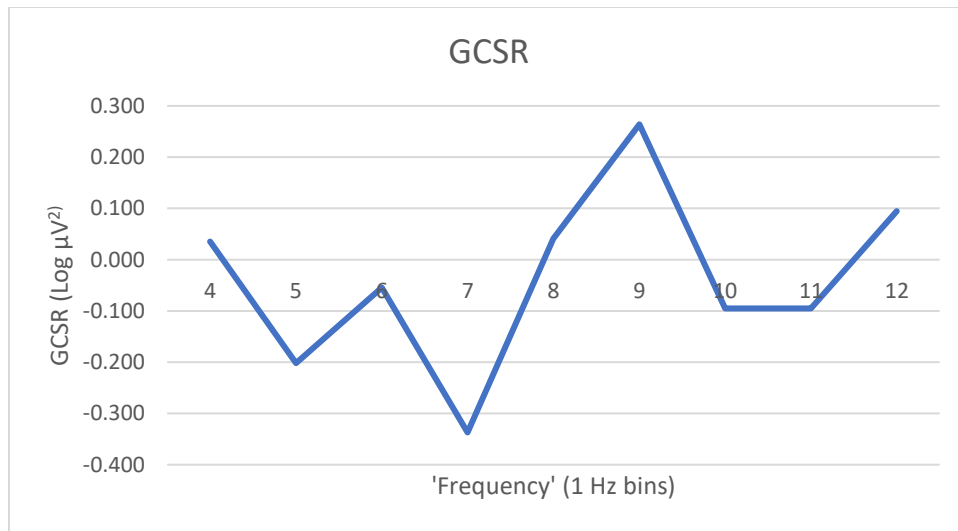


Figure 4-2. GCSR plot for the EEG Experiment. (GCSR did not reach statistical significance).

The ‘group quadratic contrast’ plot (Figure 4-2) has an absolute minimum and an absolute maximum at 7 Hz and 9 Hz that could indicate possible negative and positive GCSR, respectively — where positive GCSR would validate the hypothesis, and negative GCSR would invalidate it (for a review of positive and negative GCSR and their implications, see [16]). Before determining whether GCSR occurred at any particular subset of frequencies, however, the quadratic contrast was performed on the full (4-12 Hz) range using repeated measures ANOVA (as this contrast was the main outcome measure in Shadli et al. [1], i.e., the study that the EEG Experiment was aimed at partially replicating). Note: ‘group quadratic contrast’ plots are also referred to as “GCSR plots,” even when results do not show significant GCSR [1].

As was discussed in section 3.4.3, a within-subjects ‘type’ x ‘SSD’ (linear x quadratic) contrast tested whether GCSR occurred during the SST. While it was expected (based on Shadli et al. [1]) that ‘type’ and ‘SSD’ would have linear and quadratic effects (respectively) on the outcome variable (i.e., frontal EEG power), the hypothesis for the effect of ‘frequency’ was less specific because some studies reported significance for a linear component of a ‘frequency’ effect, while other studies found significance for higher order effects of this factor. (For example, Neo et al. [28], McNaughton et al. [16], Shadli et al. [31] and Shadli et al. [1] reported significance for quadratic, cubic, cubic and linear effects of ‘frequency,’ respectively). Vitaly, an author of (Shadli et al. [1]; Neil McNaughton, personal communication, 9 June 2021) noted that some versions of the SST seemed to elicit effects of ‘frequency’ as high as fifth order. Thus, the hypothesis was that

($p < .05$) significance would be found in the first five orders of effects for the ‘frequency’ factor in the within-subjects repeated measures ‘type’ x ‘SSD’ x ‘frequency’ (linear x quadratic x order) contrast, where Bonferroni correction would be used to offset inflation of type I errors generated by inspecting multiple (5) orders of polynomial effects for ‘frequency.’ Similarly, only orders 1-5 of ‘frequency’ effects were inspected for *all* tests in the EEG Experiment, for which p-values also had to be below 0.05 after Bonferroni correction to reach statistical significance.

Results from SPSS revealed that orders 1-5 of polynomial effects for ‘frequency’ (in the within-subjects repeated measures ‘type’ x ‘SSD’ x ‘frequency’ linear x quadratic x order contrast) had uncorrected p-values of 0.336, 0.714, 0.418, 0.047 and 0.251, respectively (see Table 4-5). Notably, the uncorrected p-value (above) for the fourth order (quartic) effect of ‘frequency’ was below 0.05 (‘type’ x ‘SSD’ x ‘frequency,’ linear x quadratic x quartic, $F(1,4) = 8.06$, $p = 0.047$); therefore, GCSR was significant *without* correction; however, GCSR failed to reach significance after Bonferroni correction (i.e., multiplying the p-value of 0.047 by 5, for the five orders tested).

Table 4-5. Main GCSR contrast results from SPSS, showing that the quartic term for the ‘frequency’ polynomial had a p-value below 0.05. After Bonferroni correction (for the five orders that were tested), however, the result did not reach significance.

Order of polynomial for ‘frequency’	Type III sum of squares	df	Mean Square	F	Sig.
Linear	0.032	1	0.032	1.196	0.336
Quadratic	0.006	1	0.006	0.155	0.714
Cubic	0.039	1	0.039	0.812	0.418
Order 4	0.080	1	0.080	8.055	0.047
Order 5	0.066	1	0.066	1.797	0.251

Notably, Shadli et al. [1] reported “clear” GCSR at F8 in “Experiment 2” of their study, “in block-1 (Stop-Go x SSD[quadratic] x frequency[linear]: $F(1, 18) = 10.19$, $P < 0.01$) and in block-3 (Stop-Go x SSD[quadratic] x frequency[linear]: $F(1,18) = 5.09$, $p < 0.05$) but not block 2” (where each of the three “blocks” consisted of 128 ‘stop-go’ trials of the SST); and the GCSR plots for blocks 1 and 3 had positive values across nearly all frequencies (Figure 4-3).

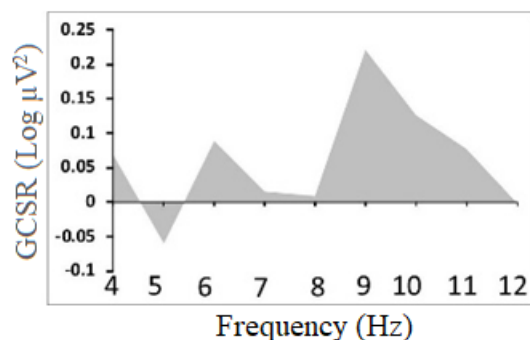


Figure 4-3. A GCSR plot in Shadli et al. [1] that appears similar to the one in the current study (in terms of frequency distribution and peak frequency). Source: Adapted from [1].

Despite GCSR not reaching significance (after Bonferroni correction) in the current study, post-hoc analyses were performed on subsets of frequencies that appeared noteworthy in Figure 4-2. First, the absolute minimum and maximum (in the centre of the 4-12 Hz range) at 7 Hz and 9 Hz that suggested possible negative and positive GCSR (respectively) were analyzed separately and revealed uncorrected p-values close to 0.10 for the ‘type’ x ‘SSD,’ linear x quadratic interaction (7 Hz: $F(1,4) = 4.48$, $p = 0.10$, uncorrected; 9 Hz: $F(1,4) = 4.77$, $p = 0.09$, uncorrected). Notably, all other frequencies in the 4-12 Hz range produced larger uncorrected p-values (vs. 7 and 9 Hz; as summarized in Table 4-6) when these other 4-12 Hz frequencies were likewise tested separately. Therefore, significant GCSR was also not found for any *individual* frequency in the 4-12 Hz range.

Table 4-6. Results of GCSR contrast for each 4-12 Hz level of ‘frequency,’ tested separately.

Frequency (Hz)	Type III Sums of Squares	df	Mean Square	F	Sig.
4	0.002	1	0.002	0.038	0.856
5	0.068	1	0.068	3.107	0.153
6	0.005	1	0.005	0.283	0.623
7	0.189	1	0.189	4.482	0.102
8	0.003	1	0.003	0.658	0.463
9	1.117	1	1.117	4.771	0.094
10	0.015	1	0.015	1.34	0.311
11	0.015	1	0.015	0.67	0.459
12	0.015	1	0.015	0.448	0.54

Additional post-hoc analyses were performed for 5-11, 6-10 and 7-9 Hz frequency ranges (that centered on 8 Hz), as some previous studies [1, 31] analyzed frequency ranges that (like hTheta) centered at 8 Hz, but were narrower than the rodent 4-12 Hz hTheta band. In the current study, the 5-11, 6-10 and 7-9 Hz ranges all yielded uncorrected p-values near 0.05, though for different orders of ‘frequency’ effect, namely fifth, third and first orders, respectively (see Table 4-7). The first order effect of ‘frequency’ on the outcome variable from 7 to 9 Hz is intuitive, as the plot of the contrast nearly forms a straight line between the two frequencies (Figure 4-2); and as the frequency range extends to include 6-10 or 5-11 Hz, the plot begins changing directions at both ends, hinting that third or fifth orders may become better fits (as the above results suggest). Notably, the above frequency ranges (that were narrower than the standard 4-12 Hz hTheta range) bore no significant GCSR (after Bonferroni correction for unpredicted ‘frequency’ effect orders).

Table 4-7. Results of GCSR contrast for 5-11, 6-10 and 7-9 Hz ranges of ‘frequency.’

Frequency (Hz)	Frequency effect order	Type III Sums of Squares	df	Mean Square	F	Sig.
5 - 11	5	0.213	1	0.213	7.891	0.048
6 - 10	3	0.257	1	0.257	7.168	0.055
7 - 9	1	0.301	1	0.301	6.677	0.061

In prior studies [1, 31], frequency ranges narrower than the 4-12 Hz range (for the ‘group quadratic contrast’) resulted from three-point smoothing,¹⁶ which is typically performed to make identifying general trends easier [1, 31]. To this end (as well as to facilitate comparison with results in prior studies [1, 31]), the ‘group quadratic contrast’ in the current study (Figure 4-2) was three-point smoothed (Figure 4-4). As can be seen in Figure 4-4, the ‘group quadratic contrast’ appears much simpler after smoothing, as it exhibits 1) a single maximum, at the same (9 Hz) frequency as the absolute maximum before smoothing, and 2) a single minimum, that unlike the 7 Hz absolute minimum prior to smoothing occurred at 6 Hz (Figure 4-4).

¹⁶ Critically, three-point smoothing causes the loss of a bin at each end of the data being smoothed; thus, if only 4-12 Hz data is available, then the final range is 5-11 Hz (as with Shadli et al [1]).

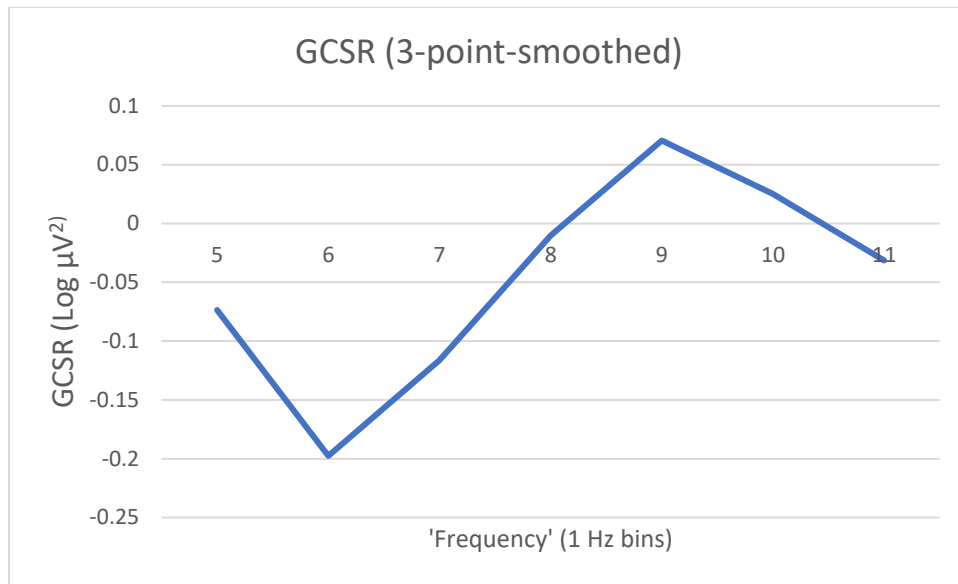


Figure 4-4. Three-point-smoothed GCSR plot from the EEG Experiment in the current study.

(Note: GCSR did not reach significance).

Further tests determined whether the SST from the current study yielded results similar to those that prior studies [1, 31] described as being predicted by (BIS) theory. First, a within-subjects ‘type’ x ‘SSD’ x ‘frequency’ (linear x linear x order) contrast tested for differences in frontal EEG power between short and long SSD conditions (independently of medium SSD conditions), but yielded no uncorrected p-values below 0.05 for ‘frequency’ effect orders 1-5 (see Table 4-8) — consistent with (BIS) theory (though not a necessary condition for GCSR, which only requires that more EEG power occurs for intermediate SSDs than for the average of short and long SSDs [1]).

Table 4-8. Results for test of variation between effects of short and long SSDs on F8 power independent of the intermediate SSD. BIS theory predicts no variation between effects of short and long SSDs. As results were insignificant, no significant variation was detected.

Order of polynomial for ‘frequency’	Type III Sum of Squares	df	Mean Square	F	Sig.
Linear	0.005	1	0.005	0.051	0.832
Quadratic	0.014	1	0.014	2.762	0.172
Cubic	0.093	1	0.093	1.591	0.276
Order 4	0.025	1	0.025	0.521	0.510
Order 5	0.014	1	0.014	0.381	0.570

Next, the within-subjects ‘type’ x ‘frequency’ (linear x order) contrast tested ‘stopping’ (averaged across short, intermediate and long SSDs) and revealed uncorrected p-values below 0.05 for both linear (‘type’ x ‘frequency,’ linear x linear, $F(1,4) = 23.19$, $p = 0.009$, uncorrected) and quartic (‘type’ x ‘frequency,’ linear x quartic, $F(1,4) = 16.55$, $p = 0.015$, uncorrected) ‘frequency’ effects (see Table 4-9), where the linear ‘frequency’ effect was significant after Bonferroni correction ($p = .045$), but the quartic ‘frequency’ effect was not ($p = .075$). Vitaly, the ($p = .045$) significant result for the linear ‘frequency’ effect indicates a significant effect of the ‘stop’ signal (averaged across short, intermediate and long levels of ‘SSD’) on EEG power at F8 because the only difference between ‘stop’ and ‘go’ trials is the ‘stop’ signal [1]. Whether the neural circuits responsible for the increases in 4-12 Hz EEG power at F8 related to 1) ‘stopping,’ 2) the color of the circle changing from green to red, or 3) some other effect of the ‘stop’ signal remains unclear.

Table 4-9. Results for test of variation between ‘stop’ and ‘go’ effects on F8 power. BIS theory predicts variation between ‘stop’ and ‘go’ effects. A ‘stopping’ effect was detected because the linear ‘frequency’ term was significant after Bonferroni correction.

Order of polynomial for ‘frequency’	Type III Sum of Squares	df	Mean Square	F	Sig.
Linear	1.135	1	1.135	23.188	0.009
Quadratic	0.097	1	0.097	2.065	0.224
Cubic	0.006	1	0.006	0.205	0.674
Order 4	0.089	1	0.089	16.552	0.015
Order 5	0.002	1	0.002	3.342	0.142

4.3 EVestG Experiment

Whereas the ‘EEG Experiment’ (in the above section) was aimed at partially replicating “Experiment 2” of Shadli et al. [1] by eliciting GCSR in frontal EEGs, the ‘EVestG Experiment’ (whose results will be outlined in this section) was a novel experiment aimed at eliciting a GCSR ‘analogue’ in EVestG data via methods *analogous* to those in “Experiment 2” of Shadli et al. [1].

4.3.1 Demographics and SST Statistics

This section will outline the demographic data and SST statistics of the EVestG group and compare these to the demographic data and SST statistics in “Experiment 2” of Shadli et al. [1]. While electrophysiological data from the EVestG Experiment were not compared with those in

Shadli et al. [1], the SST that was used in the current study was recreated based on descriptions of the SST that was employed in Shadli et al. [1]; and it was therefore necessary to compare SST statistics between the EVestG Experiment and “Experiment 2” of Shadli et al. [1] — to ensure that the SST functioned properly. Meanwhile, demographics needed to be compared between studies because differences in demographics could have contributed to differences in SST statistics.

The EVestG Experiment began with five volunteers (as was discussed in Chapter 3); however, one was excluded due to artefacts (as was explained in this chapter), leaving two males (1 left-handed) and two females with an average age of 53 ± 15 years (SD) in the EVestG group (see Table 3-1). These demographic data are quite unlike those of Shadli et al. [1] (see Table 4-1). Notably, Shadli et al. [1] included only right-handed volunteers (whereas 25% of participants in the EVestG Experiment were left-handed); and mean participant age in Shadli et al. [1] was only 20 years (or about 2.5 times lower than in the EEG Experiment). However, males and females were nearly balanced in both Shadli et al. [1] (44% males) and the EEG Experiment (50% males).

Meanwhile, the SST statistics of the EVestG group (see Table 4-10) that decided whether a volunteer’s EVestG data would be included were similar to those in previous studies [16, 28, 31] — including Shadli et al. [1]. The EVestG group successfully ‘stopped’ (pressed no key) after the ‘stop’ signal (exclamation mark): most often in short SSD ‘stop’ trials ($M=91$, $SD=12.7\%$), less often in intermediate SSD ‘stop’ trials ($M=61.3$, $SD=24.2\%$) and least often in long SSD ‘stop’ trials ($M=8.5$, $SD=5.8\%$; see Table 4-11), indicating that the ‘alignment’ of the above three SSD ‘staircases’ was correct (for the group); however, means were slightly higher than in Shadli et al. [1] ($M=83$, 44 and 8% for short, intermediate and long SSDs, respectively). Crucially, the SSD staircases were properly aligned for all participants in the EVestG group; thus, no participant’s EVestG data had to be excluded from analyses as a result of improper SSD staircase alignment. Additionally, success rates in ‘go’ trials were above 90% for all participants in the EVestG group ($M=93.3$, $SD=2.1\%$); and no participant’s reaction times in ‘go’ trials varied widely across trials (Figure 4-1), together indicating that no EVestG group participant exhibited significant ‘slowing.’

Table 4-10. SST statistics of the EVestG group participants. 'GO_RT' is the mean reaction time in 'go' trials; 'Go pass' is the success rate in 'go' trials; 'Int SSD Avg' is the average intermediate SSD value; 'SSRT' is 'GO_RT' minus 'Int SSD Avg;' and 'Short,' 'Intermed.' and 'Long SSD' are short, intermediate and long 'stop' trial success rates.

Participant (code)	GO_RT (ms)	Go pass (%)	SSRT (ms)	Int SSD Avg (ms)	Short SSD (%)	Intermed. SSD (%)	Long SSD (%)
P-2	405	96	232	173	91	45	0
P-5	404	87	238	166	73	36	11
P-6	557	93	248	309	100	82	10
P-7	610	93	307	304	100	82	13

Table 4-11. SST mean values of the EVestG group to compare with those of Shadli et al. (2016). 'GO_RT' is the average reaction time in 'go' trials; 'Go pass' is the success rate in 'go' trials; 'Int SSD Avg' is the average intermediate SSD value; 'SSRT' is 'GO_RT' minus 'Int SSD Avg;' 'Short,' 'Intermed.' and 'Long SSD' are short, intermediate and long 'stop' trial success rates.

Group	GO_RT (ms)	Go pass (%)	SSRT (ms)	Int SSD Avg (ms)	Short SSD (%)	Intermed. SSD (%)	Long SSD (%)
EVestG group	494	92	256	238	91	61	9
Shadli group	426	?	227	?	83	44	8

Other SST statistics were also found to be similar to those in Shadli et al. [1]. Most participants' intermediate SSD values (M=238,SD=79ms) tracked a horizontal line (Figure 4-1), indicating consistent performance during the task; while others' rose over time (but still oscillated), suggesting improvement with time. Notably, these two types of behaviour had been observed during the SST in prior studies (Neil McNaughton, personal communication, 13 November 2019). Additionally, 'go' reaction time (GO_RT; which is the average reaction time across all 'go' trials for a participant) when averaged across all participants in the EVestG group was only 68 ms higher (M=494, SD=106ms) than the GO_RT group average (M=426ms) in Shadli et al. [1] (see Table 4-11). Furthermore, stop signal reaction time (SSRT; M=256, SD=34ms), which is equal to the

average intermediate SSD subtracted from the abovementioned GO_RT, when averaged across all participants was similar to the group average in Shadli et al. [1] (M=227ms; see Table 4-11). Together, the results in this section suggest that the program that delivered the SST in the current study did not deviate widely from the one that delivered the SST in Shadli et al. [1].

4.3.2 EVestG Experiment Results Confirm GCSR ‘Analogue’

As was discussed in section 3.5.3, for each in-ear channel (left, right) of each EVestG group participant, 66 IHs were averaged across trials of the same ‘type’ (stop, go) and ‘SSD’ (short, intermediate, long), thus creating 6 “average” (‘short stop,’ ‘short go,’ ‘intermediate stop,’ ‘intermediate go,’ ‘long stop’ and ‘long go’) IHs, that each averaged 11 IHs. (IHs excluded in pre-processing were excluded from these averages; and if five or more IHs of the same ‘type’ and ‘SSD’ were excluded, then the associated average IH was excluded from analyses).

As was stated in Chapter 3, five volunteers were originally included; however, the EVestG data for one of the volunteers were excluded from further data analyses. These data were excluded because the volunteer had too many IHs excluded in pre-processing for all trial ‘types’ and ‘SSDs.’ After this exclusion, the remaining four participants each ended up with 6 ‘average’ power spectra, as each participant had fewer than 5 IHs of the same ‘type’ and ‘SSD’ excluded in pre-processing, leaving at least seven to be averaged for each ‘type’ and ‘SSD’ of “average” IH (see Table 4-12).

Table 4-12. IHs included in analyses for each EVestG group participant by trial type and SSD. Each participant had at least 7 included IHs for each condition and therefore 6 average IHs (short stop, short go, intermediate stop, intermediate go, long stop and long go average IHs).

Participant	shortStop	shortGo	interStop	interGo	longStop	longGo
P2	11	11	9	10	9	11
P5	7	9	11	11	7	11
P6	7	8	8	7	7	7
P7	10	9	8	8	7	9

For each in-ear data channel (left, right) of each participant in the EVestG group (N=4), the quadratic (GCSR) contrast of the 6 ‘average’ IHs associated with the channel was calculated using equation 3-3 (these results will be plotted separately and made available after publication).

The resulting four contrasts from the right ears of each participant were then averaged to form the ‘right-ear group quadratic contrast’ that is shown in Figure 4-5 (and plotted against ‘time’ intervals); while the resulting four contrasts from the left ears of each participant were averaged to form the ‘left-ear group quadratic contrast’ that is similarly plotted in Figure 4-5 (against ‘time’ intervals). Lastly, ‘ipsilateral-’ and ‘contralateral-ear group quadratic contrasts’ averaged contrasts for the ear ipsilateral and contralateral to the dominant hand of each volunteer, respectively (Figure 4-5).

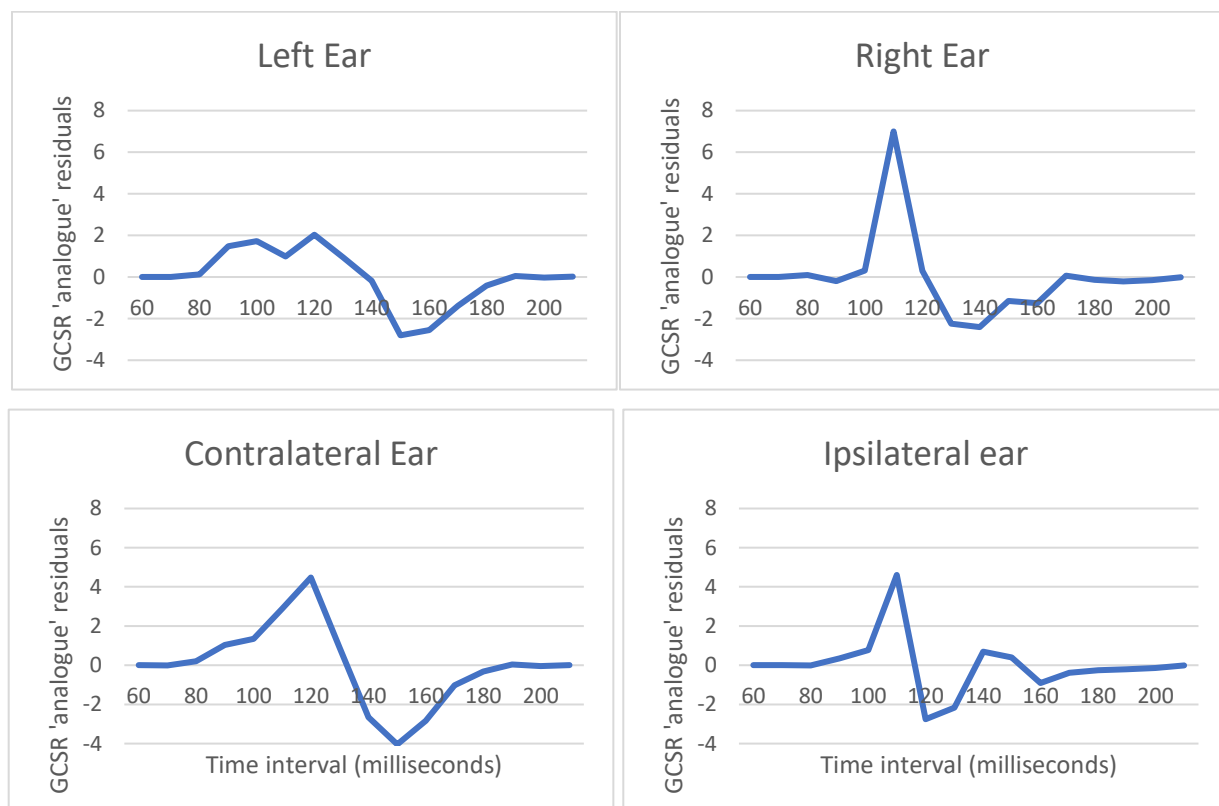


Figure 4-5. The right-ear data of the EVestG group yielded a GCSR ‘analogue’ with a tall peak at 110 ms (9 Hz). Vertical axes are the GCSR ‘analogue’ residual values (in $\log \mu V^2$ units) and the horizontal axes are ‘time’ bins (in milliseconds), centered at 125 ms (8Hz).

The ‘right-ear group quadratic contrast’ plot (Figure 4-5) has a very clear peak at 110 ms that is much taller and more well-defined than those in plots of the other group quadratic contrasts. However, before checking for statistical significance at any *particular* subset of ‘time’ intervals, the quadratic contrast was computed for the full (60-210ms) range via repeated measures ANOVA. Notably, statistical tests in the EVestG Experiment were identical to those in the EEG experiment

(though the outcome variable related to IHs of FP intervals instead of frontal EEG power spectra; and the independent variable ‘time,’ 60 - 210 ms, was analysed instead of ‘frequency,’ 4 - 12 Hz).

As was discussed in section 3.5.3, a within-subjects ‘type’ x ‘SSD’ (linear x quadratic) contrast was used to test for a GCSR ‘analogue.’ As in the EEG Experiment, ‘type’ and ‘SSD’ were expected to have linear and quadratic effects on the outcome variable, respectively; however, unlike the EEG Experiment (in which five orders of ‘frequency’ effects were tested), to increase statistical power only a quartic ‘time’ effect was tested, based on the low (0.047) uncorrected quartic ‘frequency’ effect p-value in the EEG Experiment.¹⁷ Thus, the hypothesis was that ($p < .05$) significance would be found for a quartic ‘time’ effect in the within-subjects repeated measures ‘type’ x ‘SSD’ x ‘time,’ linear x quadratic x quartic contrast. Bonferroni correction was used to offset inflated type I errors from testing four interactions because it was unclear which (‘right-,’ ‘left-,’ ‘ipsilateral-’ or ‘contralateral-ear’) ‘group quadratic contrast’ would produce statistical significance for a GCSR ‘analogue’ (suggesting all four had to be tested). Meanwhile, orders 1-9 of ‘time’ effects were inspected for all other tests in the EVestG Experiment, since this was analogous to testing the 5 of 9 (or 62.5% of) ‘frequency’ effect orders tested in the EEG Experiment (because 9 of 15, or 60% of, ‘time’ effect orders represents a similar percentage), where p-values had to be below 0.05 after Bonferroni correction to reach statistical significance.

SPSS revealed polynomial orders 1-9 for ‘time’ (in the within-subjects repeated measures ‘type’ x ‘SSD’ x ‘frequency,’ linear x quadratic x quartic contrast) showed uncorrected p-values of 0.307, 0.094, 0.385, 0.010, 0.482, $< .001$, 0.590, 0.026 and 0.938, respectively (see Table 4-13). Vitaly, the uncorrected p-value for the (predicted) quartic was 0.01 (‘type’ x ‘SSD’ x ‘frequency,’ linear x quadratic x quartic, $F(1,3) = 35.4$, $p = 0.01$) and thus significant *after* Bonferroni correction (i.e., multiplying the p-value of 0.01 by 4, for the four ‘group quadratic contrasts’ that were tested).

¹⁷ One of the authors of Shadli et al. [1] indicated that different SST versions seem to produce different orders of ‘frequency’ effects (Neil McNaughton, personal communication, 9 June 2021); however, the same version of the SST was used for both of the experiments in the current study.

Table 4-13. GCSR ‘analogue’ results. The fourth and sixth order polynomials for ‘time’ were significant after Bonferroni correction.

Order of polynomial for ‘time’	Type III sum of squares	df	Mean Square	F	Sig.
Linear	2.685	1	2.685	1.505	0.307
Quadratic	0.096	1	0.096	5.840	0.094
Cubic	8.554	1	8.554	1.027	0.385
Order 4	1.762	1	1.762	35.353	0.010
Order 5	9.752	1	9.752	0.641	0.482
Order 6	7.548	1	7.548	181.697	0.001
Order 7	5.560	1	5.560	0.361	0.590
Order 8	12.424	1	12.424	16.881	0.026
Order 9	0.061	1	0.061	0.007	0.938

Notably, the uncorrected p-value for the sixth order was 0.001, indicating that significance would have been reached even *without* a prediction for ‘time,’ as this p-value would have been significant after multiplying it by 36 (to Bonferroni correct for testing 9 unpredicted ‘time’ effect orders times 4 unpredicted ‘right-,’ ‘left-,’ ‘ipsilateral-’ or ‘contralateral-ear’ ‘group quadratic contrasts’). Critically, the other three (‘left-,’ ‘ipsilateral-’ and ‘contralateral-ear’) ‘group quadratic contrasts’ did not reveal statistical significance for any order (1-9) of polynomial ‘time’ effect.

The ‘right-ear group quadratic contrast’ data (Figure 4-5) were analyzed post-hoc, beginning with a focused analysis of the 110 ms interval, where a peak occurred that was much taller and more well-defined than any in the other ‘group quadratic contrast’ plots (as discussed; Figure 4-5). Notably, the ‘type’ x ‘SSD’ (linear x quadratic) interaction had an uncorrected p-value below 0.10 at the 110 ms interval ($F(1,3) = 7.48$, $p = 0.072$, uncorrected); while all other ‘time’ bins in the full (60 - 210 ms) ‘time’ range had higher uncorrected p-values, when they were each tested separately.

Further tests determined whether the SST in the EVestG Experiment yielded results similar to those that prior studies [1, 31] described as being predicted by (BIS) theory. First, the within-subjects ‘type’ x ‘SSD’ x ‘time’ contrast, linear x linear x order interaction tested variation in IHs between trials with short SSDs and trials with long SSDs and revealed an uncorrected p-value near 0.01 only for a seventh order ‘time’ effect ($F(1,3) = 28.09$, $p = 0.013$, uncorrected) which did not

reach significance after Bonferroni correction (for unpredicted ‘time’ effect order; see Table 4-14). Although not a necessary condition for GCSR, (BIS) theory predicts insignificant results for the above test (for a review, see [1]).

Table 4-14. Results for test of variation between effects of short and long SSDs on IH values independent of the intermediate SSD. BIS theory predicts no variation between effects of short and long SSDs. As results were insignificant, no variation was detected.

Order of polynomial for ‘time’	Type III Sum of Squares	df	Mean Square	F	Sig.
Linear	0.185	1	0.185	0.080	0.796
Quadratic	0.025	1	0.025	0.024	0.886
Cubic	0.019	1	0.019	0.003	0.963
Order 4	0.039	1	0.039	0.007	0.938
Order 5	0.839	1	0.839	0.170	0.708
Order 6	1.548	1	1.548	0.198	0.686
Order 7	3.526	1	3.526	28.091	0.013
Order 8	3.710	1	3.710	0.782	0.442
Order 9	7.089	1	7.089	5.581	0.099

Lastly, the within-subjects ‘type’ x ‘time’ (linear x order) contrast tested ‘stopping’ effects (averaged across short, intermediate, long SSDs) and had uncorrected p-values near 0.05 for odd ‘time’ effect orders 1-9, namely 0.058, 0.064, 0.059, 0.034 and 0.04, respectively (see Table 4-15); however, none of these p-values reached statistical significance after Bonferroni correction.

Table 4-15. Results for test of variation between ‘stop’ and ‘go’ effects on IH values. BIS theory predicts variation between ‘stop’ and ‘go’ effects. A ‘stopping’ effect was not detected because none of the results were significant after Bonferroni correction.

Order of polynomial for ‘time’	Type III Sum of Squares	df	Mean Square	F	Sig.
Linear	42.144	1	42.144	8.959	0.058
Quadratic	0.017	1	0.017	0.014	0.912
Cubic	132.712	1	132.712	8.189	0.064
Order 4	1.183	1	1.183	0.193	0.690
Order 5	135.548	1	135.548	8.818	0.059
Order 6	6.350	1	6.350	0.712	0.461
Order 7	70.682	1	70.682	13.679	0.034
Order 8	8.520	1	8.520	1.302	0.337
Order 9	15.055	1	15.055	12.019	0.040

4.4 Summary

The methods of Shadli et al. [1] were used to elicit and detect GCSR in the EEG group. During the analysis stage, data were compared between “Experiment 2” of Shadli et al. [1] and the EEG Experiment in the current study, starting with demographic data and results from the SST. Five volunteers participated in the EEG Experiment: two males (1 left-handed) and three females (1 left-handed) with an average age of 49 ± 17 years (SD; see Table 3-1). These demographics were quite different from those in Shadli et al. [1] (see Table 4-1). Notably, Shadli et al. [1] included only right-handed volunteers, while the EEG Experiment had roughly equal numbers of left- and right-handed individuals; and mean participant age in the EEG Experiment was about 2.5 times that in Shadli et al. [1]; however, males and females were nearly balanced in both studies. The SST statistics that determined whether a participant’s EEG data would be included in analyses were within standard ranges (see Table 4-2) and similar to those in Shadli et al. [1] (see Table 4-3); therefore, no participant’s EEG data had to be excluded from analyses because of poor SST results. Also, other less vital SST statistics were similar to those that were reported by Shadli et al. [1], together showing that the SST in the current study behaved similarly to the one in Shadli et al. [1].

For each EEG channel (F7, F8, Fz) of each participant (N=5) in the EEG group, 6 ‘average’ (‘short stop,’ ‘short go,’ ‘intermediate stop,’ ‘intermediate go,’ ‘long stop’ and ‘long go average’) power spectra (that each averaged 7-11 power spectra containing no missing values) were analyzed (see Table 4-4); however, only results for ‘F8’ are presented in this chapter (while F7 and Fz results will be available after publication). For each volunteer, the quadratic contrast of their 6 ‘average’ spectra was found (these results will be plotted separately and made available after publication); and the contrasts were averaged to form the ‘group quadratic contrast’ (Figure 4-2), where data recorded from F7 and F8 were used for left- and right-handed participants, respectively. The ‘group quadratic contrast’ was also three-point smoothed (Figure 4-4), creating a simpler plot with a single peak at 9 Hz (as before the smoothing) and a single trough at 6 Hz (vs. 7 Hz before). Repeated measures ANOVA then *together* tested every ‘average’ spectrum of every volunteer via within-subjects repeated measures ‘type’ x ‘SSD’ x ‘frequency,’ linear x quadratic x order contrast. Notably, the uncorrected p-value for the quartic effect of ‘frequency’ was found to be below 0.05 (‘type’ x ‘SSD’ x ‘frequency,’ linear x quadratic x quartic, $F(1,4) = 8.06$, $p = 0.047$; see Table

4-5); thus, GCSR was significant *without* correction; however, GCSR failed to reach significance after Bonferroni correction (i.e., multiplying the p-value of 0.047 by 5, for the five orders tested).

The main ‘type’ x ‘SSD’ x ‘frequency’ (linear x quadratic x order) contrast had uncorrected p-values near 0.05 for 5-11, 6-10 and 7-9 Hz ranges for first, third and fifth order ‘frequency’ effects, respectively ($F(1,4) = 7.89$, $p = 0.048$; $F(1,4) = 7.17$, $p = 0.055$; $F(1,4) = 6.68$, $p = 0.061$), and p-values near 0.10 when 7 and 9 Hz were tested separately (‘type’ x ‘SSD,’ linear x quadratic, 7 Hz: $F(1,4) = 4.48$, $p = 0.10$, uncorrected; 9 Hz: $F(1,4) = 4.77$, $p = 0.09$, uncorrected) for GCSR. Meanwhile, a within-subjects ‘type’ x ‘SSD’ x ‘frequency’ (linear x linear x order) contrast tested for undesirable variation between short and long SSDs and did not yield significant results (see Table 4-8). Also, a within-subjects ‘type’ x ‘frequency’ (linear x order) contrast tested for effects of ‘stopping’ and revealed uncorrected p-values close to 0.01 for linear ($F(1,4) = 23.19$, $p = 0.009$) and quartic ($F(1,4) = 16.55$, $p = 0.015$) ‘frequency’ effects (see Table 4-9); and this linear effect was significant after correction, suggesting EEG power differences between ‘stop’ and ‘go’ trials.

Main results were not compared between the EVestG Experiment and Shadli et al. [1]; however, the SST was recreated — based on descriptions of the task in Shadli et al. [1] — for both experiments in the current study; therefore, to ensure that the SST worked properly in the EVestG Experiment, SST statistics were compared between the EVestG Experiment and Shadli et al. [1]. First, however, demographic data were compared between studies as these could have confounded comparison of SST statistics. Notably, the EVestG Experiment initially included five volunteers (as was stated in Chapter 3); however, one was excluded due to artefacts (as was explained in this chapter), leaving two males (1 left-handed) and two females with an average age of 53 ± 15 years (SD) in the EVestG group (see Table 3-1). These demographics are quite unlike those in Shadli et al. [1] (see Table 4-1). Notably, Shadli et al. [1] included only right-handed volunteers (while 25% of participants in the EVestG Experiment were left-handed); and mean participant age in Shadli et al. [1] was 20 years (2.5 times lower than in the EVestG Experiment); however, males and females were nearly balanced in both studies. Meanwhile, the SST statistics that decided whether a participant’s EVestG data would be included in analyses were within standard ranges and similar to those in Shadli et al. [1] (see Table 4-11); thus, no participant’s EVestG data had to be excluded from analyses because of poor SST results; and the SST seemed to have functioned properly.

For each in-ear channel (left, right) of each EVestG group participant (N=4), 6 ‘average’ IHs that each averaged 7-11 IHs not excluded in pre-processing were computed (see Table 4-12). Next, for each of the in-ear channels (left, right) of each participant in the EVestG group (N=4), the quadratic (GCSR) contrast of the 6 ‘average’ IHs associated with each channel was calculated using equation 3-3 (these results will be plotted separately and made available after publication). Then, the resulting four contrasts from the right ears of each participant were averaged to form the ‘right-ear group quadratic contrast’ that is shown in Figure 4-5 to have a very tall peak at 110 ms; and the same was done for ‘left-, ‘ipsilateral-‘ and ‘contralateral-ear group quadratic contrasts.’

A within-subjects repeated measures ‘type’ x ‘SSD’ x ‘time’ (linear x quadratic x order) contrast then together tested every ‘average’ IH of every participant for a *quartic* ‘time’ effect, since this order of ‘time’ effect had an uncorrected p-value below 0.047 in the EEG Experiment¹⁷ (where Bonferroni correction was used to offset inflated type I errors from testing four contrasts, as ‘right-, ‘left-, ‘ipsilateral-‘ or ‘contralateral-ear’ ‘group quadratic contrast’ was not predicted). Notably, the uncorrected p-value for the quartic was 0.01 (‘type’ x ‘SSD’ x ‘frequency,’ linear x quadratic x quartic, $F(1,3) = 35.4$, $p = 0.01$; see Table 4-13), thus significant *after* Bonferroni correction. Furthermore, the uncorrected p-value for the sixth order was $< .001$, suggesting that significance would have been reached even *without* a prediction for ‘time’ because this p-value would have been significant even *after* multiplying it by 36 (to correct for testing 4 contrasts times 9 orders). Interestingly, all even orders (2-8) of ‘time’ effects had uncorrected p-values below 0.10. Critically, the other three (‘left-, ‘ipsilateral-‘ and ‘contralateral-ear’) ‘group quadratic contrasts’ did not reveal statistical significance for any polynomial of ‘time’ effect order (1-9).

Post-hoc analyses of the right-ear data revealed an uncorrected p-value for the 110 ms peak (Figure 4-5; ‘type’ x ‘SSD,’ linear x quadratic, $F(1,3) = 7.48$, $p = 0.072$); while all other ‘time’ bins (when similarly tested separately) only revealed uncorrected p-values that were all above 0.10. Next, a within-subjects ‘type’ x ‘SSD’ x ‘time’ (linear x linear x order) contrast tested (undesirable) short and long SSD effect deviation, producing a 0.013 uncorrected p-value (see Table 4-14) for a seventh order ‘time’ effect ($F(1,3) = 28.09$, $p = 0.013$) that was not significant after Bonferroni correction. Meanwhile, a within-subjects ‘type’ x ‘time’ (linear x order) contrast tested ‘stopping’ and had uncorrected p-values below 0.05 for ‘time’ effect orders seven ($F(1,3) = 13.68$, $p = 0.034$) and nine ($F(1,3) = 12.02$, $p = 0.04$; see Table 4-15) that were not significant after correction.

Chapter 5: Discussion

5.1 Overview

This chapter will begin by discussing the results of the EEG Experiment (which did not show significant GCSR, but did reveal a GCSR plot that was similar to one of the two in “Experiment 2” of Shadli et al. [1] — which the EEG Experiment was aimed at replicating). Evidence suggesting that the SST program in the EEG Experiment functioned as it should have, by creating proper conditions for GCSR, will then be explained; after which alternate explanations (besides issues with the SST) for why GCSR was not found in the EEG Experiment will be offered. Results of the EVestG Experiment (which revealed a GCSR ‘analogue’ with a single large peak at 110 ms, equivalent to a 9 Hz cycle) will then be discussed; after which statistics showing that the SST functioned properly in the EVestG Experiment will be presented. Finally, an explanation of how hTheta-like rhythmicity may have entrained FPs to elicit a GCSR ‘analogue’ will be outlined.

5.2 EEG Experiment Discussion

The EEG Experiment in the current study did not reveal GCSR at the frontal F8 EEG site. As discussed in the previous chapter, the first five orders of ‘frequency’ effects were tested via the ‘type’ x ‘SSD’ x ‘frequency’ (linear x quadratic x order) contrast; however, of these five orders, only the quartic yielded an uncorrected p-value that was below 0.05 (‘type’ x ‘SSD’ x ‘frequency,’ linear x quadratic x quartic, $F(1,4) = 8.06$, $p = 0.047$, uncorrected; for all p-values, see Table 4-5); and after Bonferroni correction, the corrected p-value (0.235) did not reach statistical significance. While GCSR was not significant, the GCSR plot in the current study (Figure 4-2) was similar to one of the two plots from “Experiment 2” in Shadli et al. [1] (Figure 4-3), namely the one in block 3, as this plot in Shadli et al. [1] had a frequency distribution similar to the one in the current study and similarly peaked at 9 Hz (though the plot in Shadli et al. [1] had more positive values, overall). Therefore, GCSR was not significant, but the GCSR plot was similar to one in Shadli et al. [1].

There are several possible explanations for why GCSR was not found in the current study. As the SST is responsible for creating the conditions that produce GCSR in participants, there may have been issues with the SST program. Notably, when Shadli et al. [1] discovered differences between their results and those in prior studies [28, 31], the authors suggested that these differences could have arisen from their use of a visual SST in place of an auditory one (since all prior studies

used SSTs that employed auditory cues). As visual cues were used *both* in the current study *and* Shadli et al [1], however, differences in results between studies could not be similarly explained.

It might be expected that other issues with the SST may have led to differences in overall results; however, SST statistics in the EEG Experiment were similar to those in Shadli et al. [1], indicating that the SST in the current study was similar to the one that was used in Shadli et al. [1]. Importantly, similar success rates in ‘stop’ trials were found across studies for the three SSD staircases (91, 58 and 22% in the current study and 83, 44 and 8% in Shadli et al. [1] for short, intermediate and long SSDs, respectively; see Table 4-3); and the three SSDs were found to be similarly aligned. All other SST statistics were also similar between studies *except* ‘mean reaction time’ in ‘go’ trials (GO_RT; 525 and 426 ms in the current study and Shadli et al. [1], respectively), though it was *expected* that increased mean age in the current study (+29 years) would decrease reaction times; and these should not have affected results, as the SST adapts to reaction time [1]. The above results suggest that the SST in the current study created the proper conditions for GCSR.

Results of post-hoc tests were also consistent with those predicted by (BIS) theory and thus further validate the SST program that was created for the current study and furthermore suggest that EEGs were properly recorded while participants performed the SST in the EEG Experiment. Notably, a within-subjects ‘type’ x ‘frequency,’ linear x order contrast tested ‘stopping’ effects and revealed uncorrected p-values close to 0.01 for linear ($F(1,4) = 23.19, p = 0.009$) and quartic ($F(1,4) = 16.55, p = 0.015$) ‘frequency’ effects (see Table 4-9), where this linear ‘frequency’ effect was significant after correction, suggesting EEG power differences between ‘stop’ and ‘go’ trials. These results imply that the EEG recordings and SST functioned properly and were synchronized.

Other possible explanations for the lack of GCSR in the EEG Experiment could relate to participant demographics. As was discussed in Chapter 4, males and females were nearly balanced in the current study (40 and 60% respectively) and Shadli et al. [1] (44 and 55%, respectively); however, nearly *half* (40%) of participants were left-handed in the current study, whereas *all* were right-handed in Shadli et al. [1]; and those in the current study were on average 29 years older. Combining F7 and F8 data of left- and right-handed participants, respectively (as was performed in the current study, though not in Shadli et al. [1] which only had right-handed participants), may not produce equivalent GCSR, as described by [62] — or, not in all age groups. (Critically, left-handed individuals tend to exhibit patterns of EEG activation different from those that are recorded

in right-handed individuals when the same task is performed [28]). Notably, Shadli et al. [62] *alone* was used to justify combining F7 and F8 data in the current study. Meanwhile, volunteers in the EEG Experiment were on average 29 years older than those in Shadli et al. [1] and had slower reaction times. While the SST is reported [1] to adapt to reaction times to establish similar levels of goal conflict for all participants, volunteers in prior studies [1, 16, 28, 31] were 18-25 years old; and it is possible that the SST only adapts to the reaction times of participants between these ages.

Two other differences between the study populations in Shadli et al. [1] and the EEG Experiment in the current study could explain the differences in outcomes between the two studies. Importantly, participants in Shadli et al. [1] were not acquaintances of Shadli et al. [1], whereas all participants in the current study were well-known to researchers in the current study. One could imagine that participants who are acquainted with the researchers in a study might worry more *or* less about aspects of the study than participants who are not familiar with the researchers; and GCSR, a putative *anxiety* process biomarker, may be sensitive to this worry (or lack thereof). Finally, it is unsurprising that GCSR was found in Shadli et al. [1] but not in the current study because of the much larger study population in the former (N=18; compared to the latter; N=5) that would tend to lower the standard deviations of measurements — and thus p-values for GCSR.

5.3 EVestG Experiment Discussion

In the EVestG Experiment, a GCSR ‘analogue’ was found in the right-ear EVestG IH data of the EVestG group (‘type’ x ‘SSD’ x ‘time,’ linear x quadratic x quartic, $F(1,3) = 35.4$, $p = 0.04$; multiplied by 4 to Bonferroni correct for testing right-, left-, ipsilateral- and contralateral-ear data; the quartic ‘time’ effect was predicted, based on the analogous EEG Experiment GCSR result).¹⁸ Vivally, this GCSR ‘analogue’ contained a single large peak at 110 ms (Figure 4-5) which was much taller and more well-defined than those in plots of the other ‘group quadratic contrasts’ (Figure 4-5). As 110 ms corresponds to 9 Hz (i.e., the peak GCSR frequency in the EEG Experiment; Figure 4-2), this suggests a possible connection to the GCSR reported in the prior section (as will be discussed). Importantly, SST statistics from Shadli et al. [1] and from the EVestG Experiment were similar, which would seem to suggest that the SST program worked

¹⁸ GCSR was significant even without the predicted quartic ‘time’ effect because the sixth order interaction p-value (‘type’ x ‘SSD’ x ‘time,’ linear x quadratic x order six, $F(1,3) = 182$, $p < 0.001$) was significant even after multiplying it by 36 to Bonferroni correct for 9 orders of ‘time’ effects (as with the other tests) and 4 (right-, left-, ipsilateral- and contralateral-ear) testing configurations.

properly in the EVestG Experiment. The above results suggest that the SST program, reported in the prior section to have failed to elicit GCSR in the EEG Experiment, successfully caused a GCSR ‘analogue’ in the EVestG Experiment.

SST statistics in the EVestG Experiment were similar to those found in Shadli et al. [1]. Similar success rates in ‘stop’ trials were found across studies for the three SSD staircases (91, 61 and 9% in the current study and 83, 44 and 8% in Shadli et al. [1], for short, intermediate and long SSDs, respectively; see Table 4-11); and the three SSDs were similarly aligned (between studies). The above results suggest that the SST in the current study created the proper conditions for GCSR.

Post-hoc tests produced mixed results: one that BIS theory predicted and another it did not. First, a within-subjects ‘type’ x ‘SSD’ x ‘time’ (linear x linear x order) contrast tested (undesirable) short and long SSD effect deviation, bearing a 0.013 uncorrected p-value (see Table 4-14) for a seventh order ‘time’ effect ($F(1,3) = 28.09$, $p = 0.013$) that was not significant after Bonferroni correction. Meanwhile, whereas the EEG Experiment results (in the above section) had a significant effect for ‘stopping,’ a within-subjects ‘type’ x ‘time’ (linear x order) contrast tested ‘stopping’ and showed uncorrected p-values below 0.05 for ‘time’ effect orders seven ($F(1,3) = 13.68$, $p = 0.034$) and nine ($F(1,3) = 12.02$, $p = 0.04$; see Table 4-15) that were not significant after Bonferroni correction. Despite this non-significant test result for EEG power differences between ‘stop’ and ‘go’ trials (from the within-subjects ‘type’ x ‘time,’ linear x order contrast), the overall quadratic “GCSR” (within-subjects ‘type’ x ‘SSD’ x ‘time,’ linear x quadratic x quartic) contrast did reach significance ($F(1,3) = 35.4$, $p = 0.04$; as discussed), and was the main contrast in the current study and Shadli et al. [1] (which did not mention testing for ‘stopping’ effects, regardless).

It is vital to exercise caution in interpreting results in this section and avoid extrapolating too much from them, given 1) the very small study population ($N=4$), 2) interpersonal relationships between participants and researchers, and 3) highly biased recruitment process in the current study. Nevertheless, the hypothesis that a GCSR ‘analogue’ would occur in the EVestG Experiment was validated by results in the prior chapter; and it is worth asking what results like these could mean.

As discussed, a GCSR ‘analogue’ was found in the right-ear IH data of the EVestG group. (‘type’ x ‘SSD’ x ‘time,’ linear x quadratic x quartic, $F(1,3) = 35.4$, $p = 0.04$, Bonferroni corrected for unpredicted right-, left-, ipsilateral- or contralateral-ear IH data; for a review, see Chapter 4). That a GCSR ‘analogue’ occurred means that IHs (of FPs) differed between SST trial conditions.

Specifically, this GCSR ‘analogue’ suggests that the average IH in intermediate SSD ‘stop’ trials differed with $p < .05$ statistical significance from the average IH in short and long SSD ‘stop’ trials (after subtracting from each average IH of each SSD the average IH in ‘go’ trials of the same SSD). Vitaly, the prediction from (BIS) theory (upon which GCSR and the GCSR ‘analogue’ are based), is that the intermediate SSD (compared to the short and long SSDs) causes increased goal conflict — a process mediated by a human analogue of (4-12 Hz) rodent type II hTheta originating in the HPC (for a review, see section 2.6). Thus, the GCSR ‘analogue’ in the current study should relate to goal conflict or a human analogue of (4-12 Hz) rodent type II hTheta that mediates goal conflict.

As discussed, the GCSR contrast of the above average IHs was found (using equation 3-3) and plotted (Figure 4-5). The plot had a single large peak at 110 ms (Figure 4-5) much taller and more well-defined than any peak in the other plots for the other ‘group quadratic contrasts’ (Figure 4-5). This peak value at 110 ms indicates that the average IH in intermediate SSD ‘stop’ trials differed maximally from the average IH in short and long SSD ‘stop’ trials for this particular (110 ms) time (after subtracting from each average IH of each SSD the average IH in ‘go’ trials of the same SSD), where the 110 ms peak was the largest residual after subtracting average IHs (with equation 3-3). This 110 ms peak is interesting because it corresponds to 9 Hz, which was also the peak frequency in the EEG Experiment (Figure 4-2) and block 3 of “Experiment 2” in Shadli et al. [1] (Figure 4-3), implying that some process operating at 9 Hz may modulate both frontal EEGs and vestibular FPs; and a human analogue of (4-12 Hz) rodent type II hTheta is implicated by BIS theory, as discussed.

What the GCSR ‘analogue’ and its 110 ms peak (Figure 4-5) entail at the vestibular FP level is that FPs occurred at a certain firing rate — higher than the average firing rate in participants — more often in intermediate ‘stop’ trials than in short or long ‘stop’ trials. It is apparent that this firing rate was *higher* than the average firing rates of participants because the residual 110 ms peak (Figure 4-5) was *below* 125 ms (which is the value that each participant’s IHs were centered around); and each participant’s average firing rate yielded a 125 ms interval (for a review, see Chapter 3). Vitaly, the 110 ms peak (Figure 4-5) shows that in intermediate ‘stop’ trials more often than in short or long ‘stop’ trials, a participant had in 110 ms the number of FPs they normally

had in 125 ms;¹⁹ or, equally, a participant had in a 9 Hz cycle the number of FPs they normally had in an 8 Hz cycle.

If a human analogue of (4-12 Hz) rodent type II hTheta in fact caused the GCSR ‘analogue’ in the EVestG Experiment, frequency or amplitude changes in this human hTheta analogue could have modulated the firing of vestibular neurons that drove the observed increase in FP firing rates. In this scenario, vestibular neurons may have fired in synchrony with this human hTheta analogue as DR neurons fire in synchrony with hTheta in REM sleep or movement [47], where burst firing occurred during hTheta activity and matched the rhythm’s frequency (Figure 2-6). Such burst firing should cause inter-FP gaps to take on small and large values in rapid spiking and quiescent periods, respectively, which should group IH data points into low and high time bins. This grouping of IH data into low and high time bins should cause these data to stand out because their peaks would shift from the center (basal firing rate) bin where tallest peaks typically occur. Such grouping of IH data points could explain the EVestG Experiment results because bursting would occur during intermediate ‘stop’ trials (causing grouping in IH data) and would decrease or altogether cease during short and long ‘stop’ trials (causing no grouping in IHs); and subtracting IHs for short and long ‘stop’ trials from IHs for intermediate ‘stop’ trials should therefore leave grouped IH data from IHs for intermediate ‘stop’ trials standing out in the GCSR ‘analogue’ plot. As the value that stood out in the GCSR ‘analogue’ plot of the current study was 110 ms (or 9 Hz), this might be interpreted as meaning that 9 Hz modulation of FPs must have occurred; however, the frequency of underlying modulation could not be discerned from the IHs in the current study because IHs were merely centered at 8 Hz to highlight shifts relative to this frequency; therefore, it remains unclear whether modulation at 8 or 9 Hz (or any other frequency) actually occurred.

Since 1) a human analogue of (4-12 Hz) rodent type II hTheta is implicated (by BIS theory) in the GCSR ‘analogue’ of the current study, as discussed, 2) GCSR is an anxiety process biomarker [1], 3) anxiety is simply “arousal with negative valence” [5], and 4) type II hTheta seems to occur in rodents whenever they are aroused [25], the human analogue of (4-12 Hz) rodent type II hTheta that is implicated in the GCSR ‘analogue’ may entrain vestibular neurons more generally (not just during the SST) when humans are aroused. This human analogue of (4-12 Hz) rodent type II

¹⁹ The same number of inter-FP gaps were used to construct each of a participant’s IHs; however, this number varied between participants because average firing rates varied between participants (and average firing rates always yielded 125 ms intervals, as discussed).

hTheta could therefore be an objective biomarker of anxiety that could be measured in patients during any task that may be anxiogenic for the patient, to monitor for conditions that trigger the patient's anxiety. For example, individuals with GAD experience anxiety in a generalized way (i.e., their anxiety is not triggered by any specific stimuli or situations [20]); therefore, for individuals with GAD, a human analogue of (4-12 Hz) rodent type II hTheta would be expected to occur in myriad situations. An individual with GAD could thus be fitted with an in-ear device that measures their type II hTheta-like rhythmicity (i.e., human analogue of rodent type II hTheta) throughout their day, and this objective data could help clinicians assess the individual's condition.

Chapter 6: Conclusion

The current study had two experiments: an ‘EEG Experiment’ and ‘EVestG Experiment,’ where the goal of the former was to elicit and detect GCSR via the methods of Shadli et al. [1]; and that of the latter was to elicit and detect a GCSR ‘analogue’ via analogous methods for EVestG. Specifically, the EEG Experiment was designed to replicate “Experiment 2” of Shadli et al. [1] to demonstrate that the SST program in the current study was capable of causing GCSR; after which the EVestG Experiment, which was novel, was meant to show that the same program that elicited GCSR in the EEG Experiment could also elicit a GCSR ‘analogue’ (for a review, see Chapter 2).

In the EEG Experiment of the current study, GCSR was not found; however, the GCSR *plot* in the EEG Experiment was similar to one of two in the experiment (“Experiment 2” of Shadli et al. [1]) that the EEG Experiment was aimed at partially replicating. As the SST program seemed to have functioned properly, the lack of GCSR in the EEG Experiment might be attributable to demographics of the EEG group. First, there was a wide age gap among participants in the EEG group; and average age was 29 years higher than in Shadli et al. [1]. Second, 40% of the volunteers in the EEG group were left-handed, while all volunteers in Shadli et al. [1] were right-handed. If demographics were not the issue, that all participants in the current study were acquaintances of the research team (because it was difficult to recruit participants during the COVID-19 pandemic lockdowns), and that very few volunteers (N=4) were recruited, may have influenced results.

Meanwhile, results in the EVestG Experiment (that involved the same SST) were more positive. The EVestG Experiment showed that the same SST that produced GCSR in frontal EEG activity in past studies [1, 16, 28, 31] caused a GCSR ‘analogue’ in EEG activity recorded from the right ear canals of the four participants in the EVestG Experiment. This GCSR ‘analogue’ occurred for a certain higher than average FP rate, indicating that vestibular neurons fired at a specific higher rate more often in intermediate than in short and long ‘stop’ trials.

According to (BIS) theory (upon which the SST and GCSR are based), GCSR is driven by a human analogue of 4-12 Hz rodent type II hTheta that mediates a process called ‘goal conflict;’ thus, the GCSR ‘analogue’ should relate to this human analogue of 4-12 Hz rodent type II hTheta. In rodents, DR neurons have been shown to fire in bursts during hTheta [47], causing small inter-FP gaps during rapid spiking and large gaps amid quiescent periods. If this occurs in humans, it should group IH data into low and high bins. This could explain the EVestG Experiment results

because, to perform the GCSR contrast, IHs for short and long ‘stop’ trials are subtracted from IHs for intermediate ‘stop’ trials, which would leave large peaks in the plot for the GCSR ‘analogue’ in IH bins that the data would be grouped into because of bursting during intermediate ‘stop’ trials; and these bins would tend to occur *away* from where tall peaks normally occur (namely the center).

It is interesting that a GCSR ‘analogue’ was found in The EVestG Experiment, given that The EEG Experiment failed to show GCSR, considering the methods for eliciting and detecting GCSR that were used in The EEG Experiment were specifically designed for EEG experiments, but had to be adapted for the (first-of-its-kind) EVestG Experiment that (by contrast) showed positive results. Despite the lack of GCSR in the EEG Experiment that could have bolstered the GCSR ‘analogue,’ this GCSR ‘analogue’ was accurately predicted based on BIS theory that has similarly predicted GCSR in several studies [1, 16, 28, 31]; and the theory in Chapter 2 of this paper established that it is plausible for a rodent hTheta analogue in humans to entrain the firing of vestibular neurons during periods of increased arousal or anxiety. The statistical significance of the contrast in the EVestG Experiment validates a GCSR ‘analogue,’ and future studies may show that this GCSR ‘analogue’ is a novel biomarker of an anxiety process that could assist clinicians in diagnosing pathologies by providing an objective measure of anxiety. Critically, however, there were many non-idealities in both experiments (including that they both had small N); therefore, it is important not to overinterpret any results from either of the experiments in the current study.

6.1 Future Work

The literature does not appear to describe any studies that attempted to measure hTheta entrainment of vestibular activity. Surely, a study aimed at simultaneously recording EEGs from peripheral vestibular neurons and the HPC (both intracranially, in animals) during a task that elicits hTheta should be capable of determining whether the rhythm entrains the firing of vestibular cells. Data from such simultaneous recordings in animals should establish that such entrainment occurs *and* reveal the nature of such entrainment — making it easier to look for an ‘analogue’ in humans.

As the EEG Experiment in the current study did not yield GCSR, the issues identified with the experiment (that were outlined in Chapter 5) should be addressed and the experiment repeated. To address these issues in a repeat of the EEG Experiment, volunteers should: 1) be of similar age, 2) be right-handed, and 3) not be acquainted with any of the members of the research team or staff; and a much larger number of volunteers should be recruited than were in the current study (N=5).

The EVestG Experiment should also be repeated because of the low number of participants (N=4) who were involved. Optionally, the experiment could be converted into a double-blind, placebo-controlled drug study, analogous to those in [1, 16, 31], where healthy participants were divided into groups that received one of three or four treatments, including buspirone, triazolam, pregabalin or a placebo. The expectation in such a study would be that groups that received one of the anxiolytics would show less or no indication of a GCSR ‘analogue.’

As was explained in Chapter 2, another way to test whether vestibular neurons become entrained by a human analogue of (4-12 Hz) type II rodent hTheta would be to record EVestG data from participants during immobile rotation. Critically, Tai et al. [50] found that rodents exhibited type II hTheta during rotation, and that vestibular neurons triggered this hTheta (though it remains unclear whether this hTheta in turn modulated the firing of vestibular neurons, as was discussed in Chapter 2). Meanwhile, Liberman et al. [32] found that auditory neurons appear to be entrained by hTheta amid auditory stimulation in rodents; and auditory and vestibular cells occupy many of the same structures (as was outlined in Chapter 2), together suggesting that vestibular cells may be entrained by hTheta during vestibular stimulation. Rotation should therefore be applied to healthy volunteers and individuals with GAD via a hydraulic chair while EVestG data is recorded (as is performed in EVestG studies) to test for a human analogue of hTheta during rotation [13]. Here, the expectation would be for type II hTheta-like rhythmicity (and its entrainment of FPs detected by NEER) to be more prominent in individuals with GAD (vs. controls) during chair motions because these individuals *generally* experience increased anxiety, in many situations [20].

Finally, auto-correlation (instead of IHS) could be used to detect burst firing in vestibular neurons caused by hTheta-like rhythmicity, as discussed. Auto-correlation was used in previous hTheta studies to show that bursting occurred amid hTheta [47] and could, in addition to detecting modulation of FPs, reveal the frequency of this modulation (and that of the resulting burst firing).

In summary, this study validated a GCSR ‘analogue’ that may represent a novel anxiety biomarker — a measure that could help clinicians form more objective anxiety disorder diagnoses. However, this biomarker should be further developed, via the study designs outlined in this section.

References

- [1] S. M. Shadli, M. J. Smith, P. Glue, and N. McNaughton, "Testing an anxiety process biomarker: Generalisation from an auditory to a visual stimulus," *Biol. Psychol.*, vol. 117, pp. 50-55, 2016, doi: 10.1016/j.biopsycho.2016.02.011.
- [2] D. F. Santomauro *et al.*, "Global prevalence and burden of depressive and anxiety disorders in 204 countries and territories in 2020 due to the COVID-19 pandemic," *The Lancet (British edition)*, vol. 398, no. 10312, pp. 1700-1712, 2021, doi: 10.1016/S0140-6736(21)02143-7.
- [3] N. McNaughton, "What do you mean 'anxiety'? Developing the first anxiety syndrome biomarker," ed: Taylor & Francis, 2017, pp. 1-14.
- [4] E. Ruzich, M. Crespo-García, S. S. Dalal, and J. F. Schneiderman, "Characterizing hippocampal dynamics with MEG: A systematic review and evidence-based guidelines," *Hum. Brain Mapp.*, vol. 40, no. 4, pp. 1353-1375, 2019, doi: 10.1002/hbm.24445.
- [5] G. G. Calhoun and K. M. Tye, "Resolving the neural circuits of anxiety," *Nat. Neurosci.*, vol. 18, no. 10, p. 1394, 2015, doi: 10.1038/nn.4101.
- [6] R. P. Vertes and B. Kocsis, "Brainstem- diencephalo-septohippocampal systems controlling the theta rhythm of the hippocampus," *Neuroscience*, vol. 81, no. 4, p. 893, 1997, doi: 10.1016/S0306-4522(97)00239-X.
- [7] T. Korotkova *et al.*, "Reconciling the different faces of hippocampal theta: The role of theta oscillations in cognitive, emotional and innate behaviors," *Neurosci. Biobehav. Rev.*, vol. 85, pp. 65-80, 2018, doi: 10.1016/j.neubiorev.2017.09.004.
- [8] A. T. Lee *et al.*, "VIP Interneurons Contribute to Avoidance Behavior by Regulating Information Flow across Hippocampal-Prefrontal Networks," *Neuron (Cambridge, Mass.)*, vol. 102, no. 6, pp. 1223-1234.e4, 2019, doi: 10.1016/j.neuron.2019.04.001.
- [9] N. Padilla-Coreano *et al.*, "Hippocampal-Prefrontal Theta Transmission Regulates Avoidance Behavior," *Neuron (Cambridge, Mass.)*, vol. 104, no. 3, pp. 601-610.e4, 2019, doi: 10.1016/j.neuron.2019.08.006.
- [10] A. D. Ekstrom, J. B. Caplan, E. Ho, K. Shattuck, I. Fried, and M. J. Kahana, "Human hippocampal theta activity during virtual navigation," *Hippocampus*, vol. 15, no. 7, pp. 881-889, 2005, doi: 10.1002/hipo.20109.
- [11] B. J. Lithgow *et al.*, "Major depression and electrovestibulography," *The World Journal of Biological Psychiatry*, 2015, Vol.16(5), p.334-350, vol. 16, no. 5, pp. 334-350, 2015, doi: 10.3109/15622975.2015.1014410.
- [12] C. D. Balaban, R. G. Jacob, and J. M. Furman, "Neurologic bases for comorbidity of balance disorders, anxiety disorders and migraine: neurotherapeutic implications," *Expert Rev. Neurother.*, vol. 11, no. 3, pp. 379-394, 2011, doi: 10.1586/ern.11.19.
- [13] B. J. Lithgow, Z. Moussavi, and P. B. Fitzgerald, "Quantitative separation of the depressive phase of bipolar disorder and major depressive disorder using electrovestibulography," *The world journal of biological psychiatry*, vol. 20, no. 10, pp. 799-812, 2019, doi: 10.1080/15622975.2019.1599143.
- [14] M. H. Pollack, "Comorbid anxiety and depression," *The journal of clinical psychiatry*, vol. 66 Suppl 8, pp. 22-29, 2005.
- [15] N. M. Simon *et al.*, "Anxiety Disorder Comorbidity in Bipolar Disorder Patients: Data From the First 500 Participants in the Systematic Treatment Enhancement Program for Bipolar Disorder (STEP-BD)," *The American journal of psychiatry*, vol. 161, no. 12, pp. 2222-2229, 2004, doi: 10.1176/appi.ajp.161.12.2222.

- [16] N. McNaughton, C. Swart, P. Neo, V. Bates, and P. Glue, "Anti-anxiety drugs reduce conflict-specific θ —A possible human anxiety-specific biomarker," *J. Affect. Disord.*, vol. 148, no. 1, pp. 104-111, 2013, doi: 10.1016/j.jad.2012.11.057.
- [17] B. J. Lithgow, Z. Moussavi, C. Gurvich, J. Kulkarni, J. J. Maller, and P. B. Fitzgerald, "Bipolar disorder in the balance," *Eur. Arch. Psychiatry Clin. Neurosci.*, vol. 269, no. 7, pp. 761-775, 2018, doi: 10.1007/s00406-018-0935-x.
- [18] N. S. Endler and N. L. Kocovski, "State and trait anxiety revisited," *J. Anxiety Disord.*, vol. 15, no. 3, pp. 231-245, 2001, doi: 10.1016/S0887-6185(01)00060-3.
- [19] A. C. Miu, R. M. Heilman, and M. Miclea, "Reduced heart rate variability and vagal tone in anxiety: Trait versus state, and the effects of autogenic training," *Auton. Neurosci.*, vol. 145, no. 1, pp. 99-103, 2008, doi: 10.1016/j.autneu.2008.11.010.
- [20] *Diagnostic and statistical manual of mental disorders : DSM-5*, 5th ed. ed. (DSM-5). Washington, D.C: American Psychiatric Publishing, 2013.
- [21] A. Adhikari, M. A. Topiwala, and J. A. Gordon, "Synchronized Activity between the Ventral Hippocampus and the Medial Prefrontal Cortex during Anxiety," *Neuron*, vol. 65, no. 2, pp. 257-269, 2010, doi: 10.1016/j.neuron.2009.12.002.
- [22] S. E. File, L. E. Gonzalez, and N. Andrews, "Comparative study of pre- and postsynaptic 5-HT_{1A} receptor modulation of anxiety in two ethological animal tests," *The Journal of neuroscience : the official journal of the Society for Neuroscience*, vol. 16, no. 15, p. 4810, 1996.
- [23] R. M. J. Deacon, D. M. Bannerman, and J. N. P. Rawlins, "Anxiolytic effects of cytotoxic hippocampal lesions in rats.(Abstract)," *Behav. Neurosci.*, vol. 116, no. 3, p. 494, 2002, doi: 10.1037/0735-7044.116.3.494.
- [24] R. Kramis, C. H. Vanderwolf, and B. H. Bland, "Two types of hippocampal rhythmical slow activity in both the rabbit and the rat: Relations to behavior and effects of atropine, diethyl ether, urethane, and pentobarbital," *Exp. Neurol.*, vol. 49, no. 1, pp. 58-85, 1975, doi: 10.1016/0014-4886(75)90195-8.
- [25] R. S. Sainsbury, A. Heynen, and C. P. Montoya, "Behavioral correlates of hippocampal type 2 theta in the rat," *Physiol. Behav.*, vol. 39, no. 4, p. 513, 1987, doi: 10.1016/0031-9384(87)90382-9.
- [26] C. E. Wells *et al.*, "Novelty and anxiolytic drugs dissociate two components of hippocampal theta in behaving rats," *The Journal of neuroscience*, vol. 33, no. 20, pp. 8650-8667, 2013, doi: 10.1523/JNEUROSCI.5040-12.2013.
- [27] N. McNaughton, B. Kocsis, and M. Hajós, "Elicited hippocampal theta rhythm: a screen for anxiolytic and procognitive drugs through changes in hippocampal function?," *Behav. Pharmacol.*, vol. 18, no. 5-6, pp. 329-346, 2007, doi: 10.1097/FBP.0b013e3282ee82e3.
- [28] P. Neo, J. Thurlow, and N. McNaughton, "Stopping, goal-conflict, trait anxiety and frontal rhythmic power in the stop-signal task," *Cognitive, Affective, & Behavioral Neuroscience*, vol. 11, no. 4, pp. 485-493, 2011, doi: 10.3758/s13415-011-0046-x.
- [29] C. K. Young and N. McNaughton, "Coupling of Theta Oscillations between Anterior and Posterior Midline Cortex and with the Hippocampus in Freely Behaving Rats," *Cerebral cortex (New York, N.Y. 1991)*, vol. 19, no. 1, pp. 24-40, 2008, doi: 10.1093/cercor/bhn055.
- [30] G. D. Logan, W. B. Cowan, and K. A. Davis, "On the ability to inhibit simple and choice reaction time responses: A model and a method," *Journal of experimental psychology. Human perception and performance*, vol. 10, no. 2, pp. 276-291, 1984, doi: 10.1037/0096-1523.10.2.276.
- [31] S. M. Shadli, P. Glue, J. McIntosh, and N. McNaughton, "An improved human anxiety process biomarker: characterization of frequency band, personality and pharmacology," *Translational psychiatry*, vol. 5, no. 12, pp. e699-e699, 2015, doi: 10.1038/tp.2015.188.

- [32] T. Liberman, R. A. Velluti, and M. Pedemonte, "Temporal correlation between auditory neurons and the hippocampal theta rhythm induced by novel stimulations in awake guinea pigs," *Brain Res.*, vol. 1298, pp. 70-77, 2009, doi: 10.1016/j.brainres.2009.08.061.
- [33] R. S. Sainsbury and C. P. Montoya, "The relationship between type 2 theta and behavior," *Physiol. Behav.*, vol. 33, no. 4, pp. 621-626, 1984, doi: 10.1016/0031-9384(84)90381-0.
- [34] B. H. Bland, "The physiology and pharmacology of hippocampal formation theta rhythms," *Prog. Neurobiol.*, vol. 26, no. 1, pp. 1-54, 1986, doi: 10.1016/0301-0082(86)90019-5.
- [35] A. Sirota, S. Montgomery, S. Fujisawa, Y. Isomura, M. Zugaro, and G. Buzsáki, "Entrainment of Neocortical Neurons and Gamma Oscillations by the Hippocampal Theta Rhythm," *Neuron*, vol. 60, no. 4, pp. 683-697, 2008, doi: 10.1016/j.neuron.2008.09.014.
- [36] R. A. Velluti, *The auditory system in sleep*, 1st ed. Amsterdam :: Academic, 2008.
- [37] L. A. Poppi, J. C. Holt, R. Lim, and A. M. Brichta, "A review of efferent cholinergic synaptic transmission in the vestibular periphery and its functional implications," *J. Neurophysiol.*, vol. 123, no. 2, pp. 608-629, 2020, doi: 10.1152/jn.00053.2019.
- [38] M. A. Mathews, A. J. Camp, and A. J. Murray, "Reviewing the Role of the Efferent Vestibular System in Motor and Vestibular Circuits," *Front. Physiol.*, vol. 8, pp. 552-552, 2017, doi: 10.3389/fphys.2017.00552.
- [39] H. Barbas, S. Saha, N. Rempel-Clower, and T. Ghashghaei, "Serial pathways from primate prefrontal cortex to autonomic areas may influence emotional expression," *BMC Neurosci.*, vol. 4, no. 1, pp. 25-25, 2003, doi: 10.1186/1471-2202-4-25.
- [40] D. Berg, N. C. Spitzer, L. Squire, A. Ghosh, S. d. Lac, and F. E. Bloom, *Fundamental neuroscience*. Academic Press, 2012.
- [41] M. A. Lebow and A. Chen, "Overshadowed by the amygdala: the bed nucleus of the stria terminalis emerges as key to psychiatric disorders," *Mol. Psychiatry*, vol. 21, no. 4, pp. 450-463, 2016, doi: 10.1038/mp.2016.1.
- [42] K. A. Michelsen, J. Prickaerts, and H. W. M. Steinbusch, "The dorsal raphe nucleus and serotonin: implications for neuroplasticity linked to major depression and Alzheimer's disease," *Prog. Brain Res.*, vol. 172, pp. 233-264, 2008, doi: 10.1016/S0079-6123(08)00912-6.
- [43] C. Peyron, J. M. Petit, C. Rampon, M. Jouvet, and P. H. Luppi, "Forebrain afferents to the rat dorsal raphe nucleus demonstrated by retrograde and anterograde tracing methods," *Neuroscience*, vol. 82, no. 2, pp. 443-468, 1997, doi: 10.1016/S0306-4522(97)00268-6.
- [44] A. N. Popper, S. M. Highstein, and R. R. Fay, *The vestibular system. / Stephen M. Highstein, Richard R. Fay, Arthur N. Popper*, 1st 2004. ed. (Springer Handbook of Auditory Research, 19). New York, New York: Springer, 2004.
- [45] E. Samuels and E. Szabadi, "Functional Neuroanatomy of the Noradrenergic Locus Coeruleus: Its Roles in the Regulation of Arousal and Autonomic Function Part I: Principles of Functional Organisation," *Curr. Neuropharmacol.*, vol. 6, no. 3, pp. 235-253, 2008, doi: 10.2174/157015908785777229.
- [46] J. P. Staab, C. D. Balaban, and J. M. Furman, "Threat Assessment and Locomotion: Clinical Applications of an Integrated Model of Anxiety and Postural Control," *Semin. Neurol.*, vol. 33, no. 3, pp. 297-306, 2013, doi: 10.1055/s-0033-1356462.
- [47] B. Kocsis and R. P. Vertes, "Dorsal raphe neurons: synchronous discharge with the theta rhythm of the hippocampus in the freely behaving rat," *J. Neurophysiol.*, vol. 68, no. 4, pp. 1463-1467, 1992, doi: 10.1152/jn.1992.68.4.1463.
- [48] E. C. Azmitia and M. Segal, "An autoradiographic analysis of the differential ascending projections of the dorsal and median raphe nuclei in the rat," *Journal of comparative neurology (1911)*, vol. 179, no. 3, pp. 641-667, 1978, doi: 10.1002/cne.901790311.

- [49] R. P. Vertes, "A PHA-L analysis of ascending projections of the dorsal raphe nucleus in the rat," *Journal of comparative neurology (1911)*, vol. 313, no. 4, pp. 643-668, 1991, doi: 10.1002/cne.903130409.
- [50] S. K. Tai, J. Ma, K. P. Ossenkopp, and L. S. Leung, "Activation of immobility-related hippocampal theta by cholinergic septohippocampal neurons during vestibular stimulation," *Hippocampus*, vol. 22, no. 4, pp. 914-925, 2012, doi: 10.1002/hipo.20955.
- [51] J. Shin, "Passive rotation-induced theta rhythm and orientation homeostasis response," *Synapse (New York, N.Y.)*, vol. 64, no. 5, pp. 409-415, 2010, doi: 10.1002/syn.20742.
- [52] V. V. Gavrilov, S. I. Wiener, and A. Berthoz, "Enhanced hippocampal theta EEG during whole body rotations in awake restrained rats," *Neurosci. Lett.*, vol. 197, no. 3, pp. 239-241, 1995, doi: 10.1016/0304-3940(95)11918-M.
- [53] V. V. Gavrilov, S. I. Wiener, and A. Berthoz, "Whole-Body Rotations Enhance Hippocampal Theta Rhythmic Slow Activity in Awake Rats Passively Transported on a Mobile Robot," *Ann. N. Y. Acad. Sci.*, vol. 781, no. 1, pp. 385-398, 1996, doi: 10.1111/j.1749-6632.1996.tb15714.x.
- [54] J. Shin, D. Kim, R. Bianchi, R. K. S. Wong, and H.-S. Shin, "Genetic Dissection of Theta Rhythm Heterogeneity in Mice," *Proceedings of the National Academy of Sciences - PNAS*, vol. 102, no. 50, pp. 18165-18170, 2005, doi: 10.1073/pnas.0505498102.
- [55] J. Winson, "Hippocampal theta rhythm. I. Depth profiles in the curarized rat," *Brain Res.*, vol. 103, no. 1, pp. 57-70, 1976, doi: 10.1016/0006-8993(76)90686-7.
- [56] P. Aitken, Y. Zheng, and P. F. Smith, "The modulation of hippocampal theta rhythm by the vestibular system," *J. Neurophysiol.*, vol. 119, no. 2, pp. 548-562, 2018, doi: 10.1152/jn.00548.2017.
- [57] J. C. Holt, A. Lysakowski, and J. M. Goldberg, "The Efferent Vestibular System," ed. New York, NY: Springer New York, 2010, pp. 135-186.
- [58] J. M. Goldberg, *The vestibular system : a sixth sense*. Oxford ;: Oxford University Press, 2012.
- [59] R. J. Croft and R. J. Barry, "Removal of ocular artifact from the EEG: a review," *Neurophysiol. Clin.*, vol. 30, no. 1, pp. 5-19, 2000, doi: 10.1016/S0987-7053(00)00055-1.
- [60] Z. A. Dastgheib, B. J. Lithgow, and Z. K. Moussavi, "An unbiased algorithm for objective separation of Alzheimer's, Alzheimer's mixed with cerebrovascular symptomology, and healthy controls from one another using electrovestibulography (EVestG)," *Med. Biol. Eng. Comput.*, vol. 60, no. 3, pp. 797-810, 2022, doi: 10.1007/s11517-022-02507-1.
- [61] B. Lithgow, "A Methodology for Detecting Field Potentials from the External Ear Canal: NEER and EVestG," *Ann. Biomed. Eng.*, vol. 40, no. 8, pp. 1835-1850, 2012, doi: 10.1007/s10439-012-0526-3.
- [62] S. M. Shadli, V. Tewari, J. Holden, and N. McNaughton, "Laterality of an EEG anxiety disorder biomarker largely follows handedness," *Cortex*, vol. 140, pp. 210-221, 2021, doi: 10.1016/j.cortex.2021.03.025.